農研機構
NARO 国立研究開発法人 農業・食品産業技術総合研究機構

Spatio-temporal Analysis of Agriculture in the Vietnamese Mekong Delta using MODIS Imagery

メタデータ	言語: eng 出版者: 公開日: 2019-12-20 キーワード (Ja): キーワード (En): 作成者: 坂本, 利弘 メールアドレス: 所属:
URL	https://doi.org/10.24514/00002981

Bull. Natl. Inst. Agro-Environ.
Sci., 1-90 (2009)

Spatio-temporal Analysis of Agriculture in the Vietnamese Mekong Delta using MODIS Imagery

Toshihiro Sakamoto *

(Received Febuary 16, 2009)

Synopsis

New methodologies using MODIS time-series imagery were developed for revealing spatio-temporal changes of agricultural environments and land use patterns in the Vietnamese Mekong Delta. The following methodologies were proposed:a Wavelet based Filter for Crop Phenology (WFCP), a Wavelet-based filter for evaluating the spatial distribution of Cropping Systems (WFCS), and a Wavelet-based filter for detecting spatio-temporal changes in Flood Inundation (WFFI). The WFCP algorithm involves smoothing the temporal profile of the Enhanced Vegetation Index (EVI) using the wavelet transform approach. As a result of validation using the agricultural statistical data in Japan, it was shown that the WFCP was able to estimate rice growing stages, including transplanting date, heading date and harvesting date from the smoothed EVI data, with 9-12 days accuracy (RMSE). The WFCS algorithm was developed for detecting rice-cropping patterns in the Vietnamese Mekong delta based on WFCP. It was revealed that the spatial distribution of rice cropping seasons was characterized by both annual flood inundation around the upper region in the rainy season and salinity intrusion around the coastal region in the dry season. The WFFI algorithm was developed for estimating start and end dates of flood inundation by using time-series Land Surface Water Index and EVI. Annual intensity of Mekong floods was evaluated from 2000 to 2004, at a regional scale. Applying a series of wavelet-based methodologies to the MODIS data acquired from 2000 to 2006, it was confirmed that the cropping season for the winter-spring rice in the flood-prone area fluctuated depending on the annual change of flood scale. It was also confirmed that the triple rice-cropped area in the An Giang province expanded from 2000 to 2005, because the construction of a ring-dike system and water-resource infrastructure made it possible to sustain a third rice cropping season during the flood season. The proposed methodologies (WFCP, WFCS, WFFI) based on MODIS time-series imagery made it clear that while the rice cropping in the Vietnamese Mekong Delta was quantitatively (annual flooding) and qualitatively (salinity intrusion) affected by water-resource changes, there were some regions where the cultivation system was changed from double rice cropping to triple rice cropping because of the implementation of measures against flooding.

*National Institute for Agro-Environmental Sciences, Ecosystem Informatics Division

Contents

Chapter I
Introduction

Japanese food self-sufficiency in terms of calorie supply decreased steadily from 79% in 1960 to 40% in 2005, and self-sufficiency in grain was only 28% in 2005 (Fig. 1). Food self-sufficiency in Japan appears to have worsened since 1961 compared with G7 countries (Fig. 2, 3). According to public opinion polls conducted by Cabinet Office in 2006 (Cabinet Office 2006), about 70% of the Japanese public consider that the current food self-sufficiency is low. With international specialization of food production, Japan is the world's largest importer of cereal grains, importing 25.9 million tons (US$5.2 billion) in 2004, 9.7% of the international cereal-grain market of 267.9 million tons (US$52.9 billion) (FAOSTAT 2007). This reliance on imports means that Japan is quite vulnerable to fluctuations in world cereal grain prices, and that its food supply security strongly depends on the global food supply-demand balance.

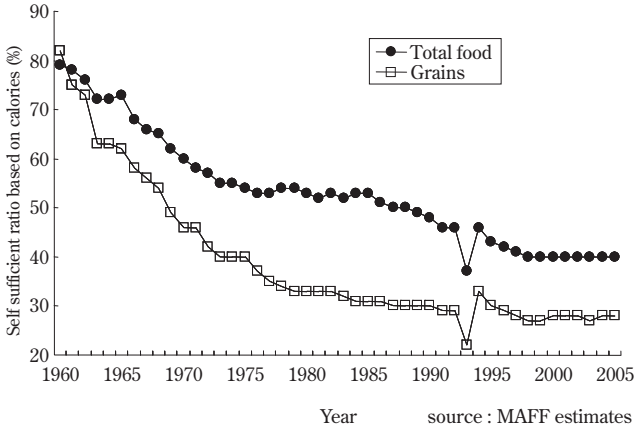

Fig. 1. Time-series self sufficiency ratio of total food and grains in Japan from 1960 to 2005

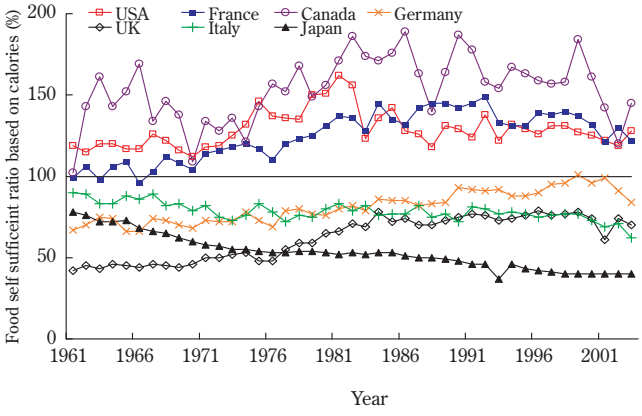

Fig. 2. Time-series food self-sufficiency ratio of the G7 from 1961 to 2003

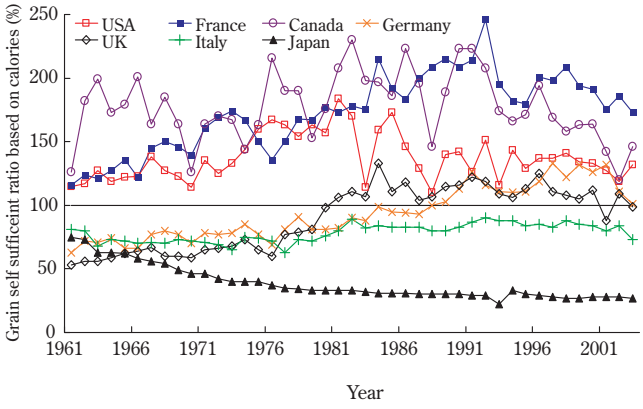

Fig. 3. Time-series grain self-sufficiency ratio of the G7 from 1961 to 2003

The global food problem is usually discussed in terms of annual statistical data (the amount of production and consumption, and the year-end stock) released by international government agencies (e.g. FAO, USDA). According to these time-series statistical data (USDA, 2007), the global cereal-grain balance between production and consumption fluctuates annually, but remains in equilibrium over the long term (Fig. 4). It seems as if the international trading system satisfy global food demand. Thus, it is easy to forget that human took a massive hit from an unprecedentedly poor harvest over a long history. Even if the world were to suffer a poor cereal harvest, the Japanese people will never suffer from hunger because Japan can compensate for any fall in national production by buying grains on the international crop

market, helped by the strength of the Japanese Yen. As in the case of the poor rice harvest resulting from record low summer temperatures in 1993, Japanese people never starve even if they are reluctant to eat imported low-quality rice or alternative foods. However, it should be remembered that 854 million people (13% of global population) suffer from hunger, mainly in the developing countries (WFP, 2007). Their demand for food to provide them with healthy life is never satisfied by increases in food production, because they cannot afford to buy food on the free market. At the same time, in developed countries where many people suffer from obesity, much food is disposed of without being eaten.

In recent years, China's imports of soybeans for oil have increased rapidly (Fig. 5), while Brazil and Argentina have increased both their soybean area under production and their export volumes (Fig. 6, 7). The U.S. has expanded the

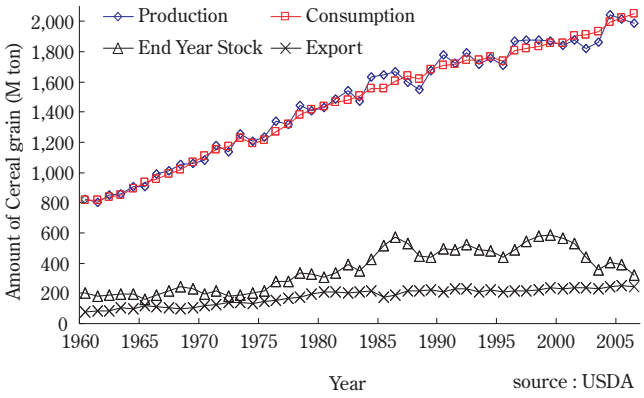

Fig. 4. Cereal grains production, consumption, export and end-year stock from 1960 to 2006

area of maize in production for ethanol extraction in response to an increased demand for bio energy and in response to government policy (Koizumi, 2006). The transforming global food supply-demand balance resulting from the increase of food-demand in developing countries and the policy changes on biomass energy in developing countries, draw international attention. Moreover, the impact of climate change on global food production systems is now an important policy issue as a subject of intense research. As the world's population increases and the rate of growth in cereal crop production slows worldwide (Fig. 4), the global food supply-demand balance may become less stable. Asian countries with rapidly growing economies and populations, especially China and India, would play an important role in the international food market. As agriculture becomes more intensive and modernized as a consequence of economic growth in developing countries, the agricultural ecosystem will become increasingly threatened, especially in rural areas. People living in poor countries with a low self-sufficiency ratio will find buying surplus food on the international market increasingly difficult, and the resulting poverty and starvation may be politically destabilizing. It is not assured that Japan can keep an adequate and continuous supply of food at an affordable price under the influence of the global climate change and changing global food supply-demand balance. Careful assessment of the changing world agricultural system and environment is an essential first step to understanding current and future food security issues of Japan within Asia. Japan should collect its own intelligence about foreign agricultural systems to help develop a comprehensive strategy in order to ensure secure food supplies and maintain peace and stability in Asia.

Rice cultivation in the Vietnamese Mekong Delta (VMD) was chosen as the subject of this study, because Vietnam is the world's second largest exporter of rice (Figs 8, 9). Most of rice exported from Vietnam is produced in the VMD at low cost and exported to Asian countries, especially the Philippine, Indonesia, and Malaysia (GSO, 2007). Additionally, Vietnam is the world's third largest country producing farmed-shrimp, and more than half of which is produced in the VMD. As a large-scale shrimp importer, Japan has an indirect connection with agricultural environmental change in the VMD. Most paddy fields in the coastal area of the VMD have been converted to shrimp ponds (Binh et al., 2005), and enabling Vietnam's share of Japan's frozen shrimp market (Figs. 10, 11) to increase more than 20% since 2003, the largest of several Asian sources.

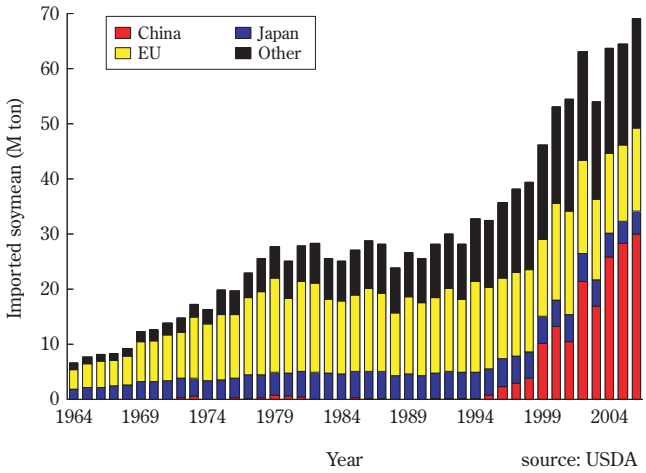

Fig. 5. Time-series data of soybean import from 1964 to 2006

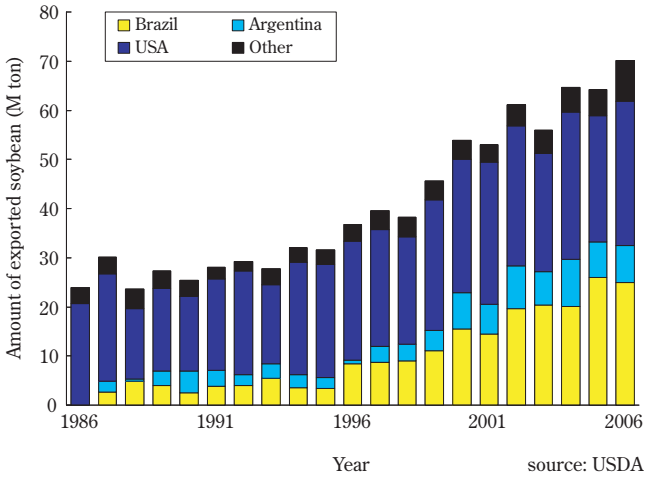

Fig. 6. Time-series data of soybean export from 1986 to 2006

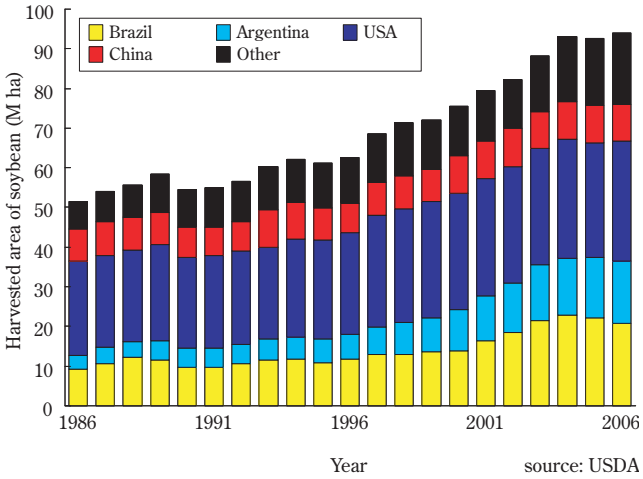

Fig. 7. Time-series harvested area of soybean from 1986 to 2006

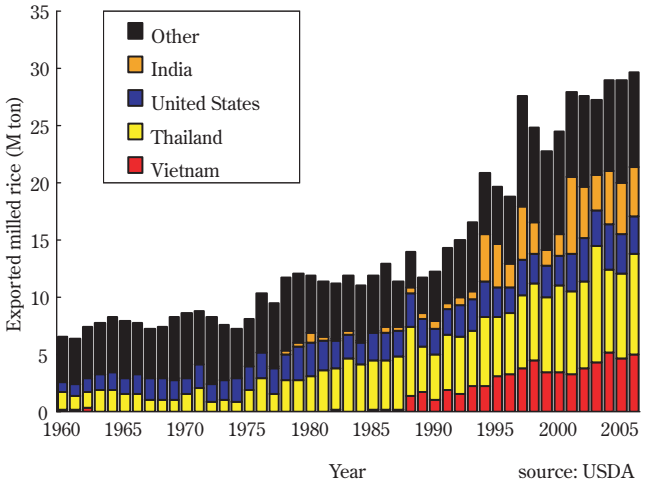

Fig. 8. Global market share trend of exported rice from 1960 to 2006

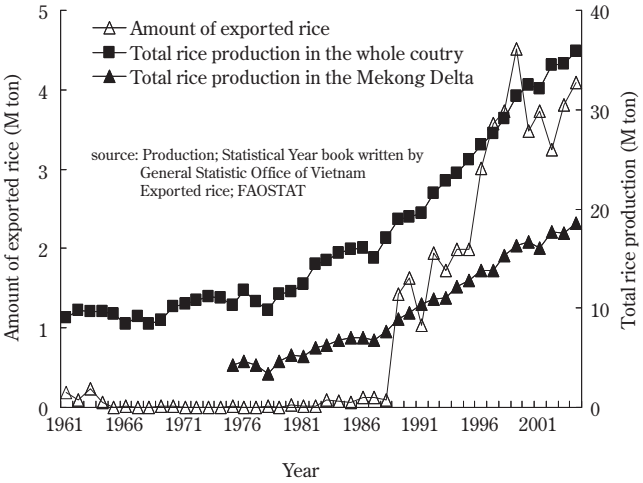

Fig. 9. Quantity of rice production and exported rice for the whole of Vietnam and the VMD from 1961 to 2004

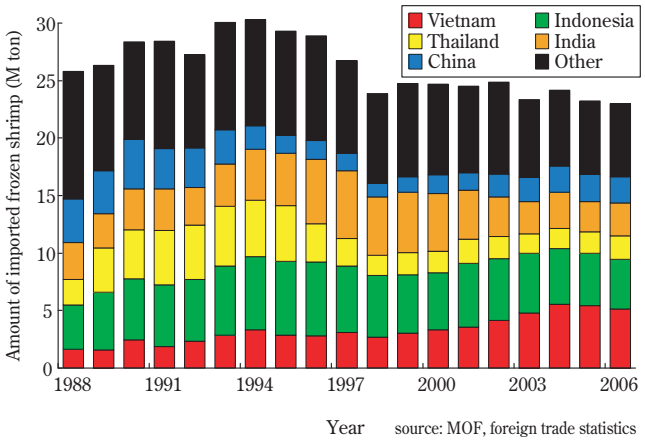

Fig. 10. Quantity of frozen shrimp imported to Japan from 1988 to 2006

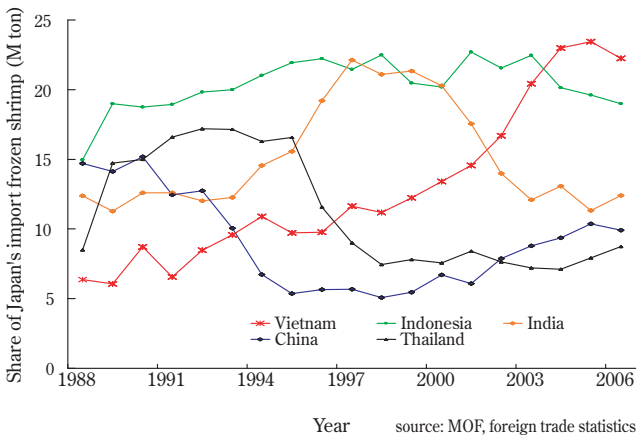

Fig. 11. Major five countries' share of Japan's imported frozen shrimp from 1988 to 2006

This study aimed to establish a new approach for detecting changes in agricultural activity and environment using remote sensing technology. The methodology using MODIS imagery is devised for monitoring the rice phenology, rice–cropping pattern and flood inundation in the VMD, in order to reveal the spatio–temporal changes in agricultural activity and its relationship with to short–to–medium variation in water resources. Such new research findings on the agricultural land–use change and the general relationships between environmental fluctuation in water resources and crop production will help us to understand the up–to–date information about the foreign agriculture and to predict the effect of global climatic change on agricultural activity and ecosystems.

Chapter II
A Crop Phenology Detection Method using Time-series MODIS Data

2.1. Introduction

Monitoring seasonal changes in vegetation activity and crop phenology over wide areas is essential for many applications, such as estimation of net primary production (Kimball et al., 2004), deciding time boundary conditions for crop yield modeling (Bormanb Am and Tuong, 2001) and supporting decisions about water supply (Dingkuhn and Le Gal, 1996). Identifying crop phenological stages from Moderate Resolution Imaging Spectroradiometer (MODIS) data may enable us to estimate crop growth under various regional weather conditions. For example, cool summers result in delayed heading and thus decreased rice yields (Mahmood, 1997; Wilson et al., 1995).

Monitoring seasonal changes in vegetation activity and crop phenology over wide areas is essential for many applications, such as estimation of net primary production (Kimball et al., 2004), deciding time boundary conditions for crop yield modeling (Bormanb Am and Tuong, 2001) and supporting decisions about water supply (Dingkuhn and Le Gal 1996). Identifying crop phenological stages from Moderate Resolution Imaging Spectroradiometer (MODIS) data may enable us to estimate crop growth under various regional weather conditions. For example, cool summers result in delayed heading and thus decreased rice yields (Mahmood, 1997; Wilson et al., 1995).

Remote sensing is often used for detecting seasonal vegetation changes. Various methods using daily Normalized Difference Vegetation Index (NDVI) data have been developed for monitoring crops and natural vegetation (Akiyama et al., 2002; Saito et al., 2002; Xiao et al., 2002b). Jakubauskas et al. (2002) applied harmonic analysis to NDVI data from the US National Oceanographic and Atmospheric Administration's Advanced Very High Resolution Radiometer (NOAA/AVHRR) and developed an innovative technique for identifying crop type from amplitude and phases of decomposed component. They stated that the application of harmonic analysis to time-series data is useful for detecting changes of land use and land cover, such as at planting and harvest. Several studies of forest phenology using MODIS data have also been made. Kang et al. (2003) used 30-year mean air temperature and MODIS/leaf area index (LAI) data to detect the onset of vegetation greenness in Korea. Their results suggested that the phenological stages can be detected more precisely through a combination of climatic data and MODIS data. Zhang et al. (2003) identified phenological dates by finding points on the time profile curve of the Vegetation Index (VI) where the rate of curvature is maximum.

In general, time-series NDVI data obtained by satellite include various noise components such as aerosols and bidirectional reflectance distribution factors. Thus, noise reduction or fitting a model to observed data is necessary before phenological stages can be determined. Tools for such preprocessing include smoothers such as polynomial and median filters (Dijk, 1987), a moving window to select the local maximum VI (Viovy et al., 1992), Temporal Window Operation (Park et al., 1999), and logistic curve fitting (Zhang et al., 2003); for a review see (Reed et al., 2003).

Several frequency analysis studies have used the Fourier transform for separating the high-frequency components of noise and the low-frequency components of seasonal changes of VI (Azzali, 2000; Roerink, 2000; Viovy et al., 1992). Sawada et al. (1999; 2000) developed the Local Maximum Fitting method by applying the Fourier transform to 10-day composite data of NOAA/ AVHRR NDVI to reconstruct a cloud-free seasonal profile of NDVI. Hara et al. (2003) modified that method and applied it to 10-day composite data of SPOT-VEGETATION NDVI.

The wavelet transform also can be used to remove noise. Its strength is the feasibility of identifying the timing of events such as localized objective signals in the presence of noise. The wavelet transform has been used for estimating forest LAI and for canopy closure mapping from EO-1 hyper-spectral data (Koger et al., 2003), and for detecting the interannual variability of NOAA/AVHRR NDVI and its relationship with El Nino/Southern Oscillation Index (Li and Kafatos, 2000). However few studies have used the wavelet transform for smoothing temporal VI data and for detecting crop phonological stages. The wavelet transform retains time components when transforming time-series data, and so can reproduce seasonal changes of vegetation without losing the temporal characteristics. In contrast, the trigonometric

functions used in the Fourier transform are not localized in the time domain, and therefore the time component of the input data is averaged after the transforming process. Thus, it is assumed that the wavelet transform could divide the noise components and reconstruct the seasonal VI time profile better than the Fourier transform. Statistics of phenological stages of paddy rice is used to compare the performance of our method using the wavelet and Fourier transforms.

2.2. Materials and methods

2.2.1. Wavelet and Fourier transforms

Time-series VI data filtered by methods using linear interpolation, such as the BISE (Viovy et al., 1992) and TWO methods (Park et al., 1999), have discontinuities with respect to first derivative, and the rates of increase and decrease of the interpolated data stay constant. Thus, it is hard to identify the crop growth stages by using inflection point or minimal point. Filtering methods using the Fourier or wavelet transform can reduce noise with reflecting the periodicity of seasonal vegetation change. The filtered VI data are continuous, and the inflection point and maximum point can be detected for delimiting growing seasons. The performance of the Fourier and wavelet transforms was compared as filtering methods in the identification of rice phenological stages from daily VI changes.

The wavelet transform is widely used; e.g., in the analysis of long-term variability of air temperature (Khan et al., 2004), noise reduction in lidar signals(Fang and Huang, 2004), and analysis of the variability of vegetation (Li and Kafatos, 2000).

The function $f(x)$ is transformed in the wavelet transform as follows:

$$Wf(a,b) = \int_{-\infty}^{+\infty} f(x) \frac{1}{\sqrt{a}} \psi\left(\frac{x-b}{a}\right) dx \qquad \cdots\cdots\cdots\cdots \quad (2-1)$$

where a is a scaling parameter, b is a shifting parameter, and ψ implies a mother wavelet. In discrete form, parameters a and b are given as follows:

$$(a,b) = (2^j, 2^j k) \qquad \cdots\cdots\cdots\cdots \quad (2-2)$$

where j and k are integers.

A wavelet is a small, localized wave in time or space and here satisfies the orthogonal condition. Since a wavelet has compact support, which means that its value becomes 0 outside a certain interval of time (Fig. 12), the time components of time-series data can be maintained during wavelet transformation. The function $f(x)$ is decomposed to linear

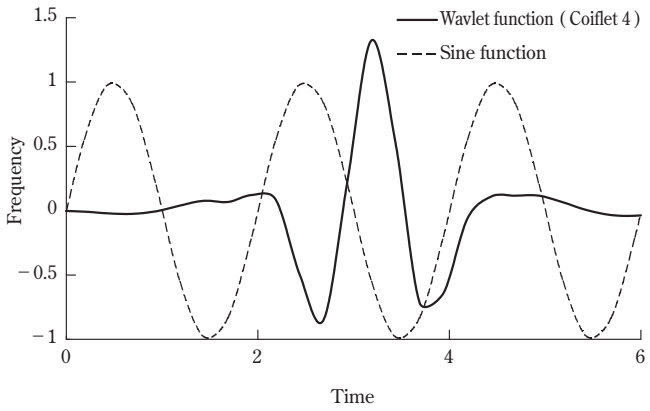

Fig. 12. Wavelet function (Coiflet 4) and sine function

combinations of wavelet functions in the multi-resolution approximation formula:

$$f(x) = f_j(x) + g_j(x) + \cdots + g_1(x) \quad \cdots\cdots\cdots\cdots \quad (2-3)$$

where the function $f_j(x)$ implies the approximate expression in level j, and $g_j(x)$ implies the high-frequency components in level j.

On the other hand, the Fourier transform decomposes a function $f(x)$ to the frequency domain by a linear combination of trigonometric functions as follows:

$$F(\omega) = \int_{-\infty}^{+\infty} f(x) e^{-i\omega x} dx \quad \cdots\cdots\cdots\cdots \quad (2-4)$$

where w is frequency and $F(\omega)$ is the Fourier coefficient with frequency ω.

It is customary to use a discrete form as follows:

$$F(k) = \frac{1}{N} \sum_{n=0}^{N-1} f_i e^{(-\frac{2\pi kni}{N})} \quad \cdots\cdots\cdots\cdots \quad (2-5)$$

where k = 0, 1, 2, . . . N-1, and N is the total number of input data. The wavelet and Fourier transform subroutines implemented in the Interactive Data Language (ITT Visual Information Solutions) were used.

2.2.2. Data description

2.2.2.1. Satellite data

The MODIS data (acquired in 2002) were provided by the EOS Data Gateway (EOS, 2007). The product name is "MODIS/Terra surface reflectance 8-day Global 500 m SIN GRID v004". The product was composed so as to have the lowest value of band 3 over every 8 days (Vermote and Vermeulen, 1999). In addition, the product had already been systematically corrected for the effects of gaseous and aerosol scattering. Each pixel includes the ground reflectance ratio. Even with correction, the effects of the Bidirectional Reflectance Distribution Function (BRDF) on VI remained as noise. Time-series analysis is necessary in order to reduce the remaining noise. The observation date and sensor zenith angle of each pixel were accounted for in this chapter to cut out misleading data.

2.2.2.2. Statistical data and digital national land information

Statistical data provided by the Ministry of Agriculture, Forestry and Fisheries (MAFF) of Japan were used as ground-truth data. The MAFF divides Japanese agricultural land into about 150 cropping zones, each with an area of about 2600 km^2. The planting, heading, and harvesting seasons in each cropping zone are recorded in the statistical data. Each phenological season is defined by three dates:the beginning, peak, and end. These data were used to assess the performance of new method for detecting phonological stages observed in 2002.

Digital national land information was published by the Ministry of Land, Infrastructure and Transportation of Japan (MLIT, 1997) for national land planning, in which Japan is divided into a grid of 30 s in latitude by 45 s in longitude (ca. 1.1 km). Each grid includes areas of paddy fields, upland fields, forest, wasteland, buildings, roads and railroads, rivers and lakes, seaside, sea, golf courses, and other types. Referring to this information, 30 test sites were selected from grids where the land coverage of paddy fields is more than 90% (Fig. 13).

2.2.3. Prescription of multi-temporal satellite data

2.2.3.1. Vegetation index

The Enhanced Vegetation Index (EVI) can be linearly correlated with the leaf area index, and has a higher sensitivity than that of NDVI in high biomass areas (Huete et al., 2002a). Since the biomass of paddy fields is low compared

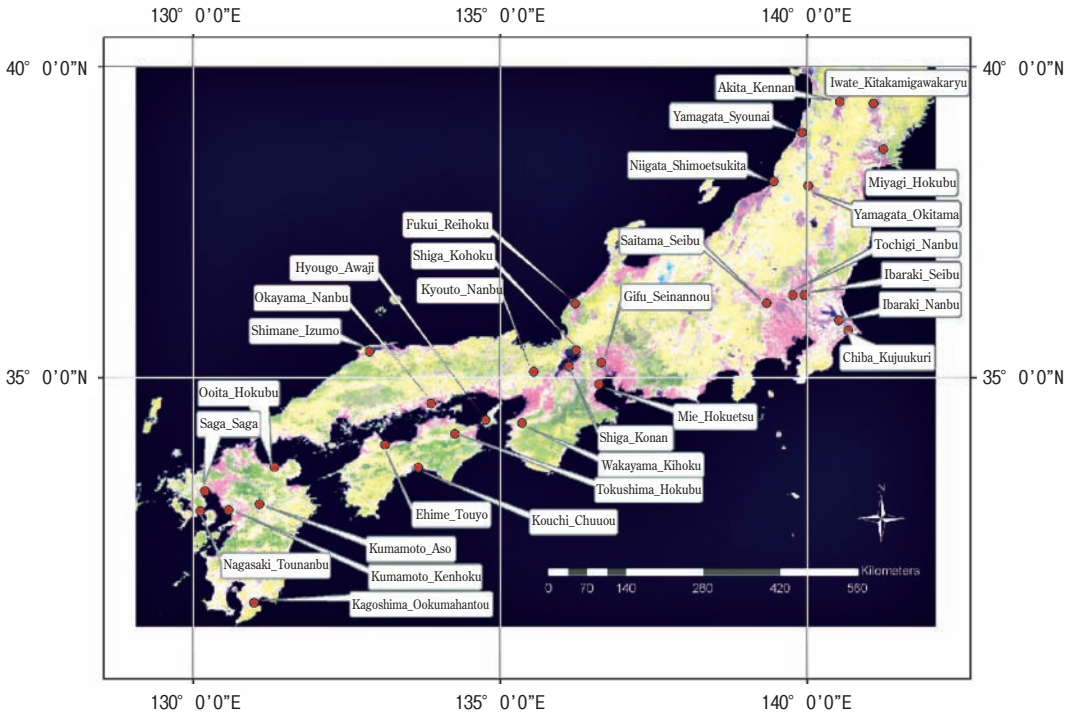

Fig. 13. Locations of the 30 test sites

with forests, EVI retains linearity in paddy fields. Therefore EVI can be used to evaluate the process of paddy growth adequately with a wide dynamic range. Furthermore, EVI is more practical than NDVI when humidity is high. Since the rice growing stage falls in the rainy season when humidity is high, EVI is a more practical than NDVI for monitoring the paddy fields in Japan. Therefore, we used EVI in our method.

2.2.3.2. Removing data affected by thick clouds, and sensor zenith angle

Even though the available satellite data were corrected for the effects of aerosols, thick clouds veiling a pixel for 8 days make it impossible to correct the surface reflectance of that pixel. To remove data affected by thick clouds, pixels whose band 3 reflectance was more than 10% were removed as abnormal data.

The MODIS data used here had already been resampled systematically to a uniform spatial resolution (500 m). However, in raw data before geometric conversion, the spatial resolution of a pixel depends on the sensor zenith angle. The larger the sensor zenith angle of a pixel, the lower the ground resolution of that pixel. For this reason, a with a broad sensor zenith angle includes a strong neighbor effect. It is essential to consider this effect of sensor zenith angle on the detection of phenological stage. We used the threshold of the sensor zenith angle to remove pixels with lower resolution, which give misleading results in time-series analysis. Because the grid resolution of the digital land-use map is about 1 km, we defined the threshold of the sensor zenith angle as 32.25° (ca. 750 m). Pixels with a sensor zenith angle of more than 32.25° were removed.

2.2.3.3. Data regulation

The number of elements in the input data array should be a power of 2 for both wavelet and Fourier transforms. To make an input array with 2048 elements, a year's VI data was continuously and recursively used to fill the array in observational date order. Missing data were linearly interpolated. We used 365 elements of the output array from the 730th to the 1094th as the smoothed time profile of EVI. This processing was used to avoid the aliasing effect.

2.2.4. Noise reduction and reconstructing the EVI profile with wavelet transform

The discrete wavelet transform can decompose time-series EVI data into scaled and shifted wavelets over a discrete set of scales. It was assumed that the frequency of noise components in time-series EVI data is higher than that of the seasonal change of VI in paddy fields. Therefore, the smoothed time profile of EVI was reconstructed by using specific frequency components. According to the statistical data, the growing period of rice is generally 90 to 160 days in Japan. To reflect a seasonal change of VI, components with a frequency lower than 128 ($=2^7$) should be taken. Furthermore, components with a frequency higher than scale 64 ($=2^6$) should be reduced in order to avoid errors caused by abnormal data. These data were not removed in preprocessing and so prevented from precisely determining the date of peak VI around the heading season. In addition, components with a frequency lower than scale 32 ($=2^5$) should be used for identifying the abrupt change in time-series VI data around the planting and harvesting seasons. A smoothed time profile of EVI was derived by averaging two time profiles, one reconstructed with the lower-frequency components divided by scale 64, the other with the lower-frequency components divided by scale 32. Three types of mother wavelets were used: (Daubechies, 1988) (order=2-24), Coiflet (1-5), and Symlet (4-15).

2.2.5. Noise reduction and reconstructing the EVI profile with Fourier transform

In using the discrete Fourier transform, the input array of the time-series EVI data is divided into 10 discrete frequencies. The length of these frequencies is a power of 2. In the same way as with the discrete wavelet transform, the smoothed time profile of EVI was derived by averaging two time profiles of EVI, decomposed by wavelengths of 64 and 128, corresponding to scales 32 and 64.

2.3. Threshold for detecting phenological stages

2.3.1. Heading date

According to time-series data of the spectral reflectance of paddy fields (Shibayama and Akiyama 1989), the maximum NDVI appears around the heading date. The reason for this is that the rice changes its growth phase from vegetative growth to reproductive growth on reaching the heading date, and leaves begin to wither and die. Therefore, it was assumed that the smoothed time profile of EVI also shows a peak on the heading date. The date of the maximum EVI in the time profile was defined as the estimated heading date.

2.3.2. Planting date

In general, paddy fields are plowed and flooded before rice planting. The VI of paddy fields decreases during this period and then increases again after rice planting. Thus, for detecting the planting date from the smoothed time profile of EVI, the following procedure was defined for determining the planting date: (i) the minimal point (the first derivative equals 0 and changes from negative to positive at this point) or inflection point (the second derivative equals 0 and changes from negative to positive at this point) earlier than 60 days from the estimated heading date was identified; then, (ii) the later one of these two points was automatically taken as the estimated planting date. The reason why two such discriminative points were used together for detecting the planting date is that the amount of biomass in the planting season is much less than that at the other phenological stages and it was difficult to detect subtle changes in EVI by only one discriminative point.

2.3.3. Harvesting date

After the heading season, VI in paddy fields begins to decrease as leaves wither and die. It then decreases abruptly because of harvesting. Therefore, the date of an inflection point (the second derivative equals 0 and changes from positive to negative) later than 30 days after the estimated heading date was defined as the estimated harvesting date.

2.4. Results and discussion

2.4.1. Validation with statistical data

Table 1 shows the performance of the method using the wavelet and Fourier transforms for detecting the phonological stages and growing period. There was no significant difference between using the wavelet and Fourier transforms in the heading and harvesting dates. However, in determining the planting date, the performance of the method using the wavelet transform was superior to that using the Fourier transform. The maximum difference of the root mean square error (RMSE) for estimating the planting date was 5.1 days between them. For estimating the growing period, the maximum difference was 7.0 days.This difference in estimating the growing period resulted mainly from the difference in estimating the planting date. Among the mother wavelets tested here, Coiflet 4 gave the best estimate. The estimated phenological stages and the statistical data are compared in Figs. 14 and 15. Table 2 indicated the number of cases that the estimated dates were within the period from beginning to end of each phenological season in statistical data. Fig. 15 shows the differences between the estimated phenological date and peak of phenological season in statistical data. The error of estimated planting date with the wavelet transform was smaller than that with the Fourier transform by 5.1 days in RMSE (Table. 1). The number of cases in which the estimation error exceeded ±16 days when using the wavelet transform were:3 (10%) in planting date, 2 (7%) in heading date, 1 (3%) in harvesting date and 6 (20%) in growing period. On the other hand, when using the Fourier transform, those were:11 (37%) in planting date, 2 (7%) in heading date, 4 (13%) in harvesting date and 8 (27%) in growing period. Except for heading date, these numbers when using the wavelet transform were smaller than that using the Fourier transform.

The performances of these methods for estimating the growing period are compared in Fig. 16. The maximum estimation error with the Fourier transform (51 days) is much more than that with the wavelet transform (−25 days), owing to the localized characteristics of the wavelet transform. The wavelet transform can detect localized changes separately in the time domain. In contrast, the trigonometric function of the Fourier transform is not localized in the time domain. Hence, the Fourier transform causes errors that occur in separate positions to interfere. Since the planting and harvesting dates estimated by using the wavelet transform did not include these errors, the growing period estimated by using the wavelet transform was also superior to that estimated by using the Fourier transform.

The method using the wavelet transform (Coiflet order=4) showed the best result. The RMSEs of the growing period and each phenological stage were around 12 days. It is assumed that the good accuracy of our method is sufficient for discrimination of rice phenology in regions where dates are not available. However, for use in crop yield models, we consider that the RMSE of the estimated planting date (12.1 days) was inadequate and has to be improved.

Table 1. Comparison of root mean square error (RMSE) of the estimated phenological date and growing period against the statistical data.

Mother wavelet	Growing period	Planting date	Heading date	Harvesting date
Daubechies 9	11.7	14.5	9.1	12.7
Daubechies 13	11.8	14.4	9.0	11.8
Daubechies 17	12.5	15.2	9.0	11.2
Symlet 6	13.5	13.2	9.6	13.1
Symlet 12	13.9	13.7	9.6	11.1
Symlet 14	13.5	14.1	9.3	10.7
Coiflet 3	14.0	12.5	9.4	12.4
Coiflet 4	11.0	**12.1**	9.0	10.6
Coiflet 5	11.0	**13.7**	9.0	10.1
Fourier	18.0	17.2	8.8	11.5

The best three results of each mother wavelet are listed.
The number after the name of the mother wavelet indicates the order number.

Table 2. Number of cases that the estimated dates are within the period from beginning to end of each phonological seasons in statistical data.

	Wavelet Analysis (Coiflet4)	Fourier Analysis
Planting date	19 (63%)	14 (47%)
Heading date	26 (87%)	24 (80%)
Harvesting date	26 (87%)	26 (87%)

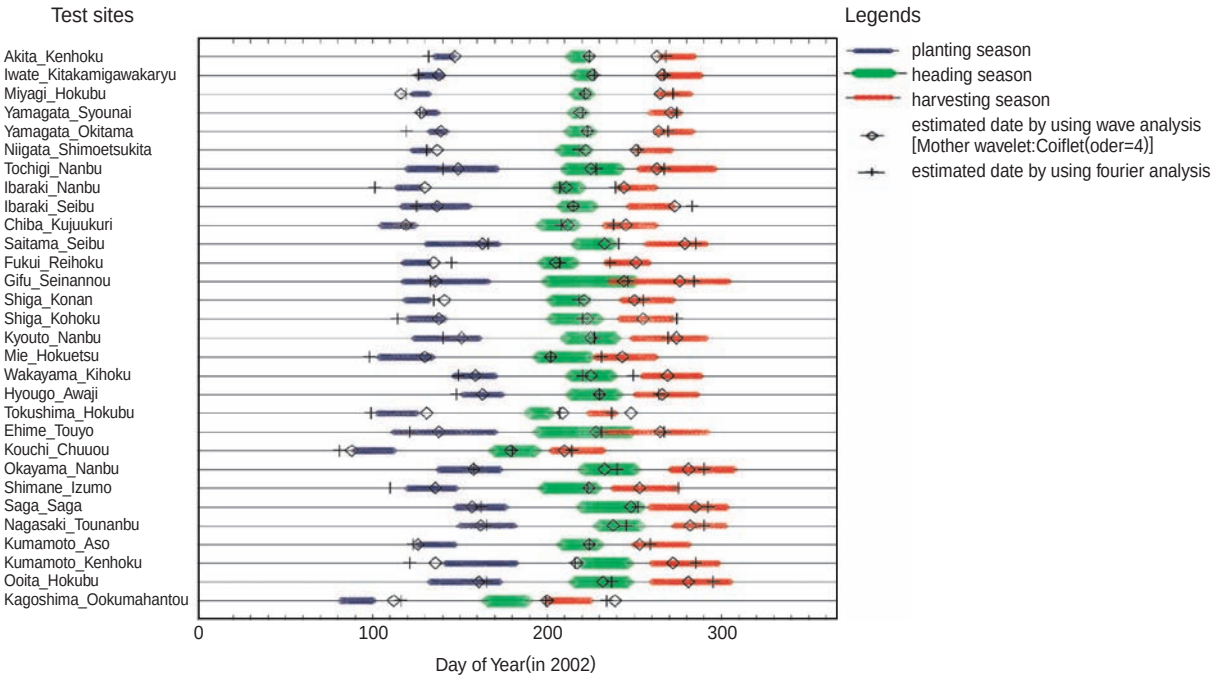

Fig. 14. Comparison between statistical data and the dates of phenological stages estimated by methods using Wavelet transform and Fourier transform.

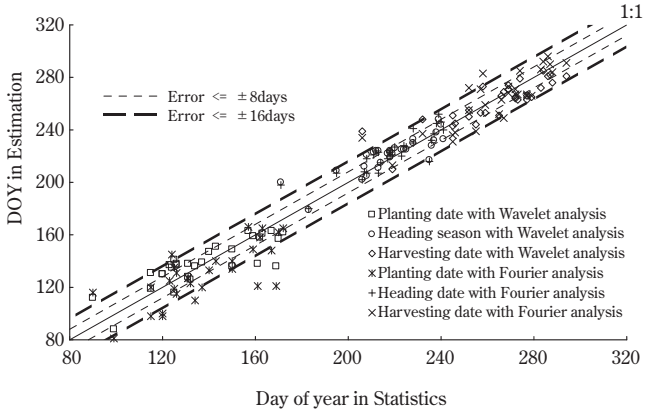

Fig. 15. One-to-one comparison between statistical data and phenological dates estimated by methods using Wavelet transform and Fourier transform. DOY = day of year

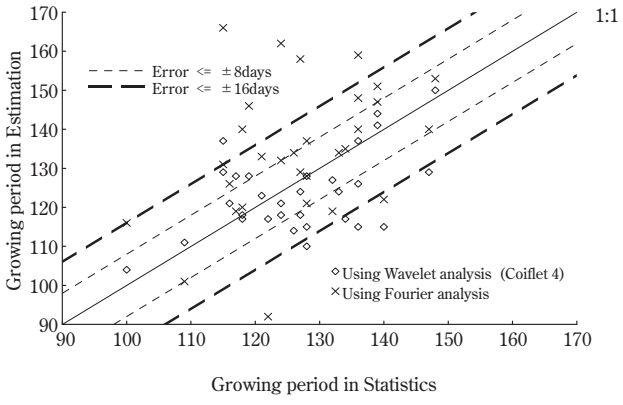

Fig. 16. One-to-one comparison between statistical data and growing periods estimated by methods using Wavelet transform and Fourier transform.

2.4.2. Smoothed time profile of EVI

The smoothed time profiles of EVI generated by both transforms are shown in Fig. 17. These time profiles show the same seasonal tendency as the original EVI data. The changes around the planting season in the second derivative of time profiles of the EVI generated by wavelet transform are larger than those by Fourier transform. The dates of the minimal and inflection points differed between profiles from wavelet and Fourier transforms (Fig. 17). In addition, local changes in the time component around the planting season were blurred in the Fourier transform (Fig. 17). The Fourier transform inadequately represents the appropriate position of the minimal and inflection points in the time domain. In the filtering process, the wavelet transform can hold the time component of temporal EVI data, but the Fourier transform cannot. It was assumed that these characteristics of the time component in temporal EVI data led to the difference in accuracy, and that the filtering method using the wavelet transform is much more sensitive to vegetation seasonal changes than that using the Fourier transform.

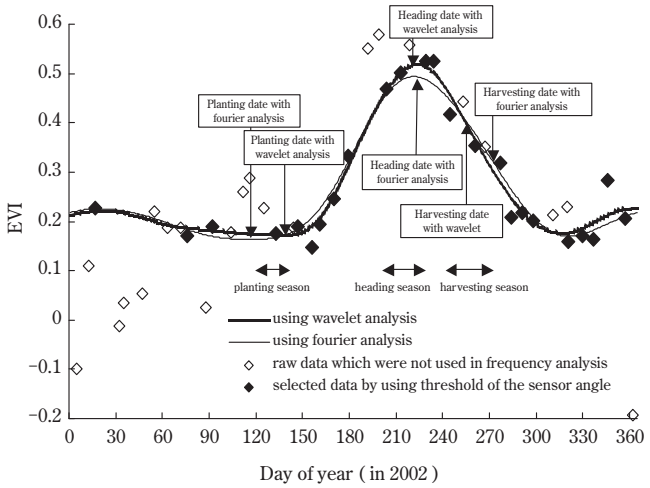

Fig. 17. Original EVI data and time profile smoothed by Wavelet transform and Fourier transform for data from Shiga_Kohoku (see Fig. 12).

2.4.3. Detecting the phenological stages on a regional scale

The mixed pixel effect and topography may affect the spectral characteristics in satellite image. However, the target areas in this section are where most of each grid is used as paddy fields. Generally such areas are located on plains formed by alluviation. Therefore, there is little topographic and mixed pixel effect on the results. The area of a parcel of paddy fields is less than about 5000 m^2 in Japan. The 500–m resolution of MODIS data is too coarse to show an individual parcel. Given that the objective in this chapter is to estimate the regional characteristics of rice phenology, it is appropriate to use MODIS data with a 500–m resolution for monitoring paddy fields on a regional scale. Additionally, compared with the resolution of NOAA/AVHRR (ca. 1.1×1.1 km) and SPOT/ VEGETATION (ca. 1×1 km), the resolution of the MODIS image is higher and offers an advantage in determining regional crop phenology.

2.5. Conclusions

In this chapter, a new systematic method was developed for detecting the phenological stages of paddy rice from timeseries MODIS data. The method consists of three procedures：(i) prescription of multi–temporal satellite data; (ii) filtering the time–series EVI data; and (iii) specifying the phenological stages from the smoothed EVI time profile. The method can determine the planting, heading, and harvesting dates in paddy fields. The estimation was validated against statistical data from 30 test sites. In filtering to reduce noise, the wavelet transform using Coiflet 4 gave the best time

profile of the EVI for detecting the phenological stages. Finally, this new method using the wavelet transform is proposed: Wavelet based Filter for determining Crop Phenology (WFCP).

As crop calendars are not available in many regions, WFCP is particularly useful for determination of regional characteristics of rice phenology. It would be appear that WFCP has potential applicability to other crops and some natural vegetation, whose EVI profile has an obvious peak with a bell-shape (e.g., wheat, deciduous forest, grassland). However the mother wavelet used and the threshold for determination of phenological stages will depend on the species.

This chapter confirms that WFCP can be applied to MODIS data with 500-m resolution for determination of rice phenological stages over wide areas and can build a smoothed EVI profile in paddy fields. In the near future, a map of rice phenology in East Asia will be released for revealing the relationship between seasonal changes in rice growth and regional characteristics of climatology. At the moment, various problems including the mix-pixel effect remain. Using MODIS/Aqua data (acquired after July 2002) together with MODIS/Terra data could improve the accuracy of our method.

2.6. Summary

Information of crop phenology is essential for evaluating crop productivity and crop management. Therefore a newmethod for remotely determining phenological stages of paddy rice was developed. The method consists of three procedures: (i) prescription of multitemporal MODIS/Terra data; (ii) filtering time-series Enhanced Vegetation Index (EVI) data by time-frequency analysis; and (iii) specifying the phenological stages by detecting the maximum point, minimal point and inflection point from the smoothed EVI time profile. Applying this method to MODIS data, we determined the planting date, heading date, harvesting date, and growing period in 2002. And the performance of the method was validated against statistical data in 30 paddy fields. As for the filtering, wavelet and Fourier transforms was adopted. Three types of mother wavelet (Daubechies, Symlet and Coiflet) were used in Wavelet transform. As the results of validation, the wavelet transform performed better than the Fourier transform. Specifically, the case using Coiflet (order=4) gave remarkably good results in determining phenological stages and growing periods. The root mean square errors of the estimated phenological dates against the statistical data were:12.1 days for planting date, 9.0 days for heading date, 10.6 days for harvesting date, and 11.0 days for growing period. The method using wavelet transform with Coiflet (order=4) allows the determination of regional characteristics of rice phenology. This new method using the wavelet transform was proposed; Wavelet based Filter for determining Crop Phenology (WFCP).

Chapter III
Spatio-temporal Distribution of Rice Phenology and Cropping Systems in the Mekong Delta with Special Reference to the Seasonal Water Flow of the Mekong and Bassac Rivers

3.1. Introduction

The optimal climatic conditions and plentiful water resources of Monsoon Asia enable intensive rice production and the cultivation of multiple crops. The high yields and considerable carrying capacity of the rice-producing regions have supported increases in the Asian population, and the surplus rice production in Thailand, India and Vietnam has enabled these countries to export rice all over the world (FAOSTAT, 2007). The cost effectiveness and considerable size associated with the Asian rice harvest is an important source of nourishment for countries where food self-sufficiency rates are low.

In its third assessment report, the Intergovernmental Panel on Climate Change predicted that average global surface temperatures would increase by 1.4 to 5.8 ℃ between 1990 and 2100. Moreover, the distribution and intensity of precipitation will change in response to this increase in temperature (IPCC Working Group I, 2001). These perturbations to rainfall will affect river flow rates and flood runoff, which will in turn likely impact upon the amount of available irrigation water. Taken together, these factors are likely to impact upon rice productivity, which is dependent upon bountiful water resources. To evaluate the likely impact of changes in global-water resources on international rice supply, it is therefore necessary to monitor the dominant rice production areas and determine how changes in water resources affect rice productivity in each area. Vietnam is second only to Thailand in rice exports (FAOSTAT, 2007) and 80% to 85% of the rice exported from Vietnam is produced in the Mekong Delta (Nguyen et al., 2004b). Within a global context, given that Vietnam kept 13.8% of global exports in 2003, approximately 11% of those were produced in the Mekong Delta in Vietnam. The high productivity of the Mekong Delta is a consequence of the perennial temperate climate, abundant water resources and organic materials transported by the Mekong and Bassac rivers (Fig. 18; Estellès et al., 2002). The expansion in the areas under rice cultivation has largely been possible due to the influence of these two major rivers. Hoanh et al. (2003) projected future hydrological cycles and food productivity for the lower Mekong River basin for the period 2010 to 2039. Their findings indicate that the maximum and minimum river flows into the Mekong Delta during the rainy and dry season would change by −9% to +1% and −7% to −33%, respectively, with the range in an average monthly river flows being −18% to 0%. This decreased river flow during the flood season would reduce the scale of flooding, and consequently, the supply of organic material to the paddy fields. Furthermore, the decreased river flow in the dry season would provide less fresh water for diluting the influx of salinity, resulting in expansion the areas affected by salinity in parts of the delta near the coast as well as a decrease in the yields of the dry-season crop (Estellès et al., 2002; Nguyen and Ashim, 2001).

It is important to assess the impact of water resource changes in the Mekong and Bassac rivers on rice productivity in the near future. Specifically, this chapter examined the general relationship between seasonal flows of the Mekong and Bassac rivers and the rice-cropping systems employed in the delta using remote sensing techniques to determine the characteristics of land use in the delta on a large scale in order to verify the hypothesis of whether rice production in the Mekong Delta is closely related to the seasonal water flow regimes of the Mekong and Bassac rivers.

Specifically, this chapter describes (i) the application of the Wavelet-based Filter for determining Crop Phenology (WFCP; Sakamoto et al., 2005) to multi-temporal satellite data acquired by the Moderate Resolution Imaging Spectroradiometer (MODIS) in 2002 and 2003, and; (ii) an investigation of the relationship between the seasonal change in the flow regime of the Mekong and Bassac rivers and the spatio-temporal distribution of rice phenology and cropping systems.

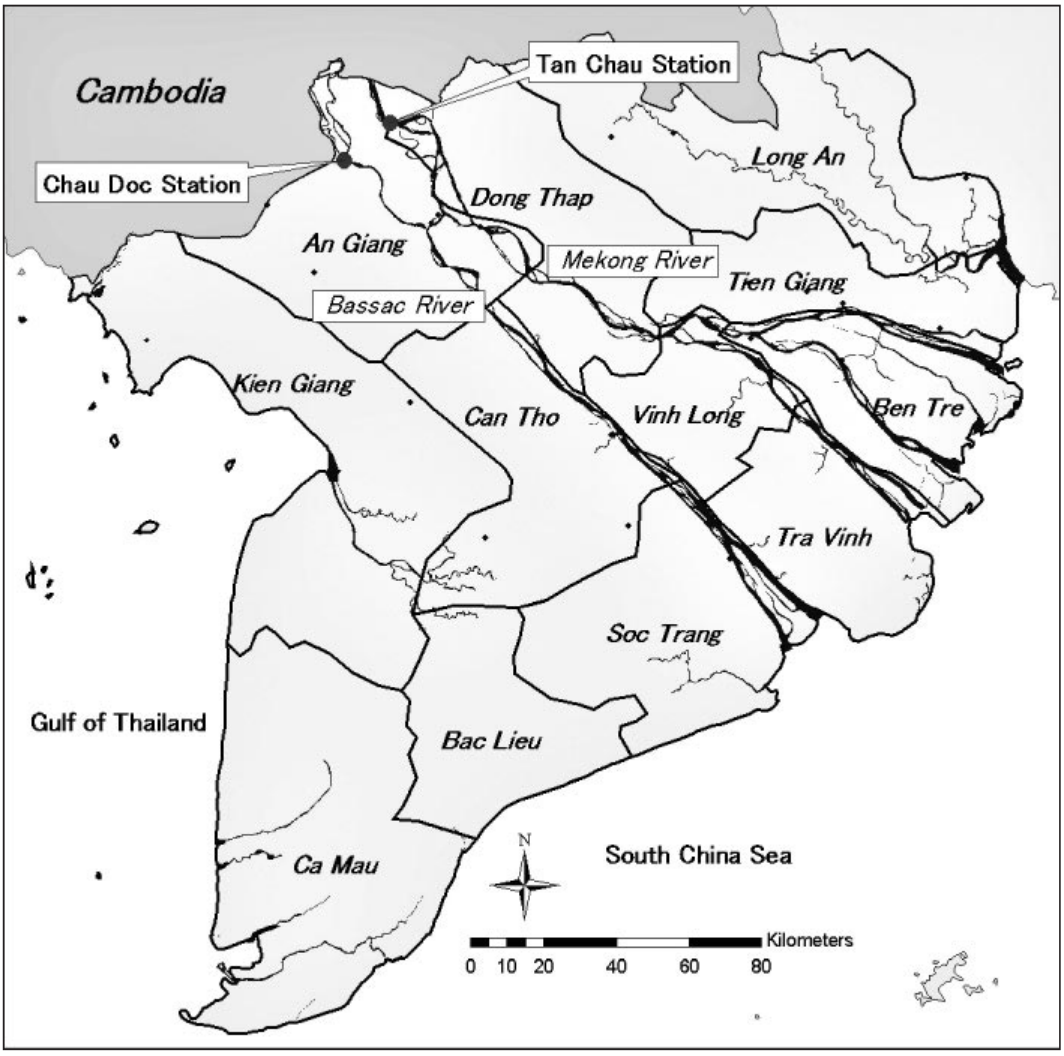

Fig. 18. The Mekong Delta showing provinces and river gauge stations.

3.2. Data and methods

3.2.1. Study area

The study area includes the 12 provinces of the Mekong Delta. These 12 provinces are located at the southernmost edge of Indochina (Lat. 8.5–11° N, Long. 104.5–106.8° E; Fig. 18). The Mekong Delta is a wide, flat plain characterized by extensive by sedimentation at the mouths of the Mekong and Bassac rivers. The total size of the study area is approximately 40,000 km^2, more than 70% of which was dedicated to agriculture in 2002 (Nguyen et al., 2004b). According to the Koppen classification, the climate of Mekong Delta is characteristic of the savanna type. Seasonal changes in precipitation caused by the monsoon divides the year into well defined dry and wet seasons, with average air temperatures in the coldest months being approximately 18℃ and over (An Giang Statistical Office, 2003; FAO, 1999; Fig. 19A) and rain lasting from May to November. Given that precipitation is concentrated in the rainy season, the Mekong and Bassac rivers overflow their banks in the northern part of the delta every year at this time and means that more than one-third of the Mekong Delta is affected by flooding (Hori, 1996). The decrease in precipitation in December marks the beginning of the dry season, which lasts through April. The monthly average water level at Chau Doc and Tan Chau stations (Fig. 19B; An Giang Statistical Office, 2003) show that the average water level of the Mekong and Bassac rivers reach their annual maxima in September or October, and their minima in around April or May. As shown in Fig. 19B, flood volumes in 2000, 2001, and 2002 were larger than previously recorded (Fujii et al., 2003).

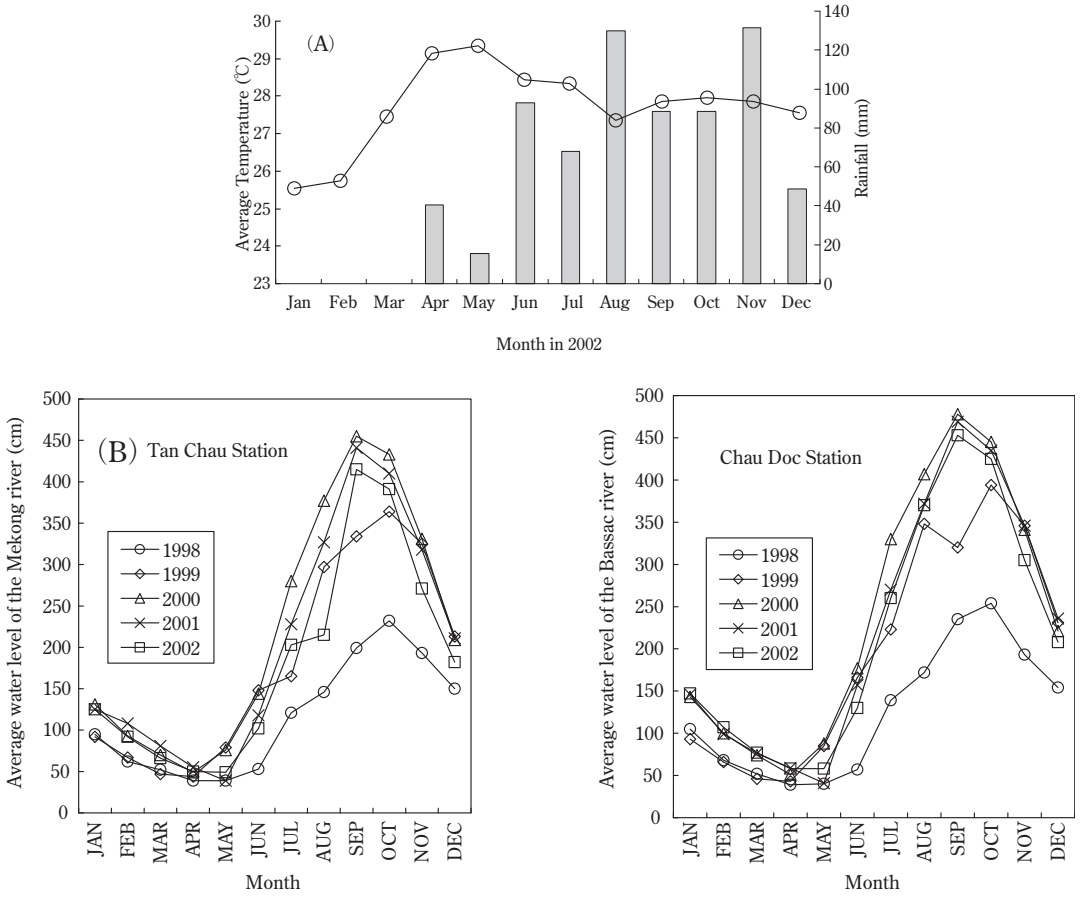

Fig. 19. Hydrometeorological data for An Giang Province. (A) Average monthly air temperature and precipitation in 2002. (B) Average monthly water level at the Chau Doc and Tan Chau stations from 1998 to 2002.

3.2.2. Satellite and land–use data

3.2.2.1. MODIS/Terra data and Landsat ETM+ data

The MODIS data were downloaded from the Earth Observing System Data Gateway (EOS 2007). The MOD09 8–day composite data for 2002 and 2003 was used, "MODIS/TERRA SURFACE REFLECTANCE 8–DAY L3 GLOBAL 500 M SIN GRID V004". The resolution of this data is 500 m and the atmospheric correction has already been done (Vermote and Vermeulen, 1999). MOD09 products give the surface spectral–reflectance for seven bands between the optical and short–wavelength–infrared regions. These composite data include the observation date as the day of year (DOY) for each pixel. LANDSAT 7 ETM+ images (path/row:125/53) were used to validate the details of the estimations of cropping systems. These ETM+ images were acquired on 12 January and 13 February 2002.

3.2.2.2. Land–use data

In this chapter, land–use data for 2002 provided by the Sub–National Institute for Agricultural Planning and Projection of Vietnam (Sub–NIAPP) was used as the ground reference data for paddy fields in the Mekong Delta (Nguyen et al., 2004b; Fig. 20). The land–use data have been updated every a few years and are recorded in vector format. This land–use data was constructed from various data, including LANSAT 7 ETM+ on 7 and 13 February in 2002, the printed map of the agricultural land use in 2002 of 12 provinces at 1/50,000 and 1/100,000 scales produced by the Department of Agriculture and Rural Development of provinces and the Department of Natural Resources and Environment, the digital land use maps in 2000 at 1/250,000 scale of the Ministry of Natural Resources and Environment, and filed survey on May and November in 2002. Then original resolution of the land–use data was 30 m.

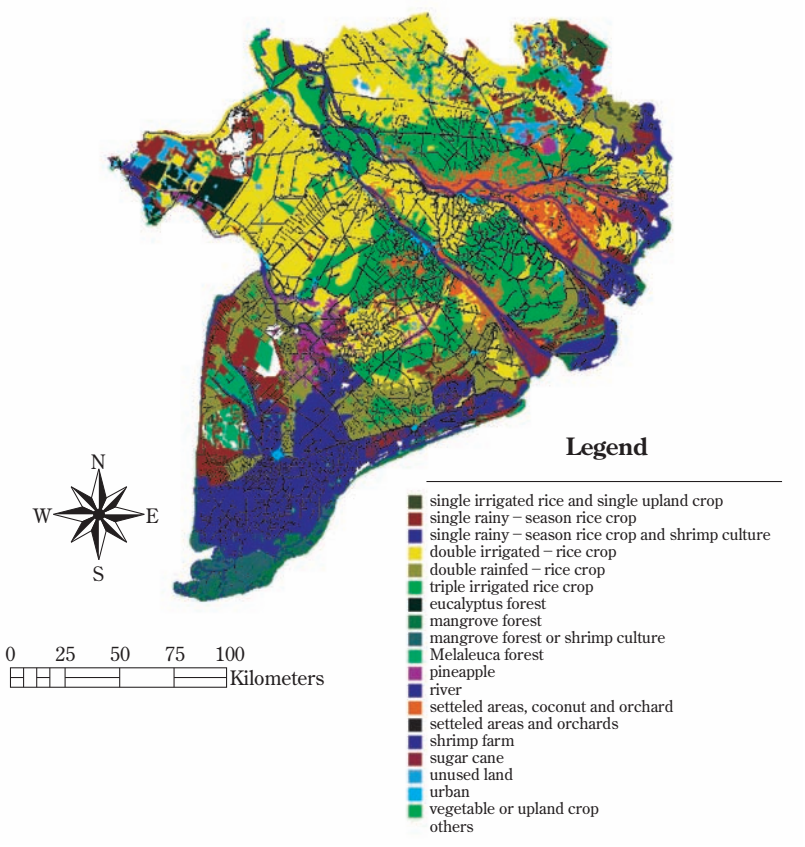

Fig. 20. Land-use map for 2002 (Source:Sub-National Institute for Agricultural Planning and Projection of Vietnam)

The land-use data (Fig. 20) was used to validate the estimated number of rice crops cultivated per year in 2002. The key land-use categories selected for analysis were single irrigated-rice and single upland rice, single rainy-season rice, single rainy-season rice and shrimp culture, double irrigated-rice, double rain-fed rice, and triple irrigated-rice crops. In terms of area, most paddy fields in the Mekong Delta are double irrigated-rice crops (with winter-spring and summer -autumn growing seasons), double rain-fed rice crops (with summer-autumn and rainy season growing seasons), or triple irrigated-rice crops (with spring-summer, summer-autumn and rainy seasons). The areas under double irrigated-rice crops were distributed mainly in the middle and upper regions of the Mekong Delta, while double rain-fed rice crops, shrimp farms and single rainy-season rice crops were located near the coastline. The areas under triple-irrigated crops are distributed along with the Bassac and Mekong rivers and not near the coastal areas. The land-use data in 2002 were converted to raster format with a 500-m resolution to facilitate comparisons with results from the MODIS data.

3.2.3. Wavelet-based filter for evaluating the spatial distribution of Cropping Systems (WFCS)

Most previous studies on the detection of cropping systems in the Mekong Delta employed multi-temporal synthetic-aperture radar data acquired by ERS-2 or RADARSAT, and have classified cropping systems based on temporal changes inferred using the backscattering coefficient for paddy fields (Kurosu et al., 1995; Liew et al., 1998; Pham et al., 2003; Ribbes, 1999). Here, this chapter used MODIS data acquired using an optical sensor designed to cover wide areas and estimated cropping systems and rice phenology by analyzing temporal vegetation index data. The WFCP was applied to the original temporal Enhanced Vegetation Index (EVI) data to smooth the EVI time profile (Sakamoto et al., 2005). The principal advantage of using WFCP is that, should EVI be underestimated due to the cloud cover, it can be interpolated by applying wavelet analysis. Accordingly, by scanning the smoothed time profile of EVI data to find characteristic points

including maximum point and inflection point, it is possible to detect phenological stages of the rice such as the timing of planting, heading and harvesting. After validating the estimated phenological dates against statistical data derived from 30 test sites in Japan, the root mean square errors of the estimated phenological dates were:12.1 days for the date of planting, 9.0 days for the date of heading, 10.6 days for the date of harvesting, and 11.0 days for the growing period. Consequently, by detecting the phenological dates of paddy fields on an annual basis we considered it possible to evaluate the spatio–temporal distribution of rice phonological patterns and their associated annual changes in the Mekong Delta. While development of this approach formed the basis of a previous chapter for detecting the crop phenology using MODIS data and its validation with statistical data in Japan (Sakamoto et al., 2005), this is the first time that WFCP has been applied to reveal the nature of a cropping system in an area the size of the Mekong Delta.

WFCP consists of a three–step process, (1) prescription of multi–temporal MODIS data, (2) filtering EVI time–series data by wavelet analysis, and (3) detecting the peaks on the smoothed EVI time profile to determine the rice–heading date. In procedure (1), the EVI time–series data are calculated. Any EVI data affected by the thick clouds is removed using the reflectance of band 3; data with band 3 reflectance values exceeding 10% are treated as missing values. Subsequent to determining the spectral qualities, the EVI data are arranged by observational date. The missing values between the observed data are substituted with dummy data calculated by linear interpolation. In the second procedure (2), the discrete wavelet transform is applied to the regulated EVI data and high frequency noise components are removed from the time–series data. A smoothed EVI profile is reconstructed through the inverse discrete wavelet transform. In the final step of the procedure (3), the rice heading dates are detected by identifying the maximum points along the smoothed EVI profile. The smoothed EVI time profile obtained by applying the WFCP is considered to represent the reflectance of the daily rice growth with minimal effects from clouds.

When using the WFCP in the Mekong Delta, two parameters was adjusted from those used in the previous chapter in Japan (Sakamoto et al., 2005). The first adjustment affected the threshold for regulating the spatial resolution of target pixels in the prescription of the MODIS data (procedure (1)). This was necessary because the spatial resolution of each pixel in the raw data differed depending on the sensor zenith angle. Sakamoto et al. (2005) used sensor zenith angle data to select only those pixels that had a real spatial resolution of less than 750 m. In Japan, given that the size of most agricultural parcels is small relative to the 500–m resolution of the satellite data, such parcels were irregularly distributed especially in the mountainous area. If applied in environments such as Japan, the spatial resolution of target pixels needs to be restricted as EVI calculated with a board sensor zenith angle will be associated with strong neighbor effects. The Mekong Delta is characterized by the occurrence of thick cloud cover during the rainy season. If the same parameters as those employed in Japan were used for regulating the pixel resolution, then the number of available data during the rainy season would be dramatically decreased in the Mekong Delta as would the accuracy of the WFCP for detecting rice phenology. Consequently, a threshold was not applied for regulating the spatial resolution in this chapter. Instead, it was assumed that the seasonal changes in EVI relative to rice growth would be adequately detected. Given that the distribution of land use in the Mekong Delta is relatively similar and more uniform, combined with the fact that the paddy fields are considerably larger compared to those of Japan, it was not necessary to regulate the spatial resolution of the target pixels in the Mekong Delta.

In addition, the threshold for noise rejection in the EVI time–series data was also altered in this chapter (procedure (2)). Generally, the duration of growth of paddy rice cultivated in Japan is 130 to 160 days (Ministry of Agriculture, 2003), whereas short–duration rice varieties (80 to 110 days) are widely cultivated in the Mekong Delta (Minh and Kawaguchi, 2002; Nguyen, 2000). It is therefore necessary to retain shorter period elements in the smoothed EVI time profile after noise removal so that the technique can be to account for the short–duration rice variety planted in the Mekong Delta. Thus, those frequency components with time cycles less than 32 days were eliminated as these were considered noise components. The mother wavelet used in this chapter (Coiflet 4) was the same as that applied in the previous chapter where its application resulted in the best performance for determining rice phenology (Sakamoto et al., 2005). This

improved method based on WFCP was named as a Wavelet based Filter for evaluating the spatial distribution of Cropping Systems (WFCS).

3.2.4. Number of rice crops cultivated per year and heading dates in study area

Rice changes its growth phase from the vegetative growth stage to the reproductive growth stage on reaching heading date when the leaves begin to whither and die. According to timeseries data for spectral reflectance from paddy fields (Shibayama and Akiyama, 1989), maximum NDVI values are obtained around the heading date. Therefore, a smoothed EVI time profile on paddy field data was employed as the local maximal point would correspond to each heading date. The heading date of Japanese rice can be estimated with a root mean square error of about 9.0 days detecting maximum point from the smoothed EVI time profile (Sakamoto et al., 2005).

However, because double and triple rice-cropping systems are employed on a wide scale in the Mekong Delta, it is difficult to determine the occurrence of the heading date using only the maximum values on the smoothed EVI time profile in the study area. Consequently, several methods had to be employed to determine the occurrence heading time, the first of which involved selecting those local maximal points with values greater than 0.4. In addition, if the interval between the two probable dates was less than 60 days, it could be possible that the two probable heading dates were misclassified due to the anomalous EVI data around the true heading date. If the EVI data around the true heading date was low and the data was not removed in the prescription of multi-temporal MODIS data, the signature of the smoothed time profile around the heading date would be revealed as two humps. Given that the growing period of rice cultivated in the Mekong Delta should be longer than 80 days, an interval of 60 days between two probable heading dates is unrealistic in terms of rice-growing periods. Therefore, the date midway between those two dates was adopted as the estimated heading date for empirical purposes. Inaccurate assignments like this may have been caused by the occurrence of low EVIs around the heading date due to cloudy days. Finally, the number of rice crops cultivated per year was then defined by the number of estimated heading dates per year.

3.3. Results and discussion

3.3.1. Number of crops cultivated per year

3.3.1.1. Comparison between the estimated number of rice crops in 2002 and land-use data

The number of crops estimated for 2002 and 2003 in the paddy fields of the study area is shown in Fig. 21. The results include the misclassified fields in which the number of crops per year was more than three. These fields were scattered around settled areas, coconut and orchard areas, or settled areas with orchards (Fig. 20, 21). The overestimation in the number of crops per year may have been due to mixed-pixel effects caused by adjacent land surfaces. The area of these misclassified fields in 2002 relative to whole paddy fields was less than 2.5%. Consequently, given the small size of the area, the fields showing more than three crops per year were excluded from the comparison of spatial patterns between the ground reference land-use data and the estimated data in Fig. 22. Conversely, the paddy fields in which the number of crops was zero were distributed mainly around the single-crop area depicted in the land-use data (Fig. 20, 22, Table 3), were located near the coastline and were susceptible to increased soil salinities. Therefore, this underestimation of single-cropped areas is related to low EVI values around the maximal points in the smoothed EVI time profile, perhaps owing to poor vegetative growth and vegetation cover.

When the number of crops estimated in 2002 and the land-use data for 2002 were compared (Fig. 22, Table 3), areas identified as triple-cropped areas in the land-use data were rarely classified as single-cropped areas. On the other hand, those identified as single-cropped areas in the land-use data were rarely classified as triple-cropped areas. Such areas accounted for 0.1% and 1.1% of the total paddy fields, respectively.

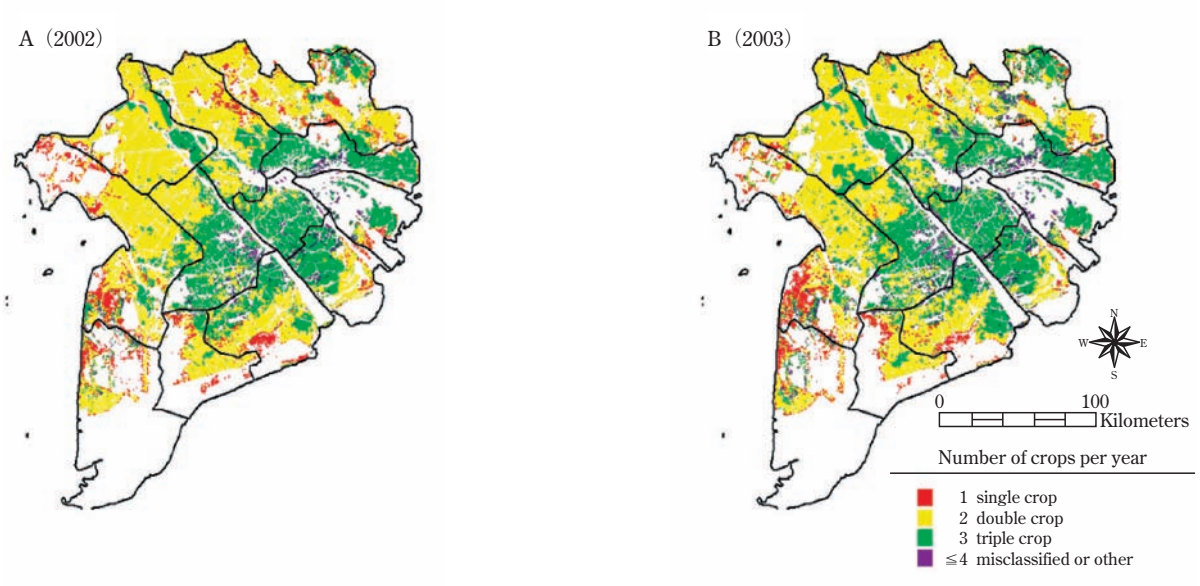

Fig. 21. Estimated number of crops per year in 2002 and 2003

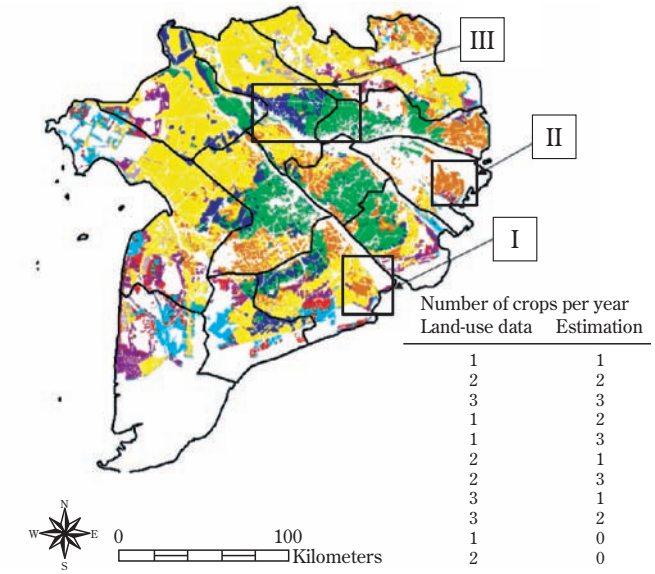

Fig. 22. Comparison of the number of crops per year between the estimate for 2002 and the reference land-use data

Table 3. Confusion matrix of the number of crops per year between the amount estimated in 2002 and the land-use data.

		Land-use data					Pixel count
		0	1	2	3	≧4	
Estimate for 2002	1	27.2（%）	25.0	38.0	7.8	1.9	13,857
	2	2.4	5.9	70.0	20.0	1.6	58,422
	3	0.2	0.4	26.8	67.5	5.1	23,025

From the smoothed EVI time profile, approximately 5.5% of all paddy fields that were overestimated as double-cropped areas were classified single-cropped area in the land-use data. Furthermore, approximately 12.3% of the areas overestimated as triple-cropped area, were classified as double-cropped area in the land-use data. Because the heading dates were defined by the peak EVI values, values of more than 0.4, consideration of the interval between the heading dates, 60 days for restricting overestimation, it is highly unlikely that these entire areas were extracted based on overestimations of the number of crops per year. It is also unlikely that these observations could be attributed to anomalous disadvantageous observation conditions, rather, these observations indicate that the actual number of crops each year was more than that identified in the land-use data. For example, a large part of region I（Fig. 22）, classified as being double-cropped based on the land-use data, was estimated as triple-cropped in 2002 from the smoothed EVI time profile. This finding of this region was further confirmed using LANDSAT ETM+images（Fig. 23B, C）.

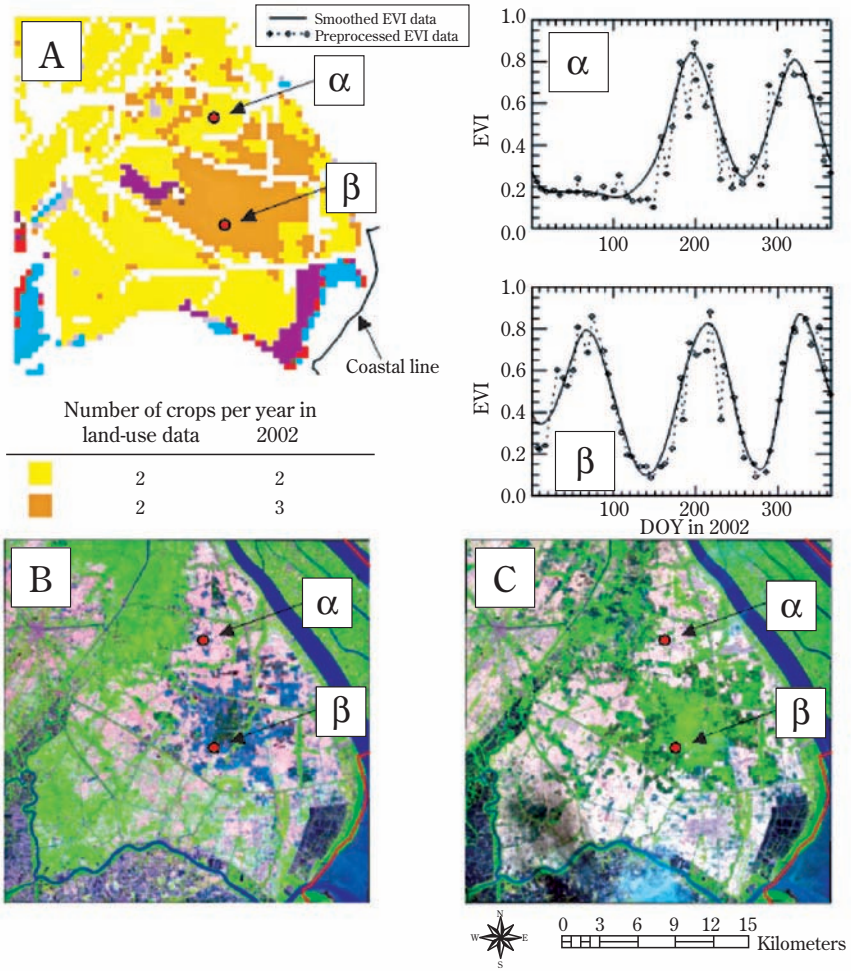

Fig. 23. Validation of the overestimated number of crops in 2002 for the eastern Soc Trang Province. (A) Comparison of the number of crops per year between the reference land-use data and the number estimated from the smoothed EVI time profile in 2002. (B) Landsat ETM+ image (R : G : B = Band 5 : Band 4 : Band 3) for 12 January 2002. (C) Landsat ETM+ image for 13 February 2002. Temporal EVI data profiles of pixels α and β are shown in the upper right.

The target area was located 5 to 20 km inland in the eastern part of Soc Trang Province (Fig. 18, 23) where coastal areas are affected by salinity intrusion every dry season. Particularly in April or May, a large amount of saline water intrudes into the aquifer from the sea and becomes mixed with the irrigation water, thus inhibiting rice growth in the dry season (Tuong et al., 2003). Therefore, dry-season cropping is impossible in such fields without countermeasures against salinity intrusion, including for example, the use of water sluices or other measures for salt removal (Estellès et al., 2002). For example, as seen in the smoothed EVI time profile (Fig. 23), the area around pixel α was double-cropped; that is, no crops were growing in March and April. Conversely, the area colored orange in Fig. 23A, which includes pixel β, was estimated as a triple-cropped area from the smoothed EVI time profile, but is shown as a double-cropped area in the land-use data. In the Landsat ETM+ false color images of the same region (12 January 2002 and 13 February 2002), the land surface indicated by pixel β (Fig. 23) was covered by water in January but was covered by vegetation in February. Therefore, it can be assumed that rice cultivation was performed in the dry-season, from March to April in 2002, and it is surmised that salinity control measures may have been applied in this area. The same interpretation applies to region II (Fig. 22) in the eastern coastal area of Tien Giang Province (Fig. 18) that was triple-cropped in 2002, including dry-season cropping from March through April. Such coastal triple-cropped areas, which were not noted on the land-use data, can therefore be identified by analysis of multi-temporal MODIS data.

On the other hand, from the multi-temporal MODIS data, approximately 3.6% of all paddy fields were underestimated as single-cropped areas, and were instead classified as double cropped areas in the land-use data. In addition, approximately 6.5% were underestimated as double-cropped areas and were classified as triple-cropped areas in the land -use data. The reason for this underestimation was because the peak EVI value at the local maximal point was below 0.4 and was due to aspects such as poor vegetation growth, disadvantageous observation conditions and a mixed-pixel effect. For example, in comparison with the land-use data, the number of crops in region III (Fig. 22) was underestimated as double-cropped areas. The estimated number of crops in 2002 and the MODIS color image of the rainy season (DOY 297 -304 in 2002, R:G:B=Band 6:Band 2:Band 1) in this area are shown in Fig. 24. Pixel γ (Fig. 24) was classified as a triple-cropped area in the land-use data, but was underestimated as a double-cropped area from the smoothed EVI time profile, whereas pixel δ (Fig. 24) was classified as a triple-cropped area by both the land-use data and our estimated results. The smoothed EVI time profiles for the two pixels are also shown in Fig. 24. The area around pixel γ (Fig. 24B) was covered with vegetation, and, at around the same time (DOY 297-304), a local maximal point appeared in the smoothed EVI time profile for pixel γ. Therefore, a triple crop system was probably used in this region. However, this third crop was not detected because the EVI value at the third peak was less than 0.4. Though a lower EVI threshold would facilitate detection of this third crop with a low peak EVI value, it would increase the risk of misidentifying minute fluctuations caused by residual noise as valid data.

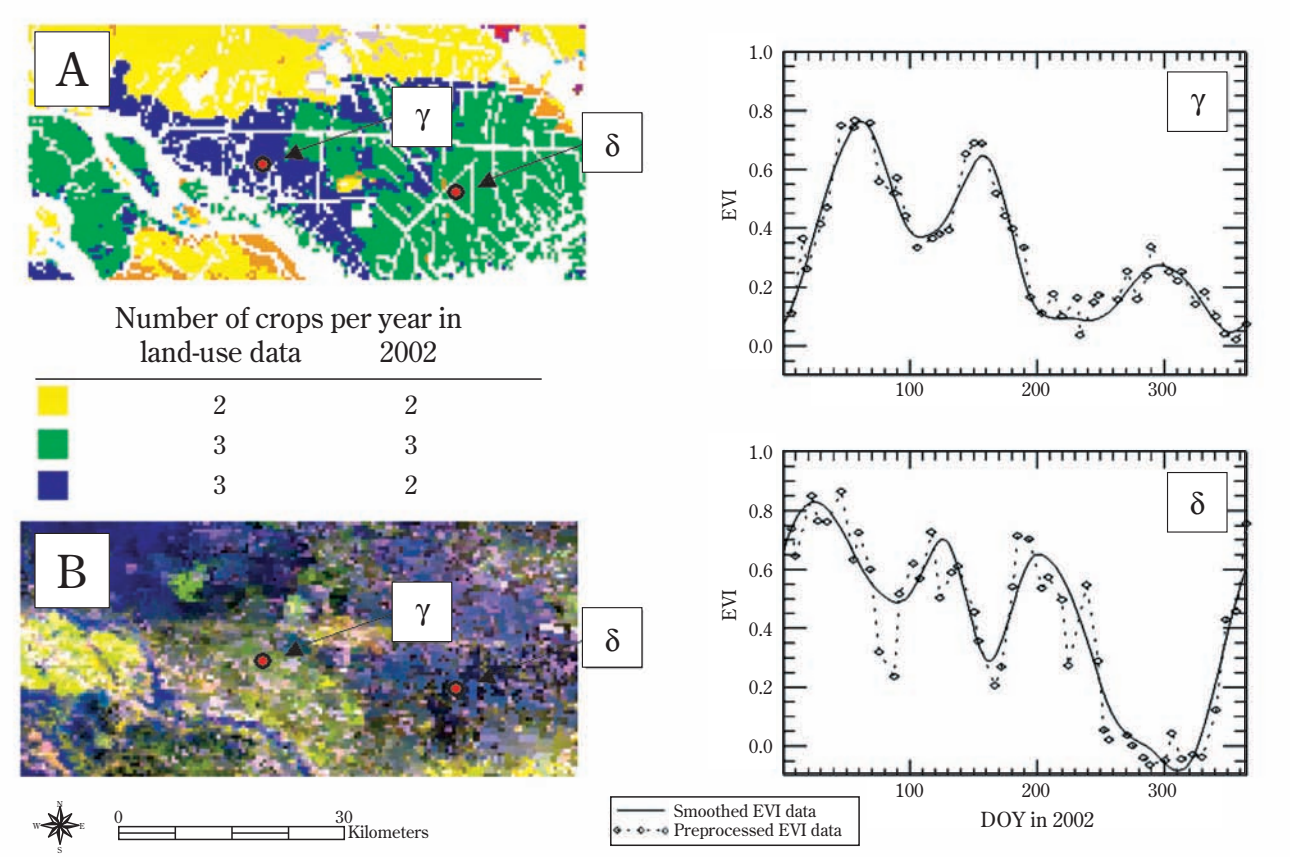

Fig. 24. Validation of the underestimated number of crops in 2002 in eastern Dong Thap Province. (A) Comparison of the number of crops per year between the reference land-use data and the number estimated from the smoothed EVI time profile in 2002. (B) MODIS false-color image (R : G : B = Band 6 : Band 2 : Band 1) acquired on DOY 297-304 in 2002. The temporal EVI data for pixels γ and δ are shown on the right.

3.3.1.2. Change in the number of rice crops cultivated per year from 2002 to 2003

A comparison of the number of crops in 2002 and 2003 (Fig. 25, Table 4) shows that the rice-cropping system changed in some areas from being a double-crop system to triple-crop system and vice versa. For example, region IV (Fig. 25) was classified as a triple-crop system in 2002, but changed to a double-crop system in 2003. For identifying the causes of these changes in crop-system, the smoothed EVI profiles in 2002 and 2003 was extracted, and these yearly changes were compared with the statistical land-use data in region ε; Hong Dan district in Bac Lieu Province, and in region ζ; Thanh Tri district in Soc Trang province (Table 5, Bac Lieu Statistical Office, 2003; 2005; Soc Trang Statistical Office, 2003; 2005). The average daily EVI data in the areas where the crop system changed from triple crop to double crop were calculated in regions ε and ζ, respectively and are shown in Fig. 26. The time profile of the EVI data for region ε in 2003 shows three marked peaks, however, the average EVI values of the second and third peaks in 2003 were lower than that observed in 2002. In region ζ, the yearly change in the EVI time profile was completely different than that obtained for region ε. Though the second crop was performed from April to June and the third crop was performed from August to October in 2002, a peak in EVI values during April to October in 2003 only appeared once. The growing season of the second crop in 2003 is likely to have occurred from May to September. Referring to the statistical land use data (Table 5), the area of summer-autumn paddies and rainy-season paddies in region (decreased by -51%, -15%, respectively between 2002 and 2003. In addition, the surface area of ponds for aquaculture increased by +47%. In region ζ, the area of summer -autumn paddies and rainy-season paddies were observed to decrease by -11% and -90%, respectively and the surface area of water for aquaculture increased by +21%. With regard to the region ε, the reason why the cropping system was changed from triple crop to double crop would be related to the land use change from rice cultivation to aquaculture and the corresponding mix-pixel effects. Therefore, the lower peak value of the smoothed EVI data for the second and third crops in 2003 was caused by the decline in the estimated number of crops per year in the region ε. In region ζ, it appears that the crop system and growing season were intentionally rescheduled because the area dedicated to rainy-season paddies in the Thanh Tri district was considerably reduced.

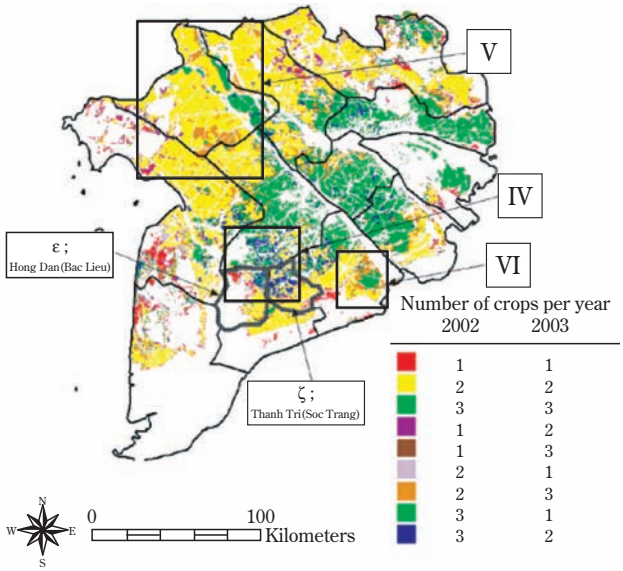

Fig. 25. Comparison of the estimated number of crops per year between 2002 and 2003.

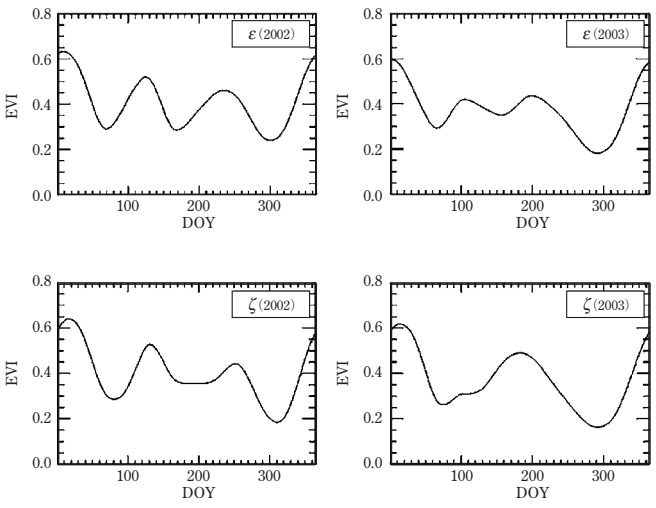

Fig. 26. Average daily EVI data in areas where the number of crops per year decreased from three in 2002 to two in 2003 in the regions ε and ζ shown in Fig. 25.

Table 4. Confusion matrix of the number of crops per year between the amount estimated in 2002 and 2003.

		Estimate for 2003					Pixel count
		0	1	2	3	≧4	
Estimate for 2002	1	73.5（%）	17.7	7.0	1.5	0.2	5230
	2	14.8	37.5	39.1	7.3	1.3	6998
	3	0.7	4.3	79.1	14.6	1.2	52,365
	≧4	0.1	0.7	13.4	78.7	7.1	28,336
		0.0	0.5	6.7	49.3	43.5	2375

Table 5. Sown paddy area and area dedicated to aquaculture from 2001 to 2003（thousands Ha）.

District	land－use	2001	2002	2003
Region ε	Spring paddy	9.5	9.5	13
(Hong Dan district in Bac Lieu province)	Summer－autumn paddy	16	21	10
	Rainy－season paddy	14	15	13
	Aquaculture	4.1	8.7	13
Region ζ	Spring paddy	30	36	37
(Thanh Tri district in Soc Tran province)	Summer－autumn paddy	40	42	38
	Rainy－season paddy	7.2	8.5	0.87
	Aquaculture	1.3	1.9	2.3

Tuong et al.（2003）monitored electrical conductivity at 14 sites and mapped the 7 dS m^{-1} isohalines for February from 1994 to 2000 in Bac Lieu Province. Our region ε is located in the northern part of their study site. The Vietnamese government has built 10 large sluices and numerous smaller ones to protect paddy fields from saline intrusion since 1994. Consequently, the area affected by the salinity intrusion has gradually decreased from the eastern to the western parts of the region（Tuong et al., 2003）. Tidal intrusion has been pushed back from the eastern to the western parts of the region using fresh water channeled from the Bassac River and this study regions e and z are located about 50–60 km from the Bassac River. It is considered likely that these regions are very sensitive to the intrusion of saline water from the sea or shrimp fields in the dry season. In addition to this environmental condition, which is a great risk to rice production in the dry season, the land–use change from rice cultivation to aquaculture is likely due to the decrease in the price of rice associated with a general increase in rice production in the whole Mekong Delta. From the point of agricultural management, it would therefore be reasonable for farmers to expand their activities into aquaculture rather than to intensify rice cultivation in areas that are vulnerable to the intrusion of saline water.

In regions V and VI（Fig. 25）, double–cropped areas in 2002 changed to triple–cropped areas in 2003. In the MODIS color images for 2002 and 2003 for region V（Fig. 27）, the smoothed EVI time profiles for pixels η and θ（Fig. 28A）show that these areas were flooded during the flood season（DOY 241–304）in 2002. However, rainy–season paddy was planted in areas around pixels η and θ during the same time in 2003（Fig. 28B）. One possible reason for this change is that Vietnam government maintains a dike and cannel system for flood control（Kazama et al., 2002）. The dikes enclosing the paddy fields prevent flooding of the dry–season rice before harvesting in the early flood season（Hori, 1996; Nguyen, 2000）and enable the farmers to seed the winter–spring and summer–autumn paddy earlier by using pumps for draining flooded water. After the several flood disasters in 2000, the Ministry of Agriculture urged authorities in the Mekong Delta to identify new ways to prevent flood inundation. The Ministry developed a drainage system and improved the dike systems（Disaster Management Unit, 2004）. These mitigation policies against flood disasters would help farmers to overcome natural flooding and expand the triple–cropped areas in susceptible regions.

Similarly, in the MODIS false color image（Fig. 29）of region VI（Fig. 25, same as region I in Fig. 22）, the orange region shows the areas where the cropping system changed from double–crop system to triple–crop system in 2003. This region forms a circular band around the area of the triple–crop system in 2002（Fig. 29B, C）and suggests that the area, which has implemented countermeasures against salinity intrusion, was expanding into coastal areas.

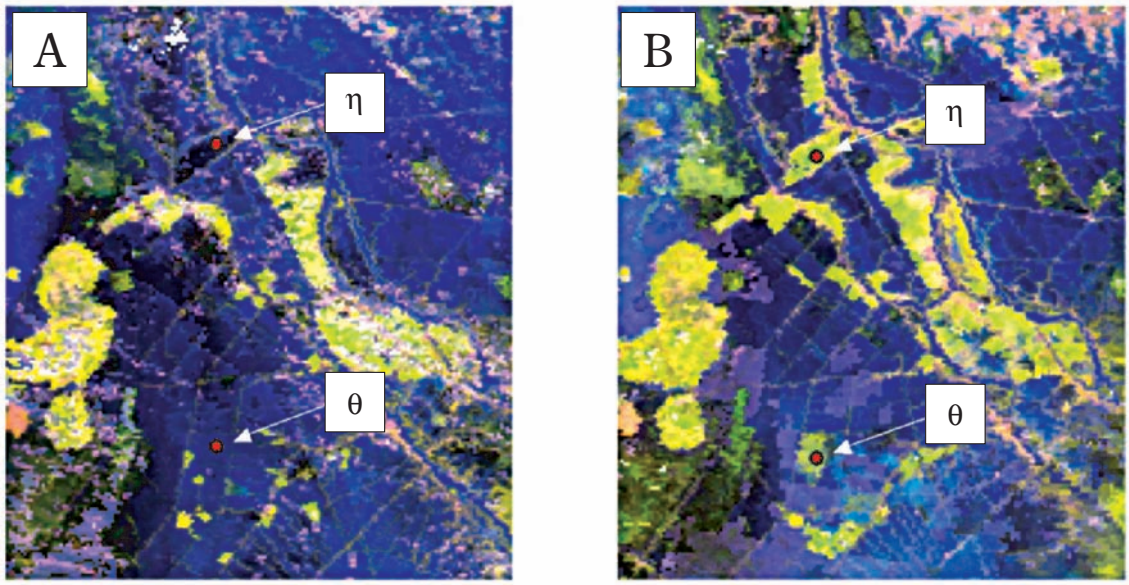

DOY 297-304 in 2002　　DOY 297-304 in 2003

Fig. 27. MODIS false-color images of An Giang Province during the same period (DOY 297-304) in 2002 and 2003. R : G : B = Band 6 : Band 2 : Band 1.

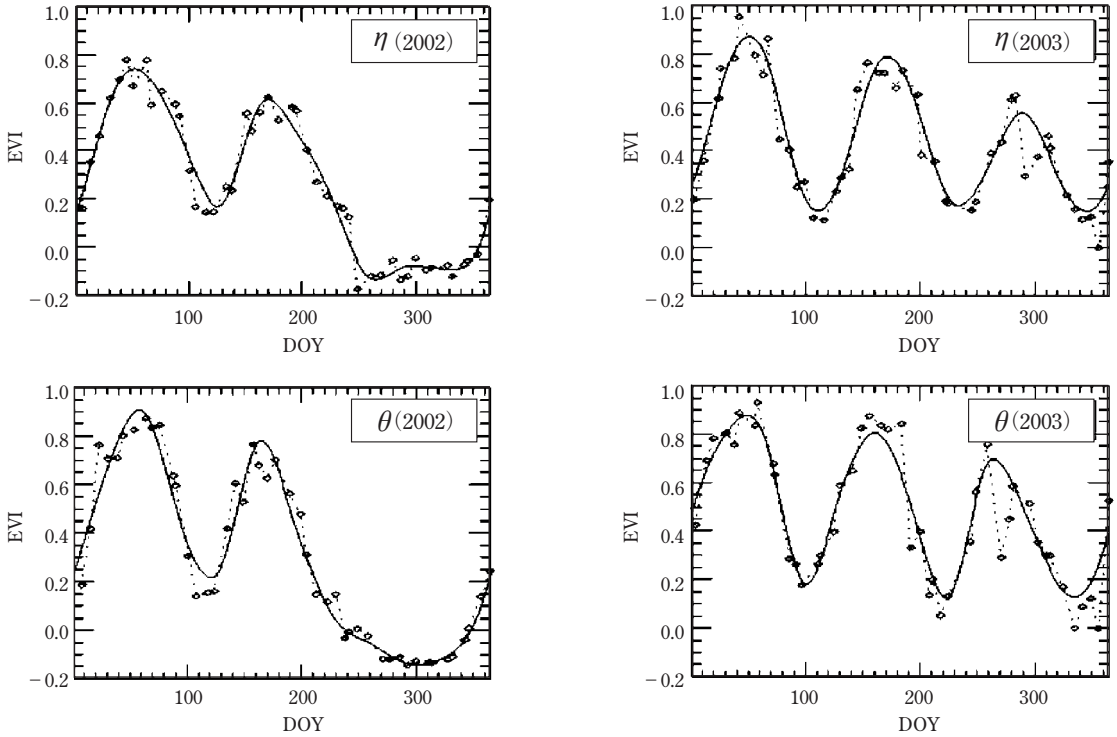

Fig 28. Temporal EVI data for areas in which the cropping system changed from double in 2002 to triple in 2003. The data refer to pixels η and θ in Fig. 27.

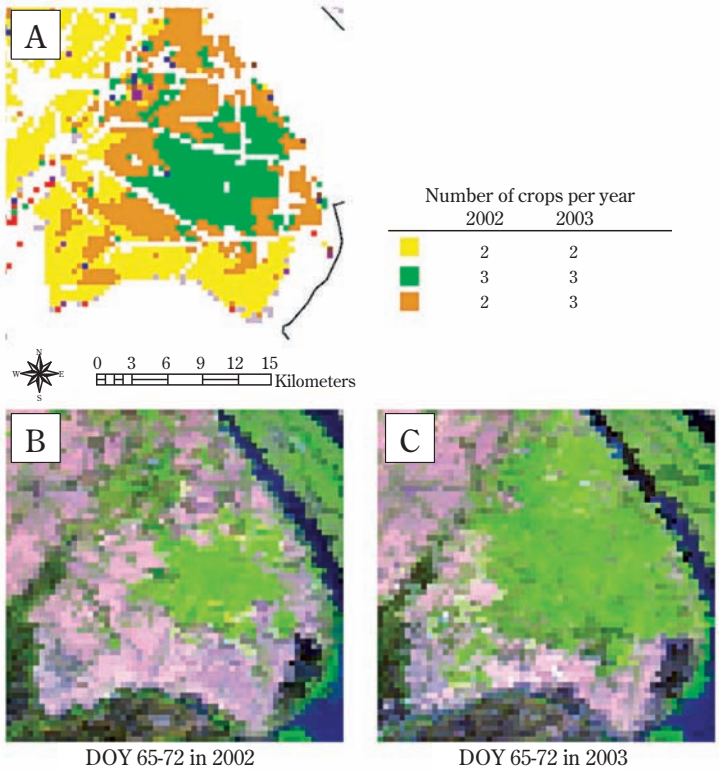

Fig. 29. Comparison of the number of crops per year between 2002 and 2003 in eastern Soc Trang Province (A) and MODIS false-color images for 2002 and 2003 (enlargement of region I in Fig. 5 and region VI in Fig. 8) of the same region. (B) MOIDS 8-day composite image for DOY 65–72 in 2002. (C) MODIS 8-day composite image DOY 65–72 in 2003. R : G : B = Band 6 : Band 2 : Band 1.

3.3.2. Phenological map

3.3.2.1. Spatial distributions of heading dates

The spatial distributions of heading dates in 2002 and 2003 are shown at 3-month intervals and categorized into four periods (Fig. 30). Period 1 is from January to March, period 2 is from April to June, period 3 is from July to September, and period 4 is from October to December. During periods 1 and 2, the heading stage appeared mostly in the upper parts of the Mekong Delta, but rarely in the coastal areas. Periods 1 and 2 corresponded to the dry season. Usually in April or May, runoff from the Bassac and Mekong rivers into the South China Sea are at their lowest. Given that intrusion of saline water due to tidal effects causes the movement of high-density salt into irrigation water, cultivation of rice is difficult in the coastal regions. In contrast, periods 3 and 4 are characterized by the appearance of the heading stage in coastal areas, but rarely in the upper parts of the Mekong Delta. The reason for this is that seasonal floods in periods 3 and 4 inhibit rice cropping in the upper parts of the Mekong Delta and the abundant runoff from the Bassac and Mekong Rivers push back the salinity intrusion. These findings confirm that salinity intrusion and flooding related to seasonal changes in the water flow from the Mekong and Bassac Rivers define the rice-cropping season.

3.3.2.2. Change in the spatial distribution of heading dates between 2002 and 2003

Comparison of heading dates during periods 1 and 2 between 2002 and 2003 (Fig. 30 a, b, e, f) revealed that the heading dates in 2003 in the upper parts of the Mekong Delta were earlier than those in 2002 by approximately 20 to 30 days. This early heading in 2003 would be related to the combination of a reduction in flood runoff in 2002 and government policy. The flood runoff in 2002 was less than that in 2001. Average water levels observed in September at the Chau Doc and Tan Chau Stations decreased by −26 cm (−5.9%) and −16 cm (−3.4%) compared to the previous year, respectively (Fig. 19B), and the water level in 2002 at the Chau Doc station decreased to the 300 cm baseline level 15 days earlier than it

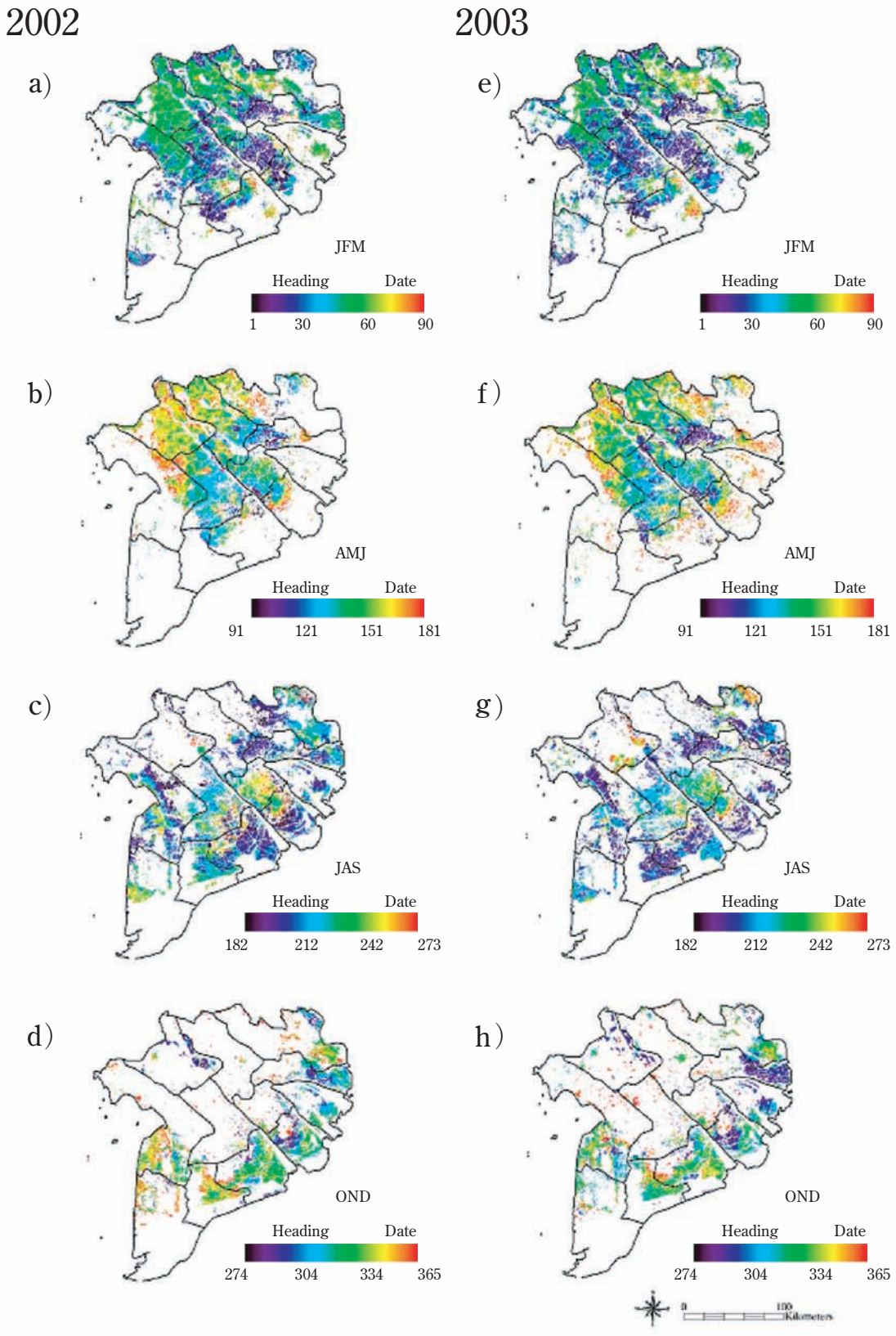

Fig. 30. Spatial distribution of heading dates in 2002 and 2003. The seasonal results for 2002 are shown on the left and those for 2003 on the right:(a, e) period 1 (January, February, March) ; (b, f) period 2 (April, May, June) ; (c, g) period 3 (July, August, September) ; and (d, h) period 4 (October, November, December).

did in 2001 (Fig. 31). Fujii et al. (2003) estimated the flood volume of the study area to the south of the Great Lake up to the Vietnam border using a combination of hydrological information and RADARSAT imagery. Their estimation of flood volume during peak flooding conditions in 2002 was 2500 million m^3 (-16.4%), less than in 2001. According to the annual damage assessment report by the Disaster Management Unit (2004), the extent of flooded and inundated paddy areas decreased from 21 thousand hectares in 2001 to 14 thousand hectares in 2002.

Gnerally, optimal sowing dates depend largely on water availability and it is thought that the best conditions are when the soil is moist but the field is not flooded (Sipaseuth et al., 2001). Consequently, prolonging field inundation increases the moist condition during harvesting of the summer-autumn paddy and causes a delay in planting the winter-spring paddies (Wassmann et al., 2004). Given that flood inundation in 2002 ended earlier and the appropriate time for sowing was also earlier than the previous year, it was possible for farmers to sow the following winter-spring paddy early in 2003. In addition to the good conditions for early sowing in 2003, the government improved rural infrastructure and accelerated crop restructuring to accommodate the floods (Disaster Management Unit, 2004). The government policies encouraged early seedling winter-spring and summer-autumn paddies to facilitate early harvesting before flooding (Neefjes, 2002; Tinh, 2003; UN/ISDR, 2004). The farmers from vulnerable areas in the Dong Thap province sowed the summer-autumn rice crop 15 to 20 days earlier than usual in 2003 (personal communication). Therefore, it was assumed that the decreased amount of flooding and the earlier termination of flood season in 2002 accelerated the drainage of flooded areas before the dry season in 2003. Furthermore, the combination of favorable soil moisture for early sowing combined with the government incentive for early sowing provided farmers with the opportunity to bring the growing season forward. As a result, the earlier heading dates detected during periods 1 and 2 in 2003 would reflect the actual situation of earlier sowing.

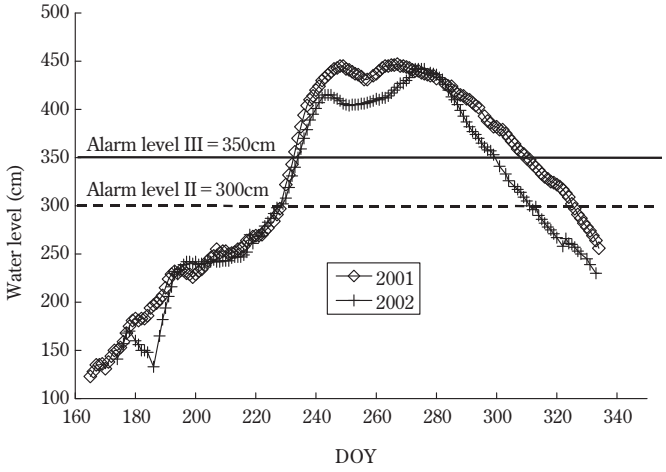

Fig. 31. Time-series rainy-season water-level data at the Chau Doc station in 2001 and 2002.

3.3.3. Rice cropping patterns in the Mekong Delta

Rice cropping patterns were classified according to the estimated heading dates (Fig. 32). Heading dates were classified into 3-month intervals and categorized into four periods. The four periods were same as those depicted in Fig. 30. For example, the legend "1-2" in Fig. 32 means that two heading dates were estimated, one in period 1 (January to March) and one in period 2 (April to June) in this area. The major cropping patterns could be characterized as being of five types : "1-2", "1-2-3", "3-4", "1-3-4", and "1-3". Based on estimations of heading date, these cropping patterns accounted for 79.7% in 2002 and 74.4% in 2003 in the Mekong Delta. These cropping patterns were distributed in a fan-like pattern that spread outward from the headwaters of the Mekong and Bassac rivers in the upper part of the Mekong

Delta to the coastline. The "1–2" double–cropped area was distributed in the inundated areas of the upper part of the delta, the "1–2–3" triple–cropped area in the central parts, and the "3–4" double–cropped area along coastal areas of the Mekong Delta. The "1–3" double–cropped area was distributed in the west and northeast of the "1–2" double–cropped area and the "1–3–4" triple–cropped area occurred in coastal areas or in marginal areas between the "3–4" double–cropped area and the "1–2–3" triple–cropped area.

These characteristics of spatial distributions in rice–cropping patterns provide valuable information about the relationship between the location of a paddy fields and the cropping system that is being used. In the upper part of the Mekong Delta, flooding limits rainy–season cropping (periods 3 and 4), while salinity intrusion in the dry season limits rice cultivation during periods 1 and 2 in coastal areas. The central part of the Mekong Delta is located between these areas and is dominated by alluvial soil without acid and saline constraints. Given that the paddy fields in this region can be irrigated throughout the year and because the risk of inundation is low, the "1–2–3" triple–crop system can be employed here.

The spatial distribution of cropping patterns (Fig. 32) makes it easier to understand the meaning of the land–use changes in regions V and VI in Fig. 25, Fig. 32 shows that the dry–season crop became practicable, and the cropping pattern could be changed from "3–4" to "1–3–4" in region VI. In the southern and northeastern parts of An Giang Province (region V in Fig. 25), rainy–season cropping became possible in some fields, and the cropping pattern tended to change from "1–2" to "1–2–3".

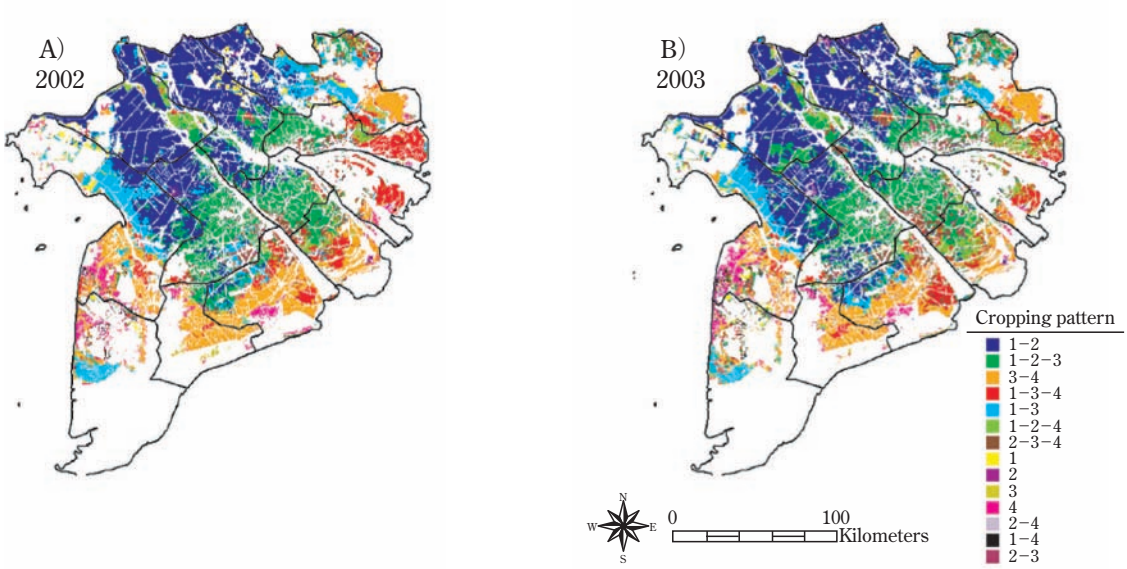

Fig. 32. Spatial distribution of cropping patterns in 2002 (A) and 2003 (B). Cropping patterns are described according to the estimated heading seasons (see Fig. 30). For example, the legend "1–2" means that two heading dates were estimated, one in period 1 (January to March) and another in period 2 (April to June).

3.4. Conclusions

WFCS, which was improved in the basis of WFCP, was applied to multi–temporal MODIS data to accurately estimate the spatio–temporal distribution of rice phenology, the number of rice crops per year, and the cropping patterns in the Mekong Delta. It was succeeded to locate triple–cropped areas that were not identified in the reference land–use data for 2002. These findings suggested that the distribution of cropping pattern depended on whether fields were located in the upper, central, or coastal areas of the Mekong Delta. Furthermore, cropping pattern was also found to be dependent upon the quality and quantity of water resources, variations in which occurred in response to the seasonal fluctuations in

runoff from the Mekong and Bassac rivers. In the upper part of the Mekong Delta, double–crop systems were dominant, with the growing season occurring from January to June to avoid flood damage. Double–crop systems were also prevalent in the coastal areas, however, the growing season in these areas occurred from July to December when salinity intrusion was ameliorated by the high water flows in the Bassac and Mekong rivers. In the central part of the Mekong Delta, triple –crop systems were employed because the threat of flooding and salinity intrusion is low. Comparison of spatial cropping patterns employed between in 2002 and 2003 revealed that the effects of flood damage and salinity intrusion were partially overcome in some areas and that the available area for cultivation was expanded from 2002 to 2003. It was also possible to identify those areas where the number of crops per year was increased from two to three. It was estimated that the heading dates during the first half of 2003 in the upper part of the Mekong Delta occurred approximately 20 to 30 days earlier compared to the first half of 2002. The earlier heading dates observed in 2003 could be attributed to an earlier termination of the flood inundation in 2003 and the promotion by government of earlier sowing in winter–spring or summer–autumn paddies for the purpose of flood mitigation. These results enabled to conclude that the cropping systems and rice phenology in the Mekong Delta are highly dependent upon the seasonal flows of the Mekong and Bassac rivers.

3.5. Summary

Multi–temporal Moderate Resolution Imaging Spectroradiometer（MODIS）data was used to estimate the spatial distribution of heading date and rice–cropping system employed in the Mekong Delta relative to seasonal changes in water resources in 2002 and 2003. Improving a Wavelet–based Filter for determining Crop Phenology（WFCP）, a Wavelet –based Filter for evaluating the spatial distribution of Cropping Systems（WFCS）was developed for the interpretation of MODIS time–series data to determine the spatial distribution of rice phenology and various rice–cropping systems from the seasonal Enhanced Vegetation Index（EVI）data. The findings correspond well the physical characteristics of the cropping system in the Mekong Delta, which have changed over time in response to localized and seasonal changes in water resources. One such example is the double–irrigated rice–cropping system commonly employed in the upper Mekong Delta in the dry season to avoid damage due to the subsequent floods. The shortage of suitable irrigation water and intrusion of saline water in the coastal regions during the dry season has constrained the practice dry–season cropping and has meant that the double– and single–rainfed rice–cropping systems are employed in the rainy season. A triple–irrigated rice–cropping system is used in the central part of the Mekong Delta which is located midway between the flood–prone and salinity intrusion areas. Analysis of annual changes in the rice cropping systems between 2002 and 2003 showed that the triple–cropped rice expanded to the flood– and salinity–intrusion areas. This expansion indicates that the implementation of measures to limit the extent of flooding and salinity intrusion by improved farming technologies and improvements in land management. The heading dates in the upper Mekong Delta in 2003 were earlier than in 2002 by approximately 20 to 30 days. The reasons for this would be due to decreased flood runoff in 2002 compared to 2001, and implementation of government policies regarding early sowing of dry–season crops. Subsequent analysis of the MODIS data confirmed that the spatial distribution of rice–cropping systems was closely related to seasonal changes in river runoff regime in the Mekong Delta.

Chapter IV
Detecting Temporal Changes in the extent of Annual Flooding within the Cambodia and the Vietnamese Mekong Delta from MODIS Time-series Imagery

4.1. Introduction

The annual flooding of the Cambodia and the Vietnamese Mekong Delta (VMD) is one of the primary factors that characterizes the local ecosystem and human activity in the region. For generations, local residents have adapted rice varieties and cropping systems to the seasonal water cycle under the influence of the monsoon regime. Riparian species are likely to have expanded their habitats and diversified in adapting to environmental variation over many years. Annual flooding links isolated water habitats and supplies various freshwater fauna such as fishes and shrimps to paddy fields and ponds. During the rainy season, Tonle Sap Lake and flooded areas along the Mekong River feed a high diversity of aquatic species (Zalinge et al., 2003); these aquatic fauna are a valuable source of protein for local people. Annual flooding also fertilizes agricultural land by spreading fertile sediment and large amounts of pure water as a natural irrigation system, although extreme flood events destroy dwellings and take the lives of many people. The water-flow regime of the Mekong River varies annually depending on rainfall patterns and typhoons. Therefore, understanding the current status of flood inundation in time and space is important in evaluating the relationships between variations in the water regime, local agricultural activity, and ecosystem behavior from a global viewpoint.

Satellite remote sensing is expected to provide powerful techniques for objectively detecting inundated areas. Flood detection is one of the classical themes of remote sensing, and many studies have been undertaken in this field for a variety of purposes, including studies of paddy fields as crop-production areas, analyses of wetlands as a source of greenhouse gas and a habitat for aquatic life and birds, and studies of flooded districts. The approaches used to detect surface water vary widely between the various sensor types used to generate different types of satellite images.

Synthetic Aperture Radar (SAR) is the most effective sensor in detecting flooded areas under cloud cover. Satellite images acquired using RADARSAT, JERS-1, ERS-1/2, and ENVISAT have previously been used to detect inundated areas in a variety of ways (Haruyama and Shida, 2006; Henry et al., 2003; Heremans et al., 2005; Hirose et al., 2001; Ishitsuka et al., 2003; Laugier et al., 1997; Liew et al., 1998; Liu et al., 2002; Wang, 2002; Wang, 2004) When using a pointing device and the selectable sensor mode, RADARSAT and ENVISAT enable the frequent monitoring of the ground surface at a large scale; however, this is not a feasible approach for this chapter because of the limitations of the recurrence period, the performance of the pointing device, and in particular the high cost of data acquisition.

With the aim of detecting variations in surface water time-series data at a regional scale, various case studies have adopted an alternative analytical approach using NOAA/AVHRR, SPOT/Vegetation, SSM/I, and MOS/SMR. Although the spatial resolution is relatively poor (NOAA/AVHRR, SPOT/VEGETATION:ca. 1 km; SSM/I:greater than 13 km; MOS/SMR:greater than 23 km), the greatest benefits of using these sensors is the availability of daily observations because of the wide swath range and the fact that these data are distributed freely via the Internet or at a reasonable cost. In terms of SSM/I and MOS/SMR, time-series variations in flooded areas are observed using a single brightness temperature or various indexes composed of different polarization/frequency brightness temperatures (Jin, 1999; Tanaka et al., 2000; Tanaka et al., 2003; Tanaka et al., 1991). Using this approach, it is possible to determine the spatial distribution of inundated areas and detect seasonal changes, but the resolution is insufficient to enable comparisons with high-resolution land-use data.

The useful spatial resolution (ca. 1km) of NOAA/AVHRR and SPOT/VEGETATION data means that they are commonly employed to detect inundation and temporal changes in the extent of flooded areas (Harris and Mason, 1989; Liu et al., 2002; Xiao et al., 2002b). The use of an optical sensor means that the ground surface is commonly partly obscured by cloud coverage. Bryant and Rainey (2002) used NOAA/AVHRR data with low cloud coverage to discriminate the surface area of a lake using a threshold value of Channel 2. The authors compared seasonal changes in the surface

area of the lake with time-series precipitation data. Sheng and Gong (2001) proposed a ratio of Channel 2 to Channel 1 of NOAA/AVHRR data to enable discrimination between water and land surfaces. They undertook a spatial and temporal assessment of flooding in the Huaihe River Basin, China, during the summer of 1991. Xiao et al. (2002a) evaluated the temporal Normalized Difference Water Index (NDWIVGT) calculated from near-infrared and short-wave infrared data acquired by a SPOT/VEGETATION sensor. The authors concluded that NDWIVGT and NDVI temporal anomalies are efficient in detecting the inundation and transplanting of rice.

Since Terra/MODIS was launched in December 1999, it has become possible to monitor continental-scale inundated areas with a moderate-resolution optical sensor (ca. 250–500 m). MODIS data are also distributed freely throughout the world (EOS 2007). In estimating the extent of paddy fields, Xiao et al. (2005, 2005) identified flooded pixels from the difference between the Land Surface Water Index (LSWI) and Vegetation Indexes (NDVI or EVI). Zhan et al. (2002) applied the Vegetation Cover Conversion Algorithm to two MODIS Level 1B datasets acquired in July and September 2000 and successfully detected inundated areas during the flooding season in Cambodia. Dartmouth Flood Observatory (2006) monitors flood disasters all over the world using MODIS data. Up to 2005, the observatory published an annual inundation map of the Lower Mekong River Flood via the Internet (Anderson et al., 2005).

The aim of this chapter is to create a methodology that can be used to detect spatio-temporal changes in the extent of flood inundation. This methodology includes a wavelet-based filter for the interpolation of missing data and noise reduction within temporal data. Using this methodology, temporal changes in the extent of the inundated region in the Cambodia and the VMD are assessed at a resolution of 500 m from 2000 to 2004.

4.2. Study area

The study area is located in the southern part of Indochina, including parts of Cambodia and Vietnam [Lat. 8.4–13.8 °N, Long. 102.9–107.1 °E] (Fig. 33). The Mekong River is the largest international river in Southeast Asia, with an extensive catchment area of 795,000 km^2. The river flows across six countries from its headwaters to the river mouth [China, Myanmar, Laos, Thailand, Cambodia, and Vietnam]. Cambodia and Vietnam are together home to 28% of the total area of the Mekong River Basin (Mekong River Commission, 2005). The mainstream from the Thailand-Laos border and the Tonle Sap River from Tonle Sap Lake converge around Phnom Penh City before branching into the Mekong and Bassac Rivers a short distance downstream. These rivers then branch off into nine different directions within the VMD, each flowing into the South China Sea. It is worth noting that excessive water volumes flow backward up the Tonle Sap River into Tonle Sap Lake during the wet season (Mekong River Commission, 2005). The area of Tonle Sap Lake during the rainy season is 3–6 times larger than that during the dry season (Zalinge et al., 2003), as water that was stored during the rainy season is discharged into the lower area during the dry season. Tonle Sap Lake therefore plays an important role as a natural regulator in the hydrological environment of the Mekong Delta. The lake moderates flood peaks during the rainy season and provides vital water resources during dry season. Most of study area is classified as savanna climate, with clear seasonal changes in precipitation between the dry and rainy seasons under the influence of the Asian monsoon. The concentration of precipitation during the rainy season (May–October) means that the water level of the Mekong River rises rapidly from May/June, leading to annual flooding along the river. The coincidence of typhoons with the flood season causes serious floods within the Mekong Delta.

4.3. Materials

4.3.1. MODIS/Terra time-series data

MODIS/Terra data are freely distributed through the Earth Observing System Data Gateway (EOS, 2007). The present study involves an analysis of MOD09 8-day composite data acquired from 2000 (after DOY 57) to 2005 (before DOY 56). The product name is "MODIS/TERRA SURFACE REFLECTANCE 8-DAY L3 GLOBAL 500 M SIN GRID V004". The resolution of this product is approximately 500 m, and atmospheric correction has already been carried out

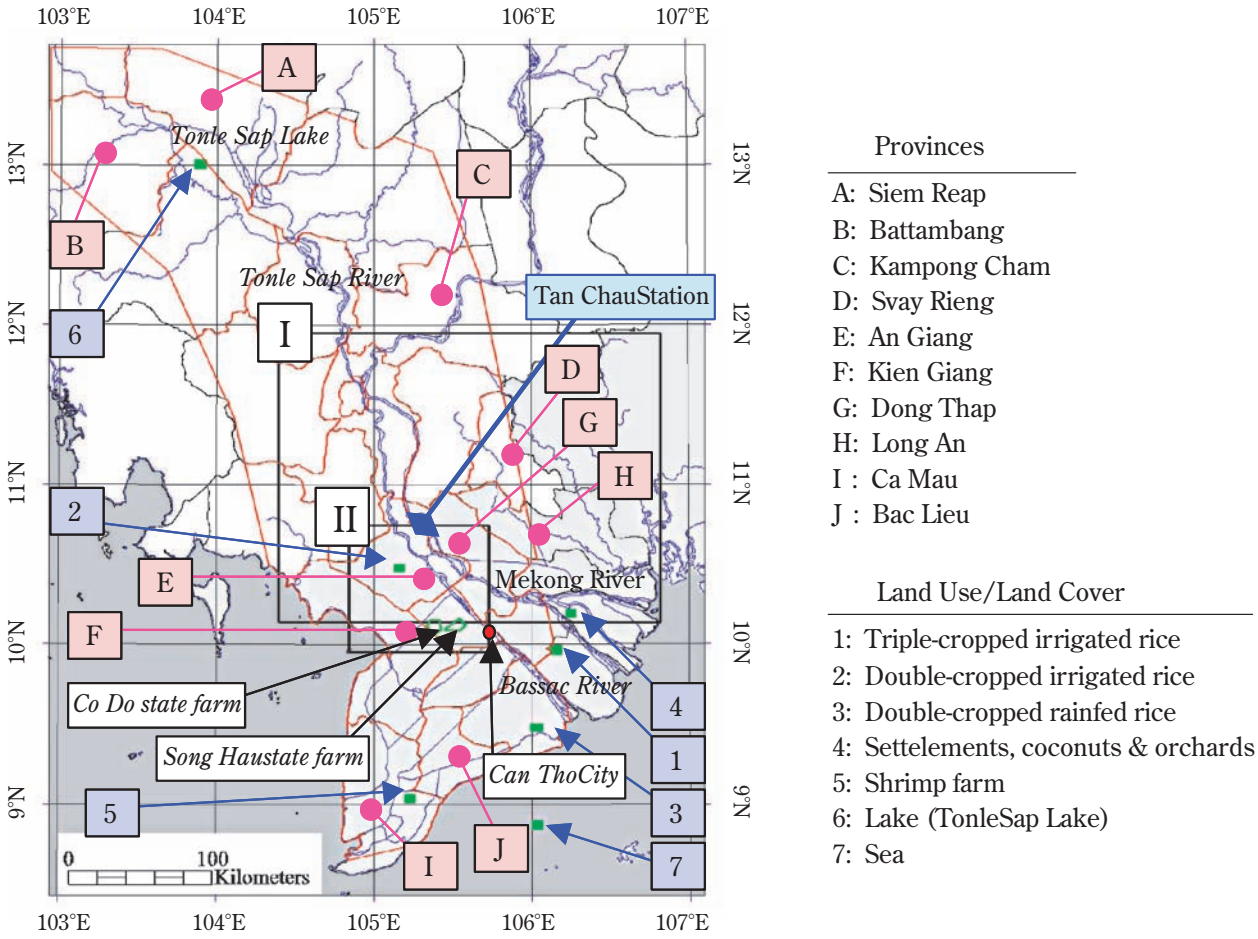

Fig. 33. Location map of the study area. The 24 provinces delineated by red boundaries are used as base units for area comparisons between WFFI and MRC products. Seven kinds of Land Use/Land Cover were selected with reference to the land use map of the Vietnamese Mekong Delta in 2002. Blue lines represent major rivers and canals. Regions I and II, as outlined by black rectangles, are further considered in Figs. 43 and 45, respectively.

(Vermote and Vermeulen, 1999). MOD09 composite products yield the best surface spectral-reflectance data for each 8-day period with the least effect of atmospheric water vapor. The observation date is also recorded for each pixel.

4.3.2. Inundation maps produced by the Mekong River Commission

Inundation maps produced by the Mekong River Commission (herein termed MRC products) are used as a reference to evaluate the estimates derived from MODIS data. The MRC products used in this study are based on Digital Elevation Model (DEM) data, hydrological data, and RADARSAT images acquired on 30th August (DOY 242), 23rd September (DOY 266), and 17th October (DOY 290) 2001 using the ScanSAR Narrow B Mode (Mekong River Commission, 2005). Bearing in mind that C-band microwaves can penetrate cloud cover and easily discriminate open water on the basis of backscatter coefficient data at a high resolution (50 m), it is assumed that the MRC products based on the RADARSAT images reveal the details of the flood distribution at a satisfactory spatial resolution, even under cloud coverage. The inundated areas in the MRC products were aggregated within each grid at 500-m resolution to enable comparisons with results derived from the MODIS data.

4.3.3. Water-surface areas identified from Landsat images

Landsat images were also used for a quantitative comparison with MODIS-derived results. Most of the images listed in Table 6 were downloaded without charge from the Global Land Cover Facility (GLCF, 2006). The transformation to

Table 6. Estimated accuracy of WFFI products relative to the inundation area derived from Landsat images.

ID	path/row	Date (DOY)	RMSE (km^2)	R^2
1	127/51	2001/11/23 (327)	9.9	0.95
2	127/51	2002/1/10 (10)	7.4	0.96
3	126/51	2001/7/11 (192)	11.0	0.88
4	126/52	2001/7/11 (192)	12.2	0.77
5	126/53	2001/1/16 (16)	10.8	0.93
6	125/52	2000/11/6 (311)	6.8	0.97
7	125/53	2000/11/6 (311)	15.2	0.92
8	125/53	2001/12/11 (345)	13.6	0.85
		Total	10.6	0.94

ground reflectance data was performed using ENVI:Remote Sensing Software（ITT Visual Information Solutions）. The objective areas were then classified into three categories using the simple method described below.

1）Non-analysis areas, including cloud cover and cloud shadow, are determined from the blue reflectance value. The cloud-cover areas are derived from the majority analysis（window size:3×3）for pixels which whose blue reflectance（Landsat Band 1）is greater than 0.2. The cloud-shadow areas are then masked by the cloud-coverage areas including 10-pixel buffer zones, where are shifted in the opposite direction from the sun orientation.

2）Water-surface pixels are identified where the Normalized Difference Water Index（NDWI; Rogers and Kearney 2004）is greater than or equal to 0.8. The equation for the NDWI used in this study is as follows:

$$NDWI = \frac{RED - SWIR}{RED + SWIR} \quad \cdots\cdots\cdots\cdots\cdots\cdots \quad (4-1)$$

where RED is the surface reflectance value（0-1; 0.63-0.69 μ m, ETM+ Band 3）and SWIR is in the short-wave infrared band（1.55-1.75 μ m, ETM+ Band 5）.

3）'Not water-surface' pixels are identified where the NDWI is less than 0.8.

After resampling the land-surface map to a grid with a resolution of 25 m using the nearest neighbor method, the areas of these different land-surface types were aggregated within each grid with a resolution of 500 m to conform with the format of the MODIS-derived results.

4.3.4. Daily-averaged water-level data recorded at Tan Chau Station

Fig. 34 shows a time-series of daily-averaged water-level data recorded at Tan Chau Station [Lat. 10.8 °N, Long 105.2 °E] from 2000 to 2004. According to the definition provided by the Hydro-meteorological Center in Vietnam, the scale of flooding in the VMD is classified into the following three categories on the basis of the peak water level recorded at Tan Chau Station:large flood, peak water level higher than 4.5 m; moderate flood, peak water level of 4.0-4.5 m; and small flood, peak water level of less than 4.0 m（Gupta et al., 2004; Long, 2003）. Based on this criterion, large-scale flooding occurred in 2000（peak water level at Tan Chau Station of 5.0 m）, 2001（4.8 m）, and 2002（4.8 m）, while moderate flooding occurred in 2004（4.4 m）. In a strict sense, the scale of flooding in 2003（4.0 m）is also categorized as moderate, although the period for which the water level exceeded 4.0 m was only 2 days; however, the water-flow pattern recorded in 2003 is clearly different from that in other years, and on this basis the scale of flooding in 2003 is classified as small for descriptive purposes in this chapter.

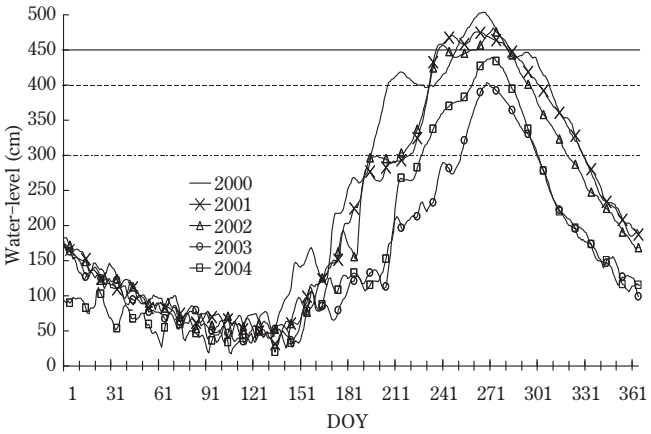

Fig. 34. Daily water-level data recorded at Tan Chau Station [Lat. 10.8°N, Long 105.2°E] from 2000 to 2004.

4.4. Methods

4.4.1. Identification of the water surface using EVI and LSWI

Short-wave infrared (SWIR) is highly sensitive to moisture content in the soil and the vegetation canopy. Various approaches have been reported that make use of the spectroscopic characterization of SWIR against water content (Gao, 1996; Jackson et al., 2004; McFeeters, 1996; Rogers and Kearney, 2004; Tong et al., 2004). Xiao et al. (2002b) showed that NDWIVGT in paddy fields exceeds NDVI derived from SPOT/VEGETATION data for the same period of flooding and rice-planting in eastern Jiangsu Province, China. Xiao et al. (2005, 2006) used anomalies between the Land Surface Water Index (LSWI) and Vegetation Indexes (NDVI or EVI) in an algorithm to estimate the distribution of paddy fields in South China and South and Southeast Asia. In accordance with their approach, a methodology is proposed in this chapter to detect the spatio-temporal flood distribution in the Cambodia and VMD from the smoothed indexes of these differences. The equations used to derive EVI and LSWI from MODIS data are as follows:

$$EVI = 2.5 \times \frac{NIR - RED}{NIR + 6 \times RED - 7.5 \times BLUE + 1} \quad \cdots\cdots (4-2)$$

$$LSWI = \frac{NIR - SWIR}{NIR + SWIR} \quad \cdots\cdots (4-3)$$

where NIR is the surface reflectance value:0-1.0 in the near infrared (841-875 nm, Band 2), RED; (621-670 nm, Band 1), BLUE; and (459-479 nm, Band 3). SWIR is in the short-wave infrared (1628-1652 nm, Band 6).

Sakamoto et al. (2005, 2006) devised a wavelet-based filter to reduce the noise component and interpolate missing information within EVI time-series data. They applied the Wavelet-based Filter for detecting Crop Phenology (WFCP) methodology to successfully detect the heading season in Japanese paddy fields. They also used the same wavelet-based filter in the VMD to classify cropping systems (e.g., double-cropping system in the rainy/dry season, triple-cropping system) and noted regions where the number of crops per year was increased from two to three over the interval 2002 to 2003 (wavelet-based filter for evaluating the spatial distribution of Cropping Systems, WFCS).

In this chapter, the same approach is applied to the EVI and LSWI time-series as well as the differences between the two to reduce the noise component and interpolate missing information. This was undertaken to determine spatio-temporal changes in flood inundation within the Cambodia and the VMD during the period 2000 to 2005.

4.4.2. Wavelet-based filter for detecting spatio-temporal changes in Flood Inundation (WFFI)

A flow-chart of WFFI is shown in Fig. 35. The previous algorithms in the WFCP and WFCS are examined on an annual basis; however, it is possible that the time component in the interpolated data may be overestimated or underestimated to some degree during the year-end period. To address this problem, the algorithm was improved to enable it to calculate the 5-year MODIS data continuously. The beginning data was set to 26th February 2000 (DOY 57) and the end date to 25th February 2005 (DOY 56). The 1st of January was not assigned as the beginning of the MODIS time-series data because MOD09 8-day composite data are unavailable for those days prior to 25th February 2000 and overflowing water usually remains in the upper region of the VMD at this time of year.

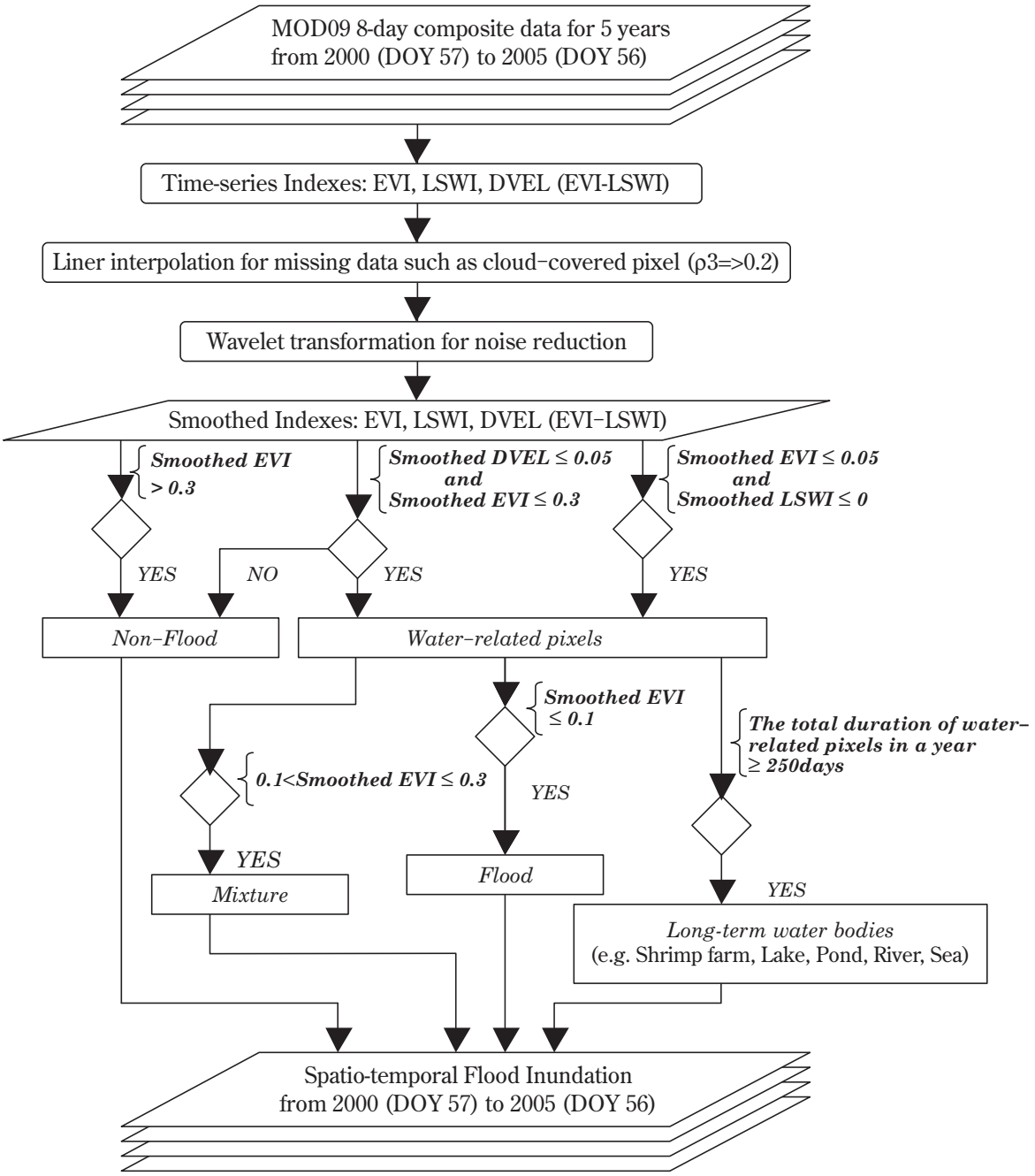

Fig. 35. Flowchart of the workings of the Wavelet-based Filter for detecting the spatio-temporal changes on Flood Inundation (WFFI).

In prescribing the time-series data, cloud-covered pixels are determined based on the Band 3 value. If the blue reflectance is equal to or greater than 0.2 (Thenkabail et al., 2005; Xiao et al., 2006), such pixels are treated as missing observation data and interpolated linearly. As with WFCS (Sakamoto et al., 2006), this chapter did not use the view angle data in the data preprocessing. The coiflet (order=4) was adopted as the mother wavelet to reduce the high-frequency component (frequency less than 32 days) considered to be noise. Fig. 36 shows the domain-averaged smoothed data for EVI, LSWI, and the Difference Value between EVI and LSWI (DVEL) for the seven Land Use/Land Cover types. In accordance with the pioneering method described by Xiao et al. (2005, 2006), DVEL was used in this chapter to discriminate between *Water-related* pixels and *Non-flood* pixels. If the smoothed DVEL is less than 0.05, such pixels are determined to be a *Water-related* pixel; however, as shown in Fig. 36, the smoothed DVEL data for the lake and sea are not always less than 0.05. The high DVEL may reflect low LSWI caused by extremely low reflectance (near 0) of open water in the NIR band. To solve this problem, the following criterion was empirically added to avoid such misclassifications. If the smoothed EVI is less than or equal to 0.05 and the smoothed LSWI is less than or equal to 0, the pixel is determined as a *Water-related* pixel. If the EVI is greater than 0.3, the pixel is categorized as a *Non-flood* pixel.

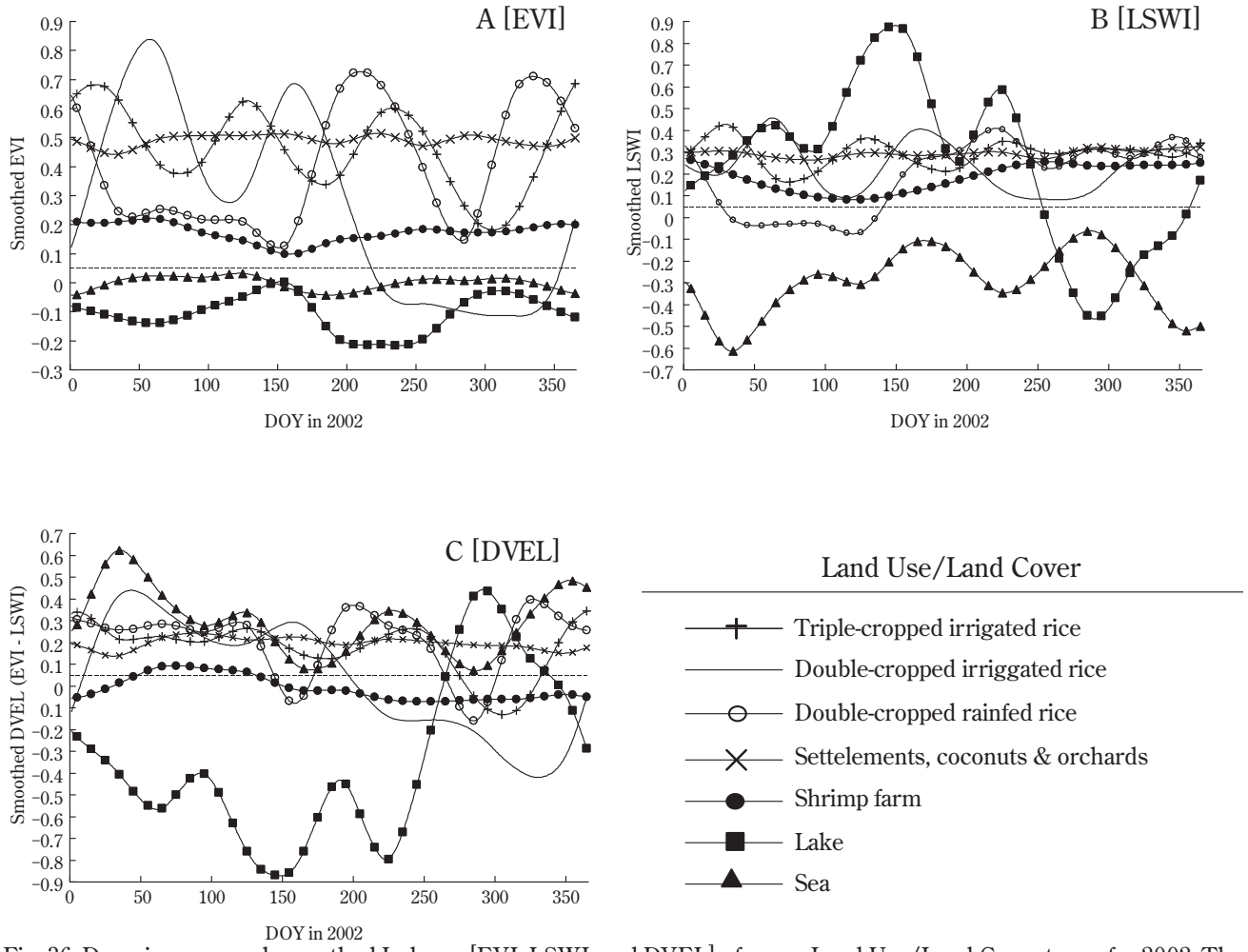

Fig. 36. Domain-averaged smoothed Indexes [EVI, LSWI, and DVEL] of seven Land Use/Land Cover types for 2002. The locations of the seven Land Use/Land Cover areas shown in Fig. 33.

Even if MODIS is superior to NOAA/AVHRR and SPOT/VEGETATION in terms of spatial resolution, it is inevitable that pixels with a resolution of 500 m come under the influence of mixtures of various types of land surfaces, especially when varying the footprint with different view angles. It is concluded that the complicated methodology used to identify sub–pixel components requires enormous computation time when treating a large dataset. There is also no method available to smooth vegetation and water indexes. Thus, *Water–related* pixels were divided into two categories (*Flood* and *Mixture*) based on the following simple method. EVI in homogeneous open–water areas such as large lakes and the sea is generally lower than that in *Mixture* pixels (mix of water, vegetation, and soil coverage). Thus, it is assumed that the smoothed EVI of the *Water–related* pixels can be used as a criterion for discriminating between *Flood* and *Mixture*. If the smoothed EVI was less than or equal to 0.1, the *Water–related* pixels were defined as *Flood* pixels. If the smoothed EVI was greater than 0.1 and less than or equal to 0.3, these pixels were defined as *Mixture* pixels.

Temporal changes in the areal ratio of *Flood* and *Mixture* pixels in the three types of paddy field and shrimp farm (equivalent to triple–cropped irrigate rice, double–cropped irrigated rice, double–cropped rainfed rice, and Shrimp farm shown in Fig. 33, 36) are plotted in Fig. 37. As a result, it would be difficult to detect short–term irrigation water from the smoothed temporal data. The short interval between the continuous cropping seasons of triple– and double–cropped irrigated rice (Fig. 36) means that EVI values are higher because of the mixture effects of residual plants and adjacent pixels. In addition, the cusp of the original data over such a short interval is smoothed to some degree with the noise component in the same way as that during the wavelet–based filter.

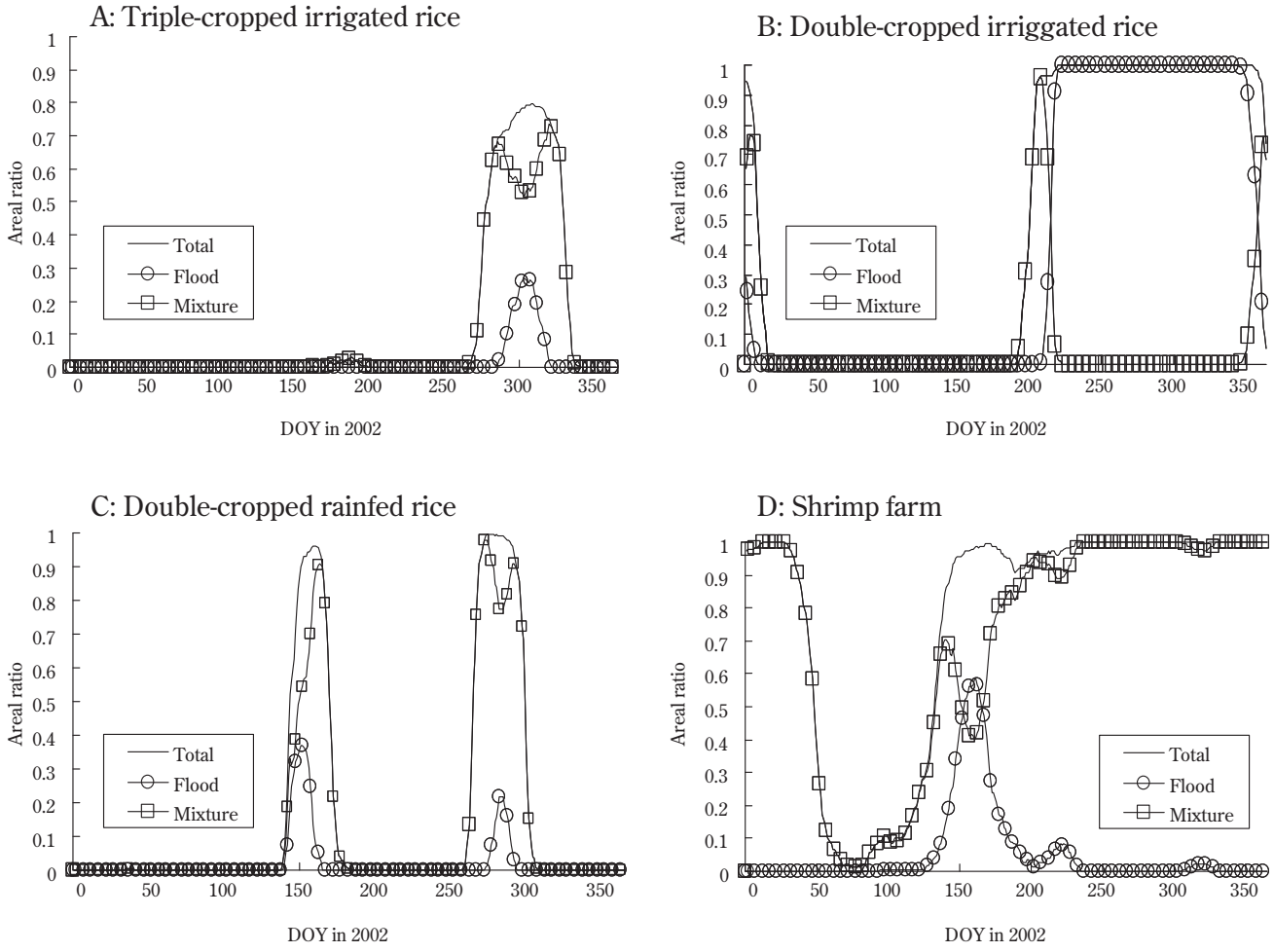

Fig. 37. Temporal changes in the areal ratio of *Flood* and *Mixture* pixels in the three types of paddy fields and shrimp farms. The locations of these areas (Triple–cropped irrigated rice, Double–cropped irrigated rice, Double–cropped rainfed rice, and shrimp farm) are shown in Fig. 33.

In terms of land-based aquaculture, shrimp farms are widely distributed throughout coastal areas. These areas with an extended inundation period (as with rivers, lakes, and the sea) should be discriminated from areas subjected to short-term and seasonal inundation, as this chapter focuses on temporal changes in annual flooding. Therefore, considering that the shrimp-growing period lasts for approximately 3-4 months and farmers grow shrimps twice per year in coastal areas, these areas are empirically defined as follows. If the total number of days as a *Water-related* pixel is grater than or equal to 250 days per year (as measured from 26th February to 25th February of the following year), the pixels are classified as *Long-term water bodies*.

Finally, this proposed methodology is termed the Wavelet based Filter for detecting spatio-temporal changes in Flood Inundation (WFFI), and the inundation map estimated using WFFI is termed the WFFI product.

4.5. Evaluation of the proposed methodology

4.5.1. Comparison of the inundated regions assessed using the WFFI and MRC products

As in the smoothed temporal data of double-cropped irrigated rice in the upper region of the VMD (Fig. 36, 37), the water surface [DOY 197-365] is clearly identified using WFFI. The distribution of inundated regions on the 30th August 2001 (DOY 242) determined using the WFFI and MRC products is shown in Fig. 38A1 and B1, respectively. Because the MRC products are based on RADARSAT data, the inundated region is clearly identified in detail without any cloud-cover effects; however, MRC products were unable to cover the entire objective area because of the limited swath range of RADARSAT. False-color images of MOD09 8-day composite data and daily MOD09 data for the same date are shown in Fig. 38C1 and D1, respectively. The WFFI products, MRC products, and MODIS false-color images for 23rd September and 17th October 2001 are also shown in the same way (Fig. 38A2, A3 [WFFI products], 38B2, B3 [MRC products], 38C2, C3 [MODIS 8-day composite false-color images], and 38D2, D3 [MODIS daily false-color images]).

Compared with daily MOD09 data for the Cambodia and VMD (Fig. 38D1, D2, and D3), the influence of cloud cover is considerably reduced in MOD09 8-day composite data (Fig. 38C1,C2, and C3); however, the unobserved data assigned to the irremovable area of cloud-cover is real, and this poses a substantive problem for the identification of the inundated region using the general methodology.

In the WFFI method, the missing observation data can be interpolated via the wavelet-based filter using available values either side of the missing data. This approach enables an understanding of a wider view of the inundated region without the influence of spatial noise (Fig. 38A1, A2, and A3); however, it should be noted that the estimated timing of the start and end of flood inundation might have a margin of error that is dependent on observation conditions. This situation occurs because the interpolation methodology will never be able to address the large number of missing values resulting from conditions of continuous cloud-cover.

As with the three subsequent MRC products (Fig. 38B1, B2, and B3), the WFFI products (Fig. 38A1, A2, and A3) simultaneously revealed the receding and expanding flood areas over a wide area (e.g., the receding inundated region around the northern part of Kampong Cham and the expanding region of inundation in the VMD). The distribution of *Flood* pixels (blue region) in WFFI products is consistent in principle with the area where the inundation ratio is 100% (red region) in MRC products, with the exception of the northwest of Tonle Sap Lake. The spatial pattern of the *Mixture* pixels (green region) is qualitatively similar to the region where the inundation ratio is less than 100% and moderate (blue to yellow region) in MRC products. Small-scale inundated areas along small tributaries in Cambodia were only partly identified in the WFFI products, and the WFFI overestimated the extent of inundated regions around the Camau Peninsula in Vietnam. These misidentifications may result from mixtures with adjacent pixels probably due to view angles. Thus, when the *Mixture* pixels are used directly for measurement of the inundated area, the estimation contains errors related to location.

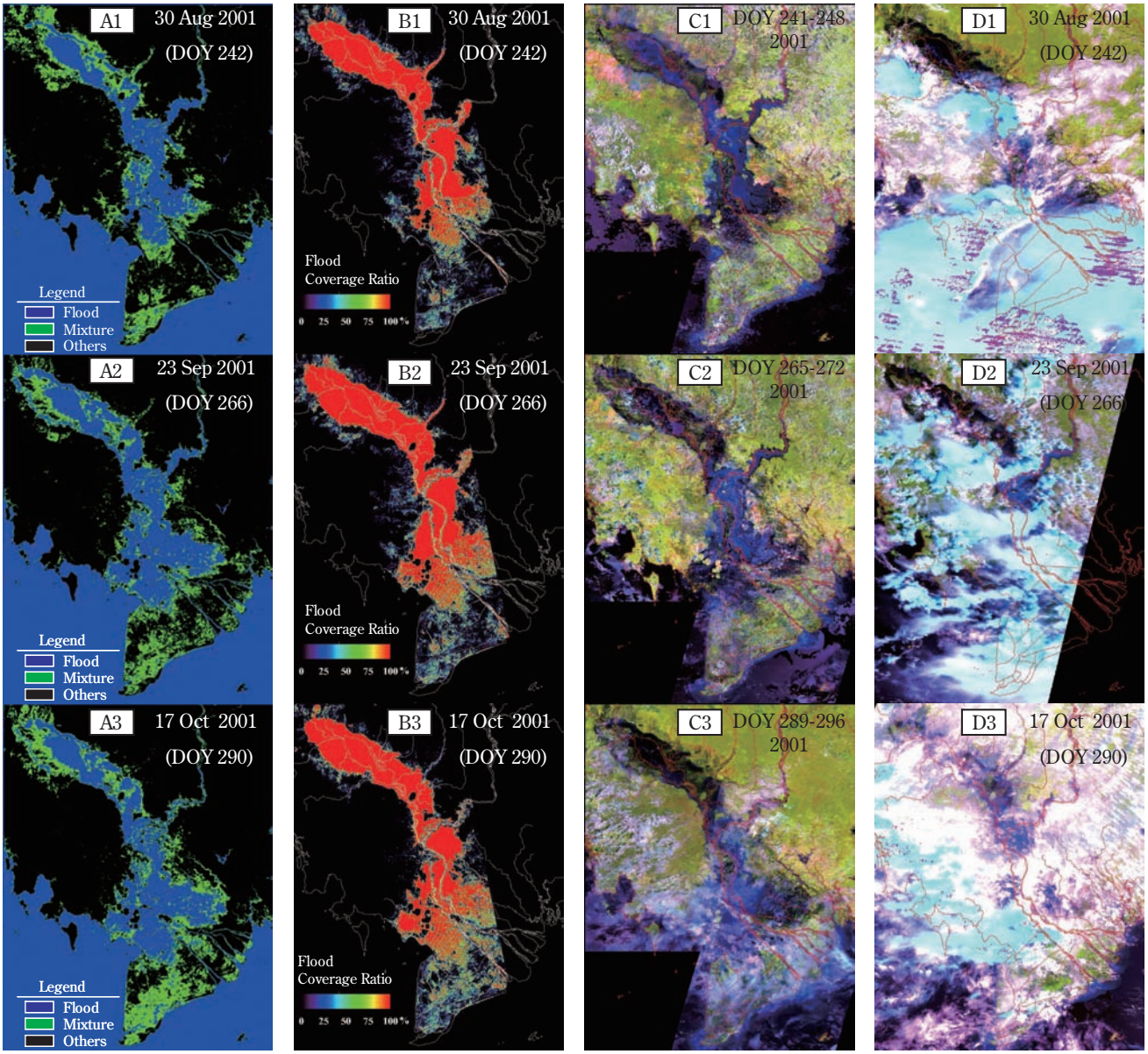

Fig. 38. Spatial comparison of WFFI products, MRC products, and MODIS 8-day composite false-color and daily false-color images for the study area, as shown in Fig. 1. (A1, 2, 3) WFFI products. (B1, 2, 3) MRC products. (C1, 2, 3) MODIS 8-day composite false-color images. (D1, 2, 3) MODIS daily false-color images. R：G：B = Band 6：Band 2：Band 1.

4.5.2. Flooded forests to the northwest of Tonle Sap Lake

Areas of flooded forests/marsh are widely distributed to the northwest of Tonle Sap Lake (Giri et al., 2000; McKenney and Tola, 2002; Xiao et al., 2005). Fujii (2004) attempted to detect the inundated area in this region from RADARSAT data; however, it proved difficult to detect the water surface under flooded forests because of the high backscatter efficiency of C-band radar. The author was able to conclusively determine inundated areas under forests and regions of high vegetation coverage using a combination of water-level data together with DEM data. In terms of MRC products, the inundated region to the northwest of Tonle Sap Lake is broadly uniform despite the presence of vegetation coverage. Thus, these areas may also be spatially interpolated using hydrological data in combination with DEM data. It is even more difficult to detect these inundated regions under high-vegetation coverage using lower-resolution optical sensors such as MODIS. Therefore, it would be difficult to accurately identify the inundated area of flooded forests/marsh in the WFFI products (Fig. 38A, C). The inundated area of flooded forests/marsh was progressively identified as the water level

of Tonle Sap Lake increased (Fig. 38A1, A2, and A3) because plant bodies are gradually submerged as the water level rises; this leads to an increase in the area ratio of the water-surface area to vegetation coverage. For this reason, there may a time lag involved in identifying inundation in flooded forests/marsh areas.

4.5.3. Comparison with MRC products at the province scale

Fig. 39 shows a comparison of the estimated inundated area at the province scale obtained from WFFI and MRC products. The 24 objective regions were defined based on the coverage area of MRC products and administrative boundary data for Vietnam and Cambodia (Fig. 33). When estimating the inundated area in each region, the result was calculated from the total number of *Water-related* pixels. Both *Flood* pixels and *Mixture* pixels were counted in equal number without weighing. In terms of the accuracy of the WFFI products compared to MRC products, low RMSE and a high determination coefficient (n=24) were obtained for the 30th August, 23rd September, and 17th October 2001. The values for these dates are 364 km^2 (RMSE) and 0.91 (R^2), 416 km^2 (RMSE) and 0.89 (R^2), and 443 km^2 (RMSE) and 0.92 (R^2), respectively. Combining these estimates (n=72) for the three different dates, the RMSE and the determination coefficient are 409 km^2 (RMSE) and 0.90 (R^2), respectively. As shown in Fig. 39, the overall inundated area estimated by WFFI products at the province level tends to be overestimated compared to estimates derived from MRC products. There are many *Mixture* pixels, especially in the Kien Giang, Siem Reap, Ca Mau, and Bac Lieu Provinces. It is clear that the inundated areas in these provinces were markedly overestimated. In contrast, the inundated areas for August and September in Battambang Province were considerably underestimated. These errors might reflect underestimates in the area around the flooded forests/marsh as explained in the previous section. It is possible to enhance the estimation accuracy using DEM data or higher-resolution data (Brivio et al., 2002; Wang et al., 2002) and this remains an issue for future studies. Although there is a fundamental overestimation problem resulting from mixed-pixel effects, it can be assumed that temporal WFFI products provide useful criteria for determining annual inundations that are early or late relative to long-term averages.

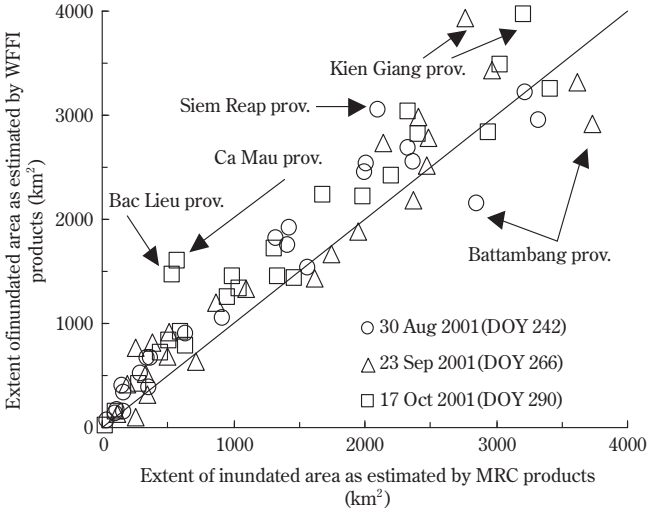

Fig. 39. Comparison of inundated areas predicted by WFFI and MRC products at the province level. Target provinces and regions are delineated by red lines in Fig. 33.

4.5.4. Comparison with Landsat-derived results at the 10-km grid level

The distribution of the water-surface area derived from Landsat images is shown in Fig. 40. In comparing these areas with the area of *Water-related* pixels in WFFI products at the 10-km grid level (Fig. 41), the estimation accuracy of WFFI products is shown in Table. 6. The RMSE vary from 6.8 to 15.2 km^2, and the determination coefficients [R^2]

vary from 0.77 to 0.97. In grids where the inundated area derived from Landsat images is greater than 50 km^2, the WFFI products yielded an overestimate (as in the comparison with MRC products) because of an over–evaluation of *Mixture* pixels. In grids where the inundation area is less than 50 km^2, the inundated area derived from WFFI products is underestimated. This problem occurs because the neighbor–pixel effect makes it difficult to detect small water–surface areas from low–resolution images. Specifically, two Landsat images (ID:3 and 4, path/row:126/51 and 126/52) were acquired at the beginning of the rainy season (July 11 2001). These numerous small water–surface areas led to an overall underestimation of the WFFI products compared with the Landsat–derived results. These results, in combination with the results from the comparison with MRC products, indicate that the WFFI products can be used to roughly measure the flood extent at regional scale.

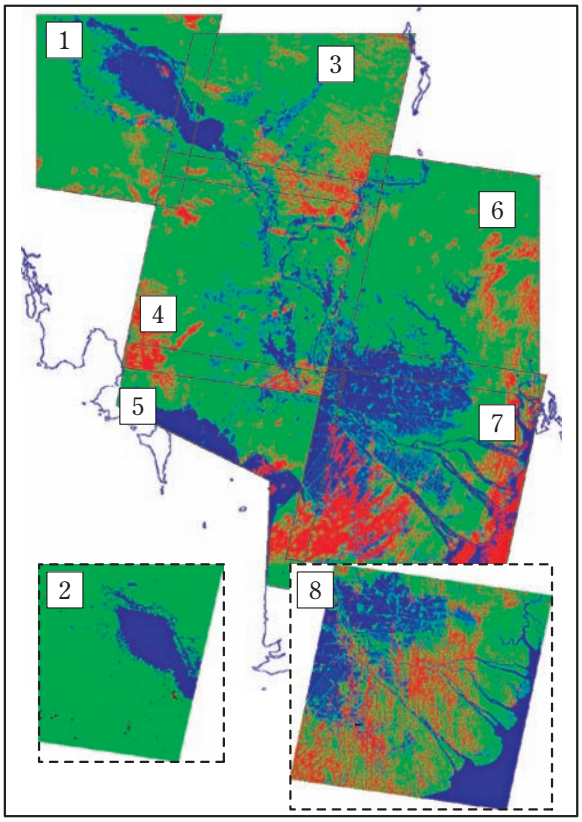

Fig. 40. Distribution of the water–surface area derived from Landsat images. The colors; Blue, Green, and Red indicate the areas of water–surface, not water–surface, and non–analysis respectively. The numbers of the Landsat images are the same as the ID numbers listed in Table 6.

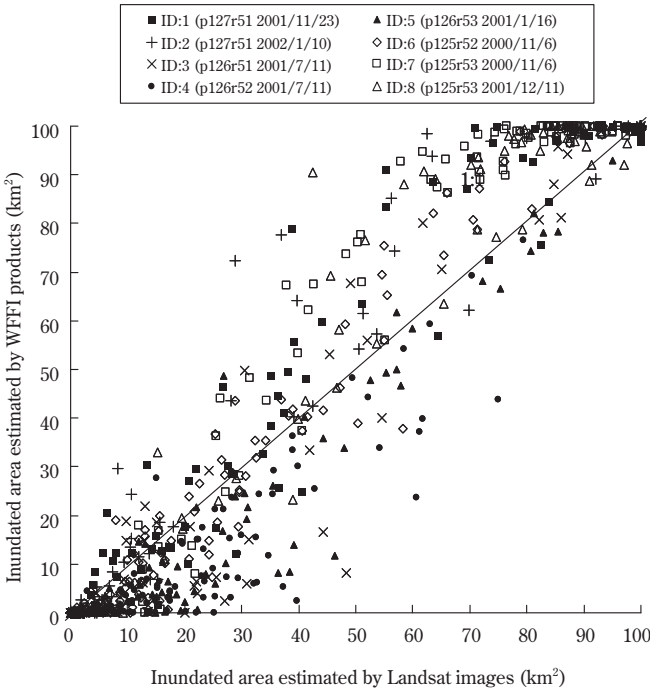

Fig. 41. Comparison of the inundated area at a 10–km grid level between the Landsat–derived results and the WFFI products.

4.6. Findings obtained from temporal WFFI products

4.6.1. Spatio–temporal changes in the extent of annual floods in the Cambodia and VMD from 2000 to 2005

Overlaying multiple images of the inundated region is effective in detecting the maximum extent of the flooded area (Sheng and Gong, 2001). Thus, the WFFI products are expected to be useful in identifying temporal changes in the simultaneous recession and expansion of flood cycles at a regional scale. Maximum flood maps estimated from the time–series WFFI product are shown in Fig. 42. Blue, green, and white colors represent areas of *Flood*, *Mixture*, and *Long–term water bodies*, respectively. Classification of the scale of flooding in the VMD according to the peak water level recorded at Tan Chau Station (Fig. 34) is in good agreement with the area of *Flood* pixels shown in Fig. 42. The area of *Flood* pixels in

2000 is the largest among the years 2000 to 2004, while that in 2003 is the smallest. In additionally, Fig. 43 shows seasonal changes in the extent of the estimated area of *Flood* pixels within Dong Thap and Long An Provinces. The temporal patterns of these inundated areas from 2000 to 2004 are very similar to the water level data recorded at Tan Chau Station (Fig. 34). During the period from July to August [DOY 182–243], the beginning of the inundation cycle was earliest in 2000, followed by 2002, 2001, 2004, and 2003 in order of the total inundated area. In addition, the order of the maximum extent of inundated areas is generally similar to the order of the peak water level, except for a reverse order between 2001 and 2002. During the period from December to January [DOY 335–31], the diminution rate of the inundated area is stable, as is the water-reducing ratio. It is clear that the start dates of the inundation cycles and the scale of flooding in the VMD vary with the amount of inflow water from the upper regions and the start date of the annual flooding season.

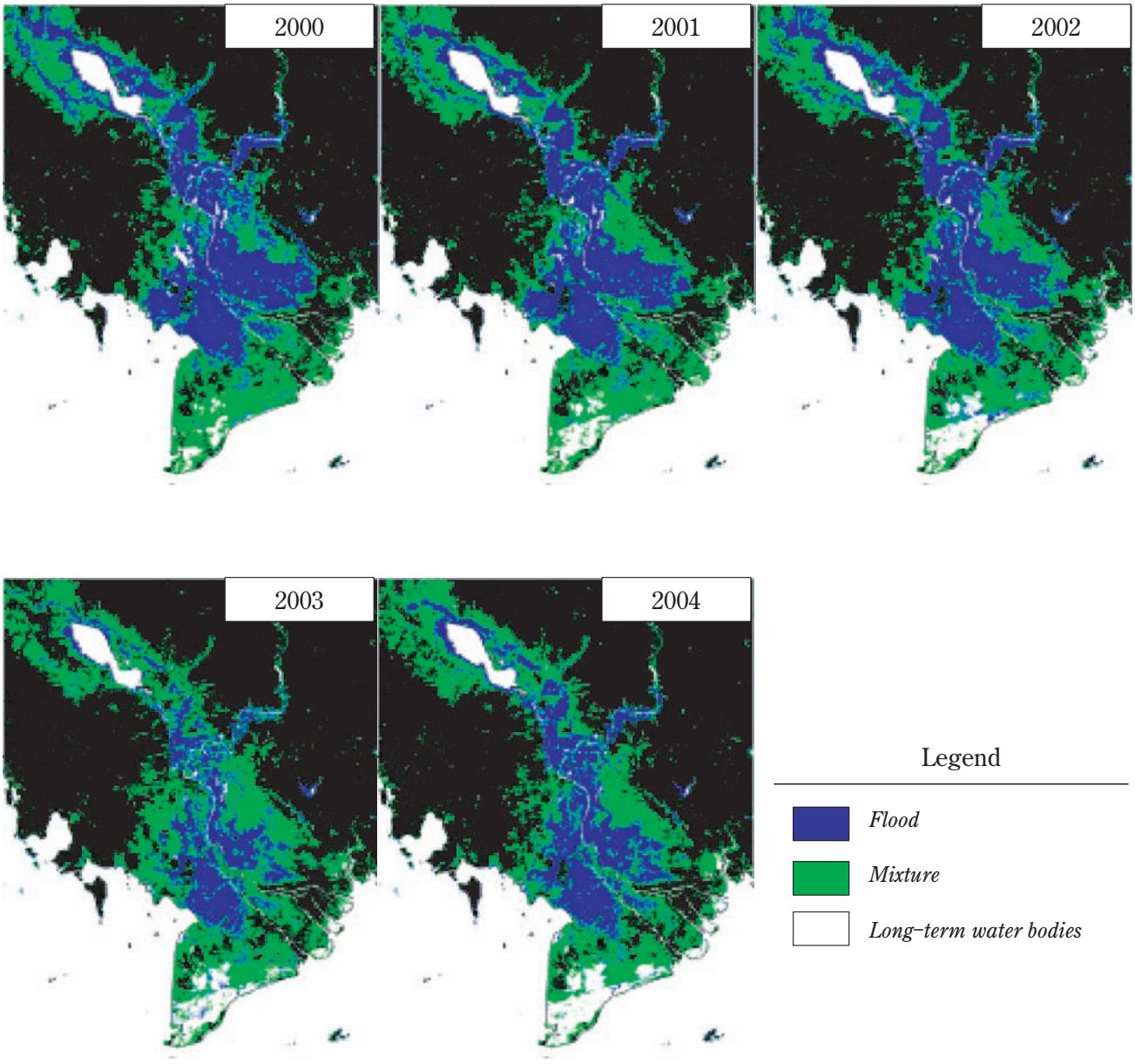

Fig. 42. Maximum estimated extent of the floodplain over the period 2000 to 2004.

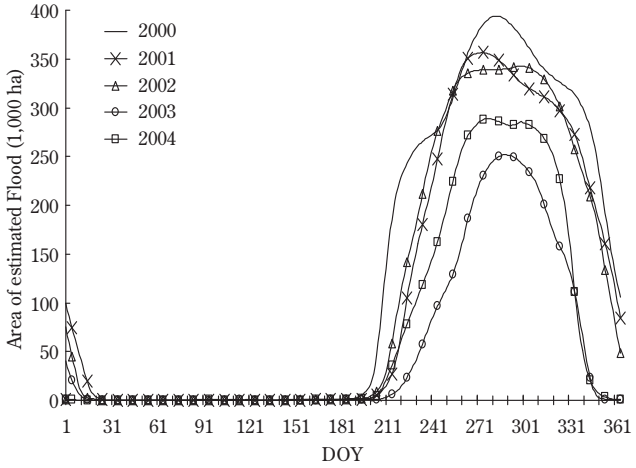

Fig. 43. Seasonal changes in the extent of the estimated area of *Flood* pixels within Dong Thap and Long An Provinces.

Fig. 44 shows the estimated flood area for the 1st day of every month (June [DOY 152] to January [DOY 1] of the following year) from 2000 to 2005. Fig. 45 shows the extent of inundated regions for every tenth day from 1st June to 17th January of the following year. Because of space limitations, the analysis focused on the region around the Vietnam–Cambodia border, including Dong Thap and Long An Provinces (Region I in Fig. 33). As is generally known, the results show that the flood started following a rapid increase in water level from July to August [DOY 182–243] (Fig. 34, 44) and reached its largest extent across the VMD during October and November [DOY 274–334] (Haruyama and Shida, 2006; Wassmann et al., 2004). Upon visualization at moderate spatial resolution (500 m) and high temporal resolution (10 days) (Fig. 45), it is apparent that the spatio–temporal distribution of the inundated area varies from year to year. Temporal changes in the area of inundation within Cambodia in 2002 (Fig. 45) are similar to the estimated progression of flooding based on RADARSAT data (Fujii et al., 2003).

The flood that inundates the Dong Thap Muoi (Plain of Reeds) is mainly caused by floodwater that flows across the Vietnam–Cambodia border. The proportion of floodwater sourced from across the border is estimated to be 88%, with just 12% from the main river and canals (Long, 2003a). Fig. 45 shows the same phenomenon, whereby floodwater is directly sourced not only from the main rivers, but also from the stream of overflowing water that passes through Cambodia. As described by Kazama (2001), the results of the present study indicate that expanding floodwater within the VMD in 2000 intruded into the southern Svay Rieng Province of Cambodia from the northern Long An Province in Vietnam (Fig. 45).

4.6.2. Temporal characteristics of annual floods:Start, end, and duration

The continuous flood period is determined according to the following procedures. 1) The continuous inundation period recorded by *Water–related* pixels (both *Flood* and *Mixture* pixels) is calculated from 5–year *Water–related/Non–Flood* data for each pixel. In this case, the continuous inundation periods include irrigation water in paddy fields. 2) If periods of continuous inundation are identified twice or more in a year, the longer period is taken as the period of annual flood inundation. 3) The duration of annual flood inundation is defined from the start and end dates of annual flood inundation. Fig. 46 shows estimates of the start dates, end dates, and duration of inundation cycles from 2000 to 2004.

The spatial distribution of the start dates varies year by year. The start dates of the largest flood (2000) are mostly earlier than those of the medium–scale flood in 2004 (Fig. 46). For 2001 and 2002, the start dates along the Bassac and Mekong rivers are similar to those for 2004 (see Fig. 46); however, in the marginal region of the floodplain, especially the coastal area near the Gulf of Thailand, the start dates for 2001 and 2002 are much earlier than those for 2004 (Fig. 46, 45 [DOY 242–262]). As for the smallest flood (2003), the start dates along the two main rivers shows similar patterns to those for 2004 (Fig. 46); however, when focusing on the *Flood* pixels in Fig. 45 [DOY 202–232], the timing of the

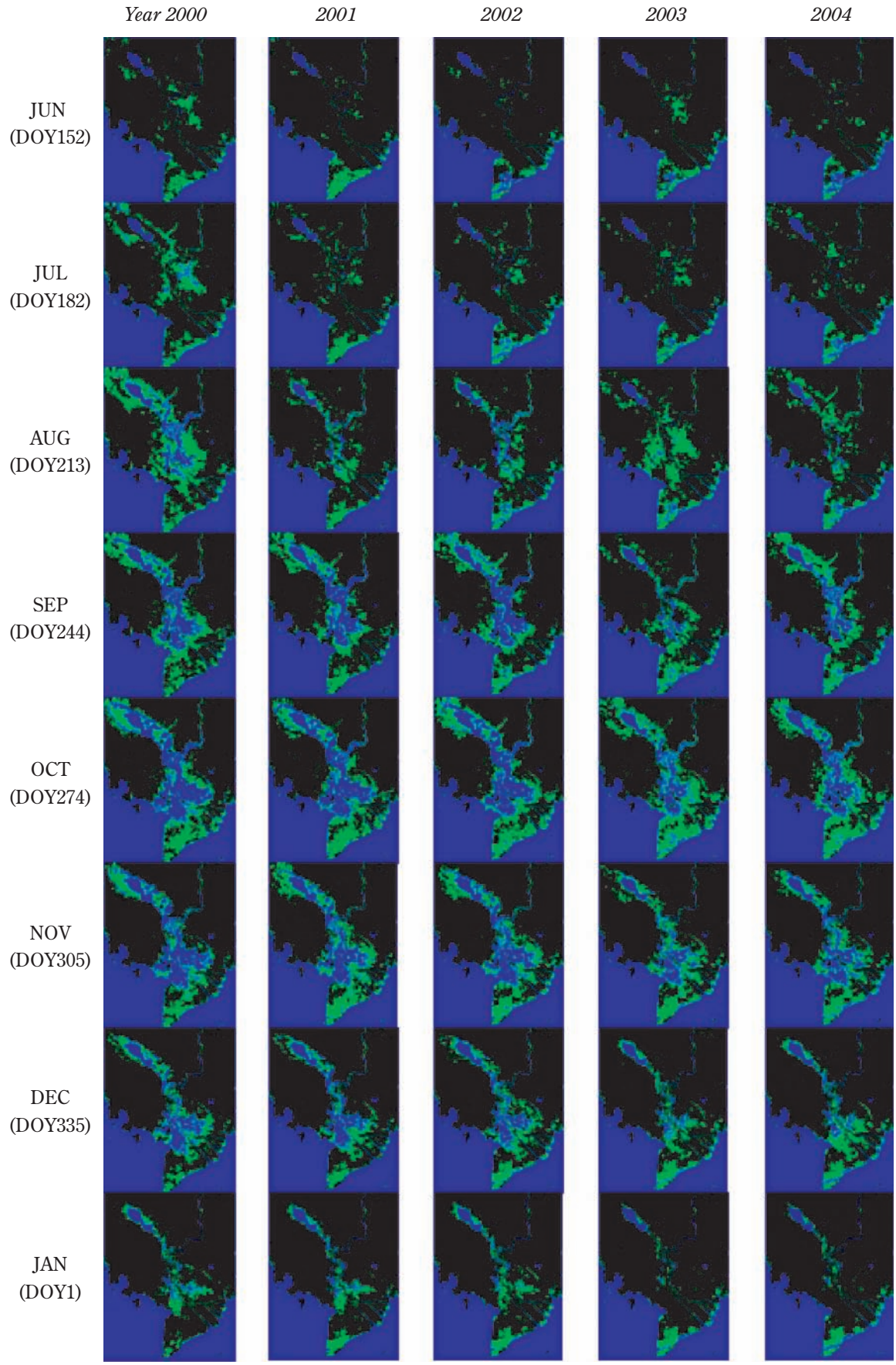

Fig. 44. Spatial distribution of inundated areas on the first day of every month from June to January of the following year. Areas of blue indicate the distribution of *Flood* pixels and areas of green indicate *Mixture* pixels.

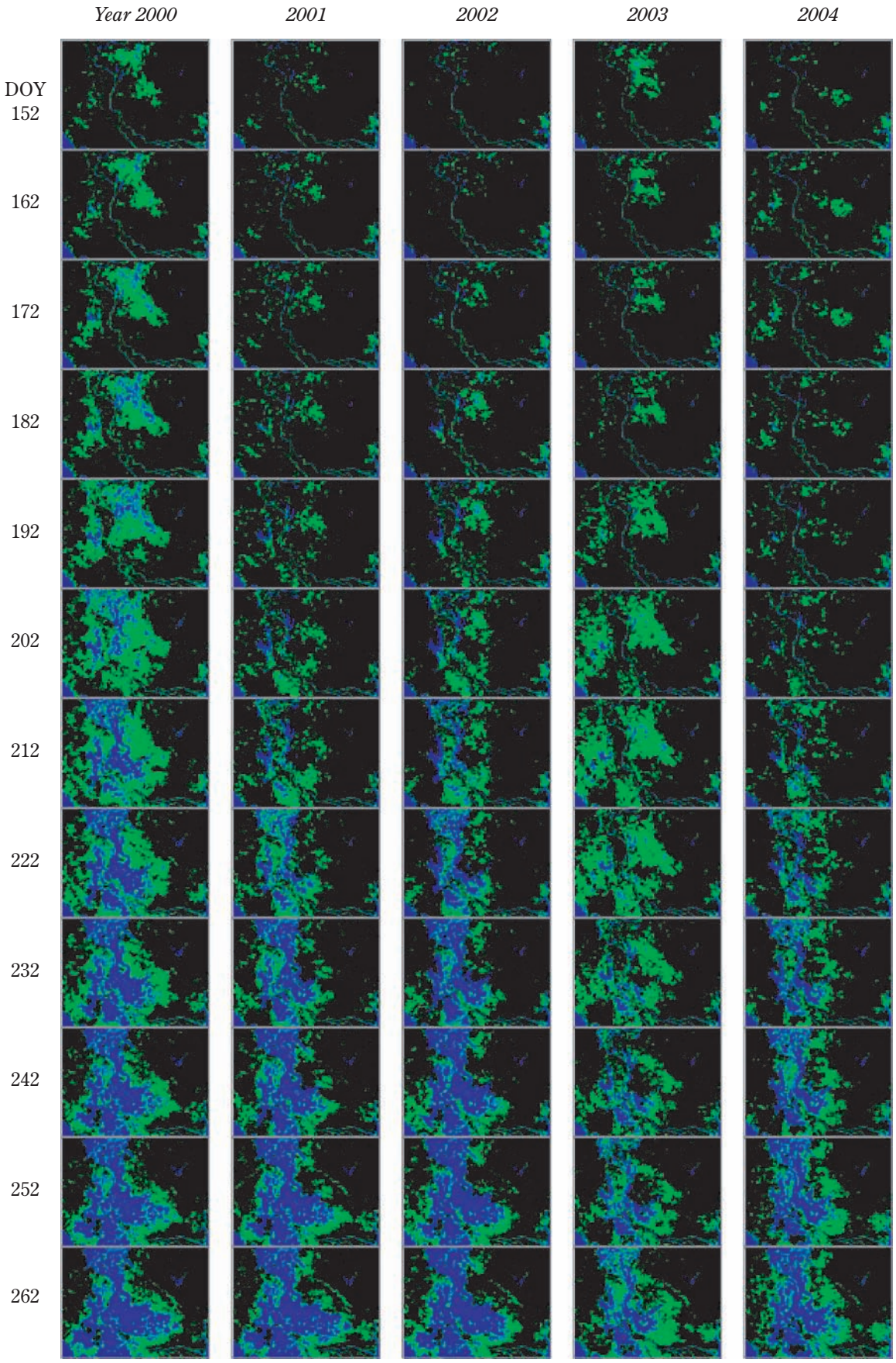

Fig. 45. Temporal changes in flood inundation around the Cambodia–Vietnam border during flood seasons over the period:2000–2004 (enlargement of Region I in Fig. 33). Areas of blue indicate *Flood* pixels, while areas of green indicate *Mixture* pixels.

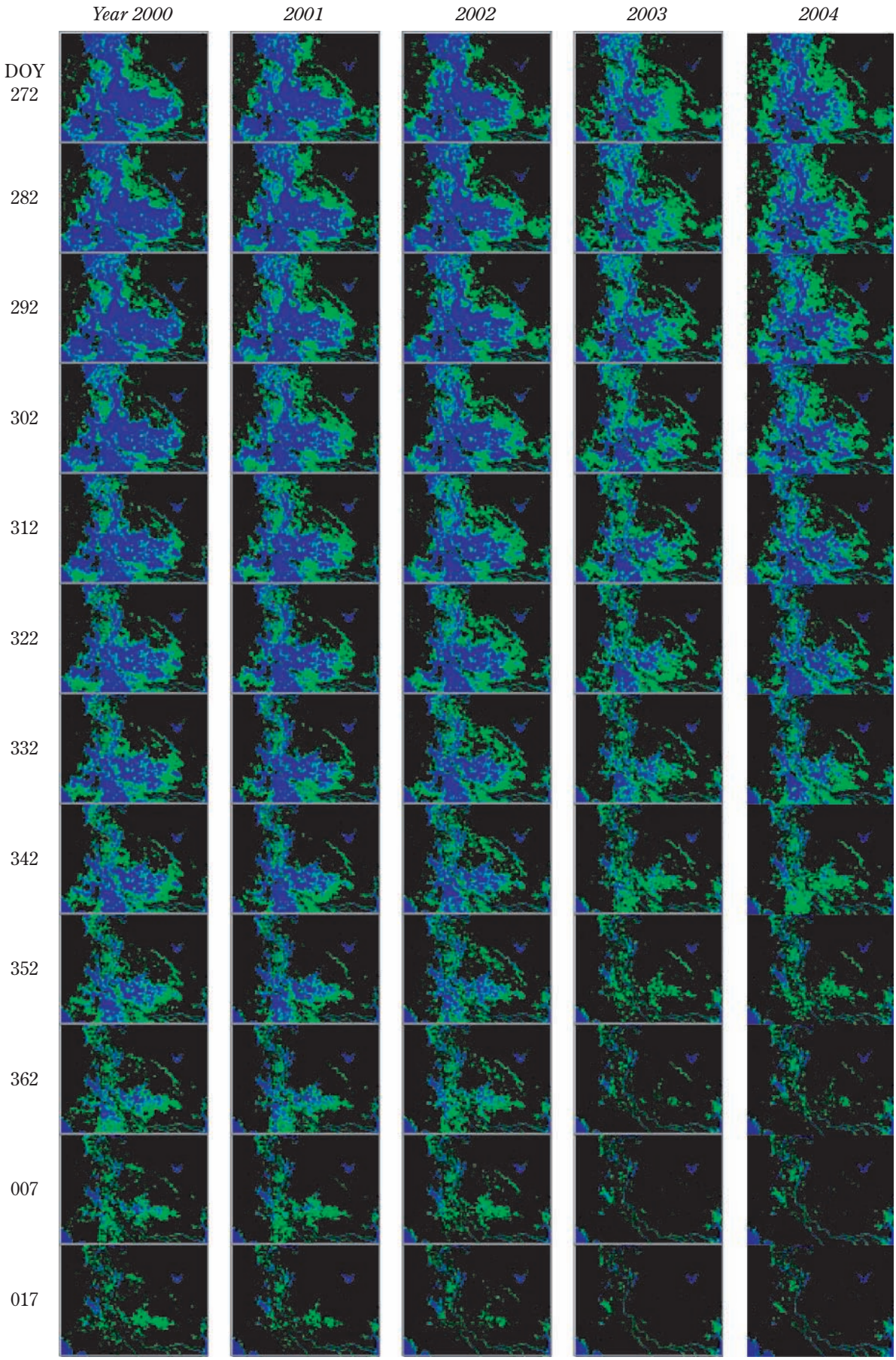

Fig. 45. (continued)

appearance of *Flood* pixels in 2003 is obviously later than that in other years. In additional, the start dates of flooding around the border between Syey Rieng and Long An Provinces in 2003 were clearly later than those in other years (Fig. 46). This observation might reflect the fact that sufficient overflowing water failed to arrive in the northern marginal region of Long An Province (Vietnam) and that new embankment and canals were constructed at the province borders in 2003.

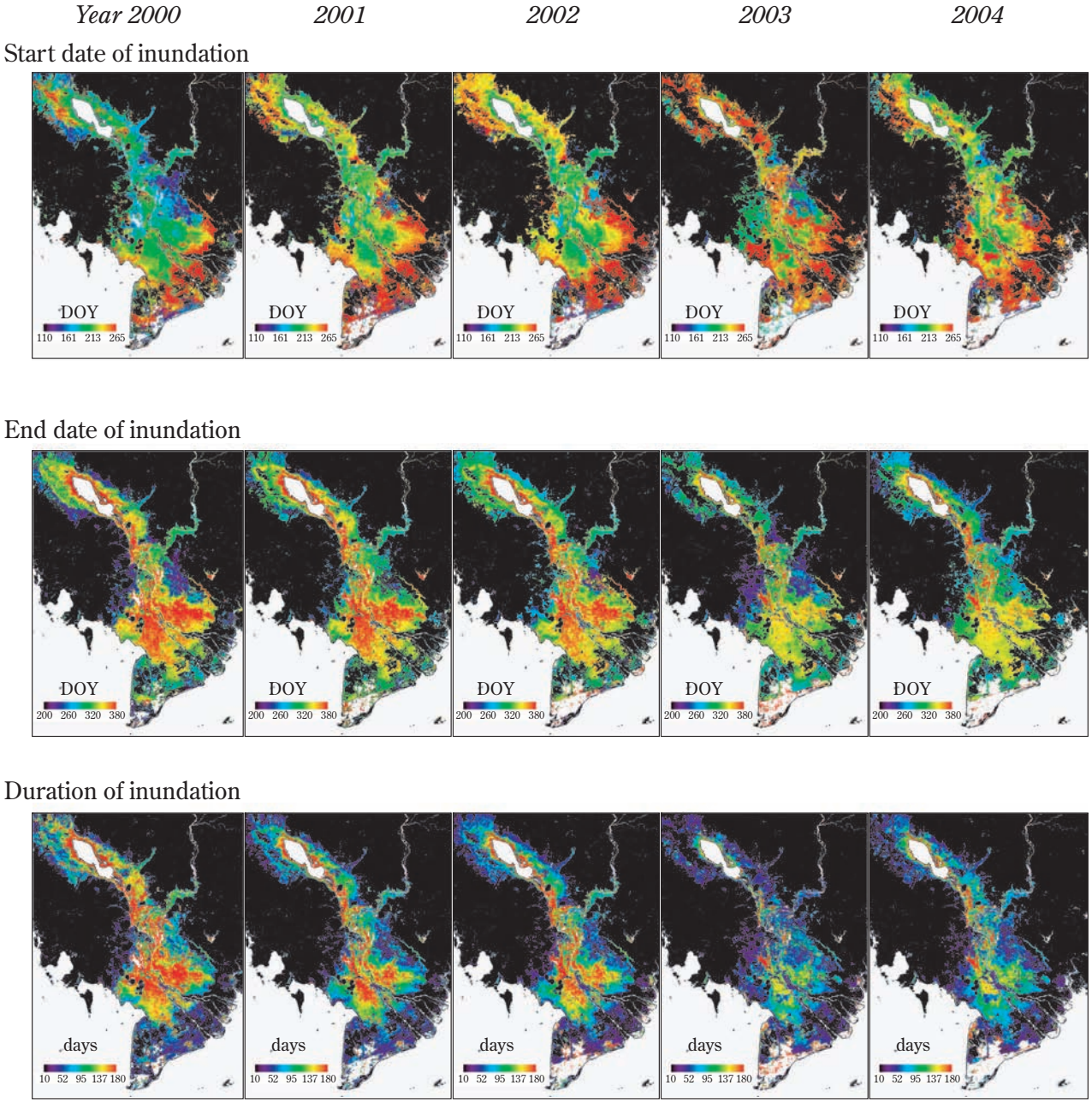

Fig. 46. Spatial distribution of the start date, end date, and duration of inundation cycles over the period from 2000 to 2004.

These early and late start dates of annual flooding appear to be in good agreement with the dates that the water level increased (Fig. 34). The water level recorded in 2000 started to increase earlier in the season than that recorded in other years. The flood damage during 2000 was the most severe in over 70 years, and the seasonal flood hydrograph began 4–6 weeks early Mekong River Commission (2005). Although an arbitrary measure, the first date that the water level

exceeded the given level of 300 cm was earliest in 2000, followed by 2002, 2001, 2004, and 2003 (Fig. 34).

There is a clear contrast in the estimated end dates of inundation cycles between large-scale floods (2000, 2001, and 2002) and small- to medium-scale floods (2003 and 2004) (Fig. 46) :the end dates for large floods are much later than those for the medium- to small-scale floods. It is also possible to determine the approximate differences in flood scales from the duration map. It is assumed that this reflects differences in the natural discharge period that are related to the annual flood intensity.

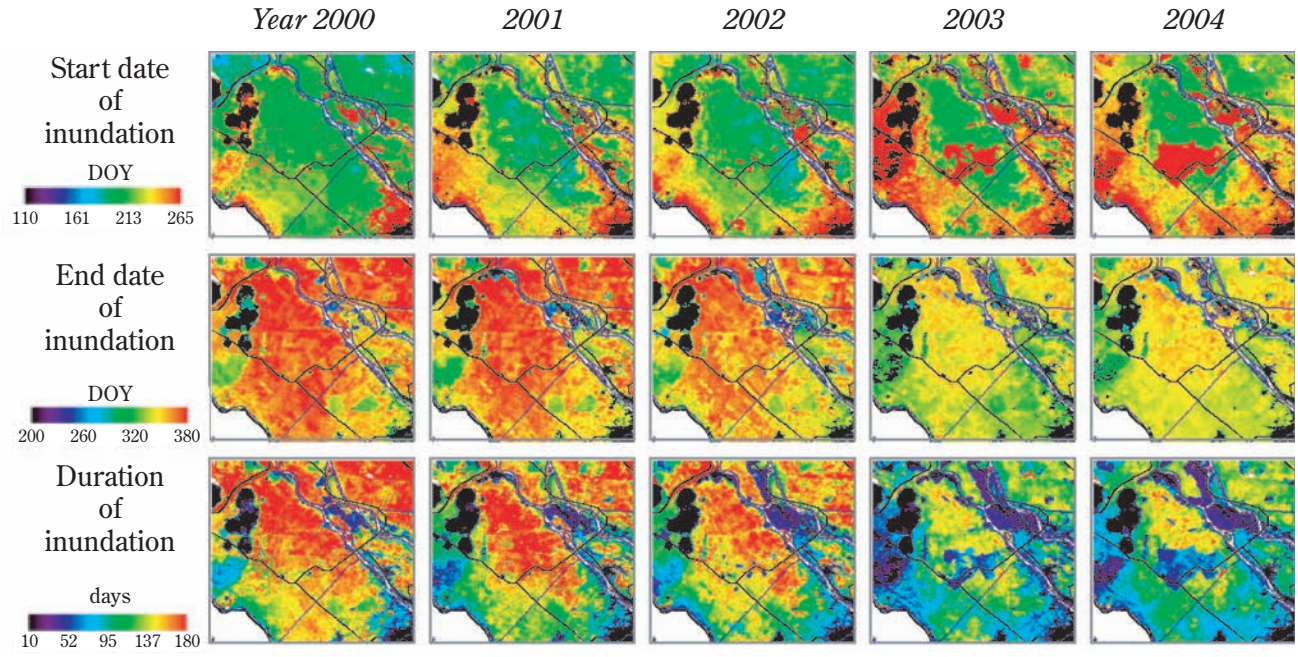

Fig. 47. Start date, end date, and duration of inundation cycles within An Giang and Can Tho Provinces (enlargement of Region II in Fig. 33). The colors used for the start date, end date, and duration are the same as those used in Fig. 46.

A more detailed analysis of the estimates of the timing of inundation cycles (Fig. 47) reveals that the estimated start dates for the years 2003 and 2004 in the southern part of An Giang Province (the central parts of each window in Fig. 47) were distinctly later than those in surrounding areas. A comparison of seasonal EVI patterns in 2002 and 2003 suggests that harvesting in the early part of the flood season was possible for the first time in 2003, enabling a change in the cropping system in this area from double- to triple-cropping (Sakamoto et al., 2006). New findings that arose from this study include the fact that these triple-cropping regions protected by an embankment expanded in area from 2003 to 2004. In contrast, the end date of the same triple-cropping area is similar to that in surrounding areas. In the flood-protected areas of southern An Giang province, at the end of the flooding season (from November) when the flood water is gradually receding and the third of the annual paddy crops (autumn-winter crop) has already been harvested, local farmers open their embankment systems to take the remainder of the flood water into the fields. The objectives of this practice are: (1) to flush pollution and pests (e.g., agro-chemicals, insects, and rats) and provide natural fertilizer via sedimentation (Long, 2003), and (2) to maintain a volume of water for the preparation of land or sowing of the winter-spring paddy crop (starting from the end of November), as this practice reduces the irrigation cost in the dry season.

The inundation season on the Co Do and Song Hau State Farms located in Can Tho Province (Fig. 33; southeast parts of the windows in Fig. 47) shows distinctive features observed in the southern part of An Giang Province, as described above. Although the start date for both state farms is similar to that for surrounding areas, the end dates are clearly earlier.

The farming systems of both state farms are different from those of surrounding areas, which are dominated by mono –paddy cultivation. The diversified systems of crops（paddy and upland crops）and the integrated system（paddy and fish/prawn）are used in both state farms. The reason for the earlier end dates in both state farms is that drainage pumping is performed early for the seeding of upland crops（cash crops in the dry season）and preparation for harvesting the fish cultured within paddy fields.

4.6.3. Shrimp farming

The estimated area of *Long–term water bodies* increased from 2000 to 2004, especially in the Ca Mau and Bac Lieu Provinces（Fig. 33, 42）. This trend may be closely linked to rapid land–use changes related to growth of the Vietnamese economy. Fig. 48 shows statistical data on the total rice–planted area, the area of water surface for aquaculture, and the production figures for shrimp breeding in both provinces. The total rice–planted area tends to decrease over time, while the area of water surface for aquaculture and shrimp production increased from 2000 to 2004. Because the coastal area has geographical advantages in terms of brackish–water aquaculture and its good cash income, local farmers are easily able to shift from rice cultivation to aquaculture, especially shrimp farming（Binh et al., 2005）. There is also a remarkable change in the extent of *Long–term water bodies* estimated from 2000 to 2004（Fig. 42）. While the estimated extent of *Long–term water bodies* increased each year, the area of water surface used for aquaculture and the production of farmed shrimp also increased over the same period, especially during 2000 and 2001（Fig. 42, 48）. According to estimated changes in Land Use/Land Cover within the Cai Nuoc district in Ca Mau Province（Binh et al., 2005）, large amounts of agricultural land were converted to shrimp farming from 1997 to 2003. This is directly related to a policy decision of the Vietnamese Government in 2000. According to the government No.09/NQ–CP（Binh et al., 2005）, where cultivation is impossible because of environmental constraints（e.g., soils, salinity, and acidity）, paddy fields can be converted to other farming systems that provide increased benefits to local farmers. In the case of the delta coast, most of the paddy fields along the coast can only be used for cultivation in the rainy season because of the high risks imposed by physical conditions（e.g., typhoon, drought, salinity intrusion, and soil acidity）. This restriction leads to reduced benefits and hardship for the farmers. Shrimp farming is an attractive alternative, because of the high price commanded by exported shrimp.

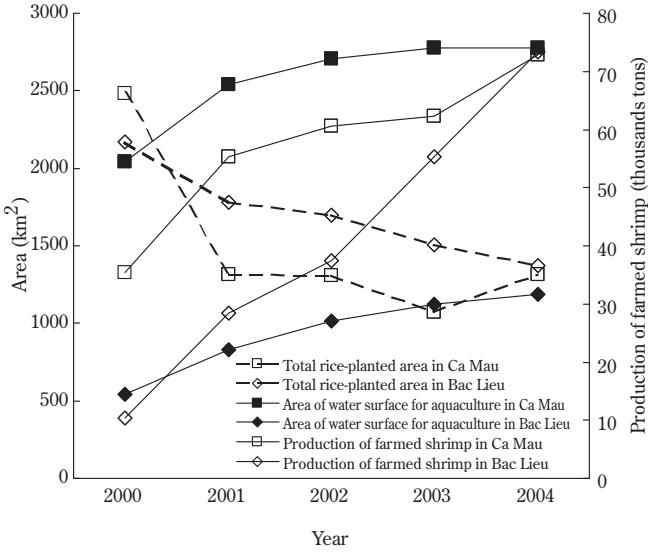

Fig. 48. Total area planted in rice, and Area of water surface used for aquaculture and the production of farmed shrimp in Ca Mau and Bac Lieu Provinces from 2000 to 2004. Sources:Bac Lieu Statistical Office（2005）, Ca Mau Statistical Office（2005）, and General Statistics Office（2005）.

4.7. Conclusions

In this study, the methodology termed the Wavelet-based Filter for detecting spatio-temporal changes in Flood Inundation (WFFI) was devised to use in assessing seasonal and annual changes in inundation cycles from time-series MODIS data. The WFFI products are in good agreement with the water-surface area derived from Landsat images at a 10-km grid level and three inundation maps based on RADARSAT data, hydrological data, and digital elevation model data in terms of temporal changes and spatial distribution. Although the inundated area estimated by WFFI has a margin of error associated with the low resolution of the sensor, the estimates show a strong correlation with the inundated area derived from MRC products [R^2:0.89-0.92] and Landsat images [R^2:0.77-0.97]. The WFFI products derived from MODIS 500m imagery show the ability to study flood dynamics and performs similar to Radarsat based flood assessments. Considering that MODIS products have a great advantage in the high-frequent observation, it is concluded that the WFFI is a useful method to clarify the entire extent of the temporal Mekong flood. In Vietnam, collaboration between provinces is sometimes weak in terms of water-resource management, and such management is conducted according to local interests rather than an integrated and collaborative approach that considers the river basin as a whole (Trang, 2005). With the aim of changing the mindsets of policymakers in this regard, the WFFI products may be the most effective information to put forward. The WFFI products enable us to visualize and understand a spatial and temporal overview of flood dynamics on the wide floodplain that spans political boundaries. As with satellite remote sensing, thematic maps and animation movies produced from satellite images do not require specialized knowledge to understand environmental change from a global viewpoint. It is considered likely that anybody, even those who are not scientists or administrative officers, can understand that the management and control of water resources is not a private matter to be considered solely at the province or national level. In considering climate change associated with global warming, the focus of international corporations and global attention to changes in the water-resource cycle will become increasingly important for the coexistence of riparian countries in the near future. It is hoped that the methodology and WFFI products proposed in this chapter will contribute to consensus-building in terms of water-resource management and the maintenance of wetland ecosystems at an international level.

4.8. Summary

This chapter presents the methodology used to detect temporal changes in the extent of annual flooding within the Cambodia and the Vietnamese Mekong Delta (VMD) based on MODIS time-series imagery (Wavelet-based Filter for detecting spatio-temporal changes in Flood Inundation; WFFI). This methodology involves the use of a wavelet-based filter to interpolate missing information and reduce the noise component in the time-series data, as proposed in a previous study. The smoothed time profiles of Enhanced Vegetation Index (EVI), Land Surface Water Index (LSWI), and the Difference Value between EVI and LSWI (DVEL) are obtained from MOD09 8-day composite time-series data (resolution:500 m; time period:2000-2005). The proposed algorithm was applied to produce time-series inundation maps (WFFI products) for the five annual flood seasons over the period from 2000 to 2004. The WFFI products were validated via comparisons with Landsat-derived results and inundation maps based on RADARSAT images, hydrological data, and digital elevation model data. Compared with the RADARSAT-derived inundation maps at the province level, the obtained RMSE range from 364 to 443 km^2 and the determination coefficients [R^2] range from 0.89 to 0.92. Compared with Landsat-derived results at the 10-km grid level, the obtained RMSE range from 6.8 to 15.2 km^2 and the determination coefficients [R^2] range from 0.77 to 0.97. The inundated area of flooded forests/marsh to the northeast of Tonle Sap Lake were underestimated, probably because of extensive vegetation cover in this area. The spatial characteristics of the estimated start dates, end dates, and duration of inundation cycles were also determined for the period from 2000 to 2004. There are clear contrasts in the distribution of the estimated end dates and duration of inundation cycles between large-scale floods (2000-2002) and medium- and small-scale floods (2003 and 2004). At the regional scale, the estimated start dates for the southern part of An Giang Province during 2003 and 2004 was distinctly later than that for surrounding areas. The

results indicate that these triple–cropping areas enclosed by dikes increased in extent from 2003 to 2004. In contrast, the estimated end dates of inundation at the Co Do and Song Hau State Farms were clearly earlier than those for surrounding areas, although the estimated start dates were similar. Temporal changes in the inundation area of *Flood* pixels in the Dong Thap and Long An Provinces are in excellent agreement with daily water–level data recorded at Tan Chau Station. The estimated area of *Long–term water body* increased in size from 2000 to 2004, especially in coastal areas of the Ca Mau and Bac Lieu Provinces. Statistical data for Vietnam indicate that this trend may reflect the expansion of shrimp–farming areas. The WFFI products enable an understanding of seasonal and annual changes in the water distribution and environment of the Cambodia and the VMD from a global viewpoint.

Chapter V
Agro-ecological Interpretation of the Relationship between Annual Flood Inundation and Rice-cropping System in the Vietnamese Mekong Delta based on MODIS Time-series Imagery

5.1. Introduction

The establishment and improvement of suitable cultivated crops and farming systems for a given regional climate has traditionally been undertaken by local farmers based on observations of the seasonal change in the environment over a period of many years. However, the recent acceleration of land-use change and the crop breeding for purpose of increasing crop production and agricultural revenue may no longer relies on such long-term observations or considerations of suitability, and there is emerging concern for the impact of such human activity on the regional environment, natural ecosystems, and biodiversity in many areas of the world.

As a result of the introduction of market-oriented economic system and reformation of the agricultural system in line with the reform policy of "Doi Moi" in the late 1980's, the rice planted area in Vietnam was substantially expanded, and a range of methods for improving the efficiency of rice productivity was applied. Prior to the late 1960's, most rice growers employed the traditional single rice-cropping system using the photosensitive local variety of rice, which has a growing period of 7-9 months (Cho, 2005). The introduction of non-photosensitive high-yield rice varieties in the late 1960's and the large-scale development of canals, dikes, irrigation/drainage systems, and water sluices has lead to widespread adoption of the double/triple rice-cropping system (Cho, 2005; Kono, 2001). The adoption rate of modern rice varieties in Vietnam has increased from 16.9% in 1980 to 94.2% in 2002, and the irrigated area has increased from 46% in 1980 to 85% in 2002 (Ut and Kajisa, 2006). As a result, the total rice-planted area, production and yield in Vietnam increased from 4.9M ha, 10.3M ton and 2.1t/ha in 1975 to 7.4M ha, 36.1M ton and 4.9t/ha in 2004 (General Statistics Office, 2000; 2006). The breakthrough of rice-output expansion has allowed Vietnam to become an exporter of rice. Vietnam has now reached an eminent position as a rice exporter since the first exports in 1989. The international share of the exported rice from Vietnam was the second largest only to Thailand in 2003 (FAOSTAT, 2007).

The Vietnamese Mekong Delta (VMD) is most remarkable region in examining the land-use change relating rice production of Vietnam. The adoption rate of modern variety and the rate of irrigated area in 2002 of the VMD are the highest level (99.5% and 91% respectively) in whole country, as well as those of the Red River Delta (96.3% and 100%). Accordingly, the VMD accounted for 54% of the total rice production of whole country in 2005, and 52% of the total planted area (General Statistics Office, 2006). The rice produced in this region also accounts for 80-85% of the rice exported from Vietnam (Nguyen et al., 2004a). Thus, the VMD also occupies an important position in terms of the international rice market and hence global food security.

While infrastructure development for water resource management allows rural farmers to conduct multiple rice cropping for improving rice productivity, the seasonal cycle of the agricultural ecosystems in flood-prone areas have changed drastically under the anthropogenic influence of human activity. Rapid land-use change may have a negative impact on the regional environment and the watershed ecosystem through the material/hydrologic circulation of chemicals and nutrition (Kuusemets and Mander, 2001). Thus it is important to understand the agro-ecological meaning of interplay between the variable environmental condition and the agricultural activity, towards to a sustainable growth of agricultural activity in the VMD. The spatial information such as the district-level maps of cropping system is needed for regional policy assessment, increasing water-use efficiency and water-irrigation management (Frolking et al., 2006; Humphreys et al., 2006).

The spatial distribution of the rice-cropping system of the VMD is closely related with the seasonal water regimes of the Mekong and Bassac rivers (Sakamoto et al., 2006). Furthermore, the rice phenology in the upper region of the VMD would be strongly affected by the annual flooding in rainy season. Normal-scale flooding provides various benefits for local farmers including the freshwater resources with fertile sediments, the introduction of freshwater fish into the

paddy fields, and the flushing of pollutions. However, catastrophic floods such as in 2000 cause significant and widespread damage to human life and the rice cropping (Tinh and Hang, 2003). Since this experience of severe flooding in the VMD, the Vietnamese government has promoted a policy entitle "Living with Floods" to take advantage of the positive effect of annual flood inundation while implementing various countermeasures against the negative impact of flood disasters.

In this chapter, the multi-temporal MODIS imagery was used to examine the spatio-temporal relationship between the annual flood inundation and the rice cropping system in the VMD, because remote sensing using satellite imagery is a powerful tool to reveal the land-use pattern, the land-use and land-cover change in the wide area periodically (Brandt and Townsend, 2006; Echeverria et al., 2007; Heinl et al., 2006; Ji et al., 2004; Kerr and Cihlar, 2003; Ludwig et al., 2007; Sivanpillai et al., 2006) and to identify the current ecosystem functional types (Alcaraz et al., 2006). Specifically, the phenology information of the plant growth detected from the temporal satellite data help us to understand the spatial pattern of vegetative activity (Wardlow et al., 2006) and the relationship with the climatic and geographical features (Karlsen et al., 2006). The annual change of the rice-cropping system is also detected by using a original methodology, because the assessment of the current land-use pattern is important issue for projecting the impact of climate change on the biodiversity (Higgins, 2007). In Thailand, the spatial pattern and the number of rice cropping per year is correlated with the number of free grazing duck density, which is key link between agricultural activity and Highly pathogenic avian influenza outbreak (Gilbert et al., 2007). Therefore, the study approach proposed in this chapter is helpful for interpreting agro-ecological meaning of the agricultural activity against the relevant environmental fluctuations as an important aspect of the symbiosis of agricultural activity and spatio-temporal fluctuation of the natural environment.

5.2. Vietnamese Mekong Delta (Cuu Long Delta; alias in Vietnam)

The Vietnamese Mekong Delta (VMD) is located in southern Indochina (8.5-11°N, 104.5-106.8°E) near the mouth of the Mekong River, which is the largest international river in the Southeast Asia. The catchment area of the Mekong River Basin (795,000km^2) spreads beyond or along the boundaries of China, Myanmar, Laos, Thailand, Cambodia, and Vietnam. This region is classified as a savanna climate in Koeppen climatic division with clear seasonal changes in precipitation between the dry (ca. Nov-Apr) and rainy seasons (ca. May-Oct) due to the Asian Monsoon effect. The massive precipitation in the rainy season and the outflow from the upper riparian countries cause the water level to rise rapidly from May/June, leading to annual flooding in the VMD. Approximately 17 million people currently live in the VMD, 80% of whom live in rural areas. While the rural population in the VMD has increased by half from 9.0 million in 1976 to 13.7 million in 2005, the total rice-planted area in the VMD has also expanded from 1.86 MHa in 1975 to 3.82 MHa in 2004 (General Statistics Office, 2000; 2004; 2006). The temperate climate and plentiful water resources carried by the Mekong and Bassac rivers make it possible for double or triple rice cropping to be conducted in the VMD. This chapter considers *the winter-spring rice* (recession rice) production affected by the fluctuating flood inundation, and the triple rice-cropping system started recently in An Giang Province following the construction of a dike system and water -resource infrastructures (Figs. 49, 50).

5.3. Data and Method

5.3.1. MODIS/Terra

Data acquired by the Moderate Resolution Imaging Spectroradiometer (MODIS) onboard the Terra satellite (EOS-AM) are generally available from 2000. The instrument has a 2330-km viewing swath, taking spectral imaging data of the earth surface every 1-2 days in 36 spectral bands. The MOD09 data used in this study are distributed freely by the Earth Observing System Data Gateway (EOS, 2007). MOD09 data includes the atmospheric-corrected surface spectral-reflectance for 7 spectral bands at 500-m resolution (Vermote and Vermeulen, 1999). The 8-day composite products yield the best surface spectral-reflectance data for each 8-day period with the least effect of atmospheric water vapor, and also record the observation date for each pixel. The temporal MOD09 8-day composite data acquired from 2000 (after DOY

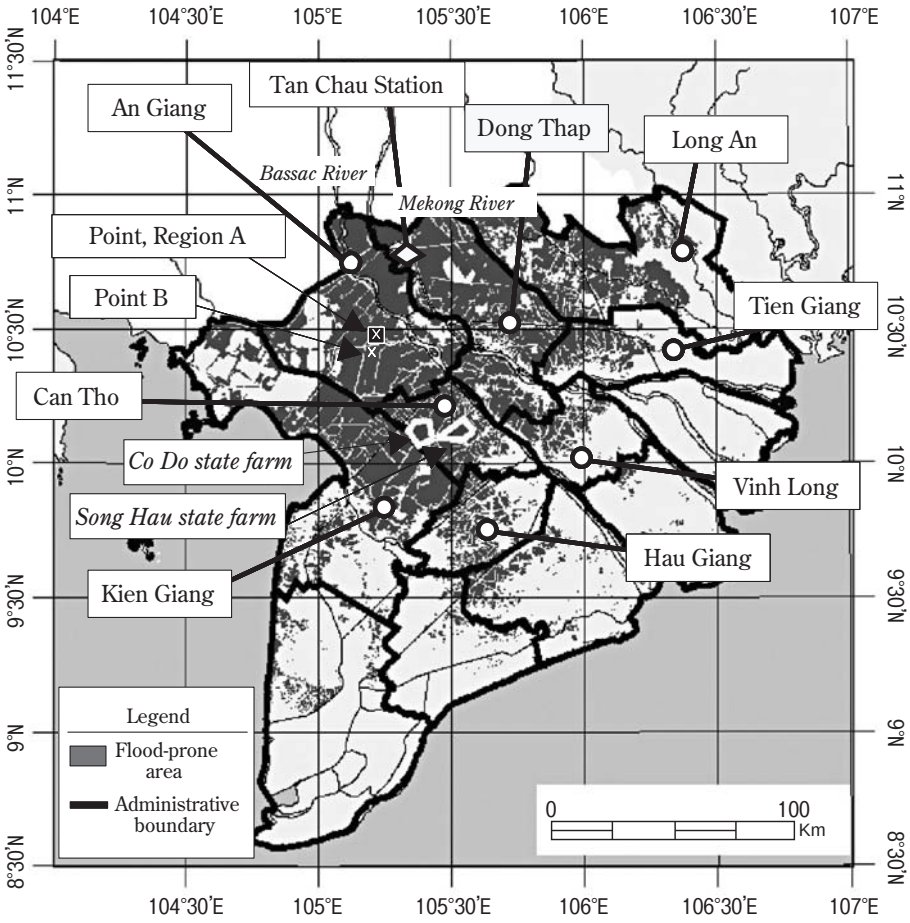

Fig. 49. Location of study area. The objective flood-prone area is defined by the inundation period (2–6 months) of *"Flood"* pixels in 2000 estimated by the WFFI methodology.

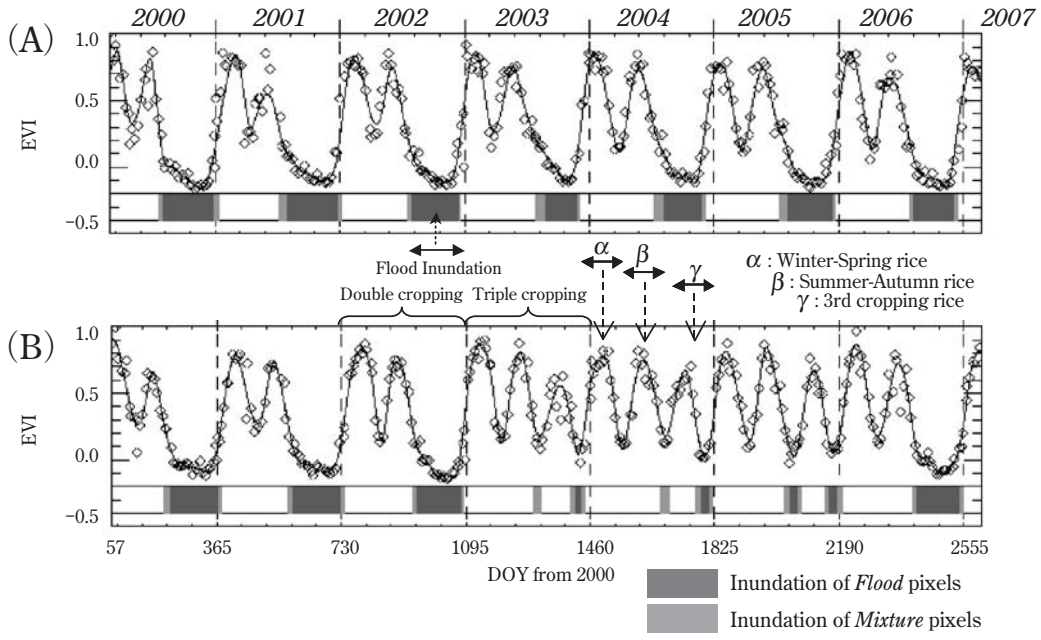

Fig. 50. Smoothed EVI time profile with observed EVI data from 2000 (DOY 57) to 2007 (DOY 56) in (A) an area in which the cropping system did change in the observation period (area A in Fig. 49), and (B) an area in which the cropping system changed from double cropping to triple cropping (area B in Fig. 49).

57）to 2007（before DOY 56）are used in this chapter. The spatial resolution of this data set（ca. 250/500m）is sufficiently fine to monitor the vegetation activity and flood inundation on a regional scale. The 500–m resolution MODIS data are mainly used in this chpater, while the 250–m resolution MODIS data are used for analyzing the triple rice cropping area in An Giang Province. Because MOD09 data at 250–m resolution includes only two spectral–reflectance data（band 1; red, band 2; near infrared）, the reflectance data of band 3（blue）at 500–m resolution, which was interpolated by ***the nearest neighbor method***, was substituted for calculating the Enhanced Vegetation Index（EVI）at 250–m resolution. Although the higher–resolution image（ca. 250m/pixel）provides clearer results for agricultural land–use change with less mixed pixel effect, calculation for the entire the VMD in 250–m resolution would take too long time for the purpose of the present chapter.

5.3.2. New wavelet–based algorithms for detecting spatio–temporal patterns

5.3.2.1. Wavelet–based filter for detecting crop phenology

The previous chapter focused on the characteristic pattern of the time–series vegetation index due to rice growing, and proposed an original methodology for detecting rice phenology based on multi–temporal EVI data. The EVI derived from MODIS data would be linearly correlated with the leaf area index, and has a higher sensitivity in high biomass areas than normalized difference vegetation index（NDVI; Huete et al., 2002）.

$$EVI = 2.5 \times \frac{NIR - RED}{NIR + 6 \times RED - 7.5 \times BLUE + 1} \qquad \cdots\cdots\cdots\cdots\cdots\cdots \quad (5-1)$$

where NIR is the surface reflectance value:0–1.0 in the near infrared（841–875 nm, Band 2）, RED;（621–670 nm, Band 1）, BLUE; and（459–479 nm, Band 3）.

The greatest advantage of MODIS data for crop monitoring is the high sampling frequency（1–2 days）of optical images. However, optical sensors such as MODIS are unable to image the surface reflectance under thick clouds conditions. Thick clouds veiling a pixel for continuous period of 8 days cause a missing/error value in the temporal EVI profile. Thus, a wavelet–based filter was devised to reduce the noise component and interpolate missing value, utilizing the advantages of time–frequency analysis. In analysis of Japanese paddy fields in 2002, the local maximal points in the smoothed EVI profile were found to correspond to the peak date of crop heading season in the statistical data, with the RMSE of 9.0 days. This wavelet–based filter for determining crop phonology（WFCP）can thus be used to identify rice–heading dates and the rice–growing process（Sakamoto et al., 2005）.

5.3.2.2. Wavelet–based filter for evaluating the spatial distribution of cropping systems

A wavelet–based filter for evaluating the spatial distribution of cropping systems（WFCS）has also been developed（Sakamoto et al., 2006）as an advanced algorithm that maps the spatio–temporal distribution of rice phenology and cropping systems. This algorithm has been used to map the spatial pattern of the multiple cropping areas, revealing that the cropping systems and rice phenology in the VMD were highly dependent on the seasonal water–flows regime of the Mekong and Bassac rivers. Double irrigated rice–cropping system（including ***the winter–spring*** and ***the summer –autumn*** rice, from Nov/Dec to Jul/Aug）is dominant in flooding zone of the upper region of the VMD. Double rain–fed rice–cropping system（including ***the summer–autumn*** and ***the rainy–season rice***, from May to Nov/Dec）is mainly located in coastal areas, because little precipitation and salinity intrusion through the canal and river networks in the dry season cause lack of fresh–irrigation water in dry season. The triple rice–cropping area was mainly sustained widely in an intermediate region where the geographical conditions protect against flood inundation in the rainy season and salinity intrusion in the dry season.

5.3.2.3. Wavelet-based filter for detecting spatio-temporal changes in flood inundation

To quantify the annual variation in the intensity of the Mekong flood, the present authors have proposed a wavelet-based filter for detecting spatio-temporal changes in flood inundation (WFFI; Sakamoto et al., 2007). This algorithm also applied the wavelet analysis to reduce the noise component from the temporal data of the EVI, Land Surface Water Index (LSWI;Xiao et al., 2006), and the Difference Value between the EVI and LSWI (DVEL), and the missing value due to continuous thick clouds were interpolated.

$$LSWI = \frac{NIR - SWIR}{NIR + SWIR} \quad \cdots\cdots\cdots\cdots\cdots\cdots \quad (5-2)$$

$$DVEL = EVI - LSWI \quad \cdots\cdots\cdots\cdots\cdots\cdots \quad (5-3)$$

where NIR is the surface reflectance value:0–1.0 in the near infrared (841–875 nm, Band 2), SWIR is in the short-wave infrared (1628–1652 nm, Band 6).

In this methodology, the ground surface condition is divided temporally into *Flood* pixels, *Non-flood* pixels, and *Mixture* pixels including water, vegetative coverage, and soil. The spatio-temporal inundated area indicated by WFFI data is in good agreement with the reference water-surface images derived from Landsat Enhance Thematic Mapper (ETM +) images and inundation maps generated using RADARSAT, digital elevation model (DEM), and hydrological data. When using the WFFI methodology, it is clearly revealed that the flood intensity in the period from 2000 to 2004 varies annually in the time and space (Sakamoto et al., 2007).

5.4. Data Analysis

5.4.1. Definition of flood-prone area

The distribution of flood-prone paddy field in the VMD is shown in Fig. 49. The first target of this study is to examine the phenology of *the winter-spring rice* that is affected by the annual flood inundation in the upper VMD. The flood-prone area was defined using the WFFI products in terms of the flooding periods to exclude the temporal water-surface area during irrigation scheme or long-term water bodies such as aquaculture ponds, river, and sea. The flood-prone area is empirically defined as being inundation for longer than 60 days and less than 240 days in 2000 based on the WFFI algorithm. Areas not occupied by paddy fields in the flood-prone area were masked using the land-use map. The cropping season of *the winter-spring rice* was determined by detecting the heading date after the estimated end date of flood inundation.

5.4.2. Detecting the triple cropping area in An Giang Province

The second target of the present study is to detect the annual change in the rice cropping system in An Giang Province from 2000 to 2006. Over these 6 years, the area of triple cropping can be easily detected by the WFCS algorithm. However, it is impossible to detect the rice cropping system in 2000, since MODIS data start from DOY 56 of the year 2000. The area of triple cropping in 2000 is defined if the heading date is estimated to occur after July, as farmers in the upper region of the VMD usually finish harvesting the second crop before the next flood season. A thematic map of the annual change of the triple rice cropping area was created by combining the years in which a third rice crop is detected. A kind of image processing "majority analysis" was conducted for reducing the spatial noise in the thematic map.

5.5. Results and Discussion

5.5.1. Annual flood scale

The annual flood scale in the VMD is divided into three categories on the basis of the peak water level recorded at Tan Chau Station (see Fig. 49, 51) and the definitions (Long, 2003). The floods in 2000, 2001, and 2002 are categorized as

large-scale floods with peak water levels higher than 4.5 m. The floods scales in 2004 and 2005 are classed as moderate, with peak water levels between 4.0m and 4.5 m. Although the flood scale in 2003 with a peak water level higher than 4.0m should be classed as moderate in a strict sense, the 2003 flood was classified as small for the purposes of the present study because the flooding behavior is substantially different from that in other years. Additionally the peak water level in 2003 exceeded 4.0 m for only 2 days (Table 7).

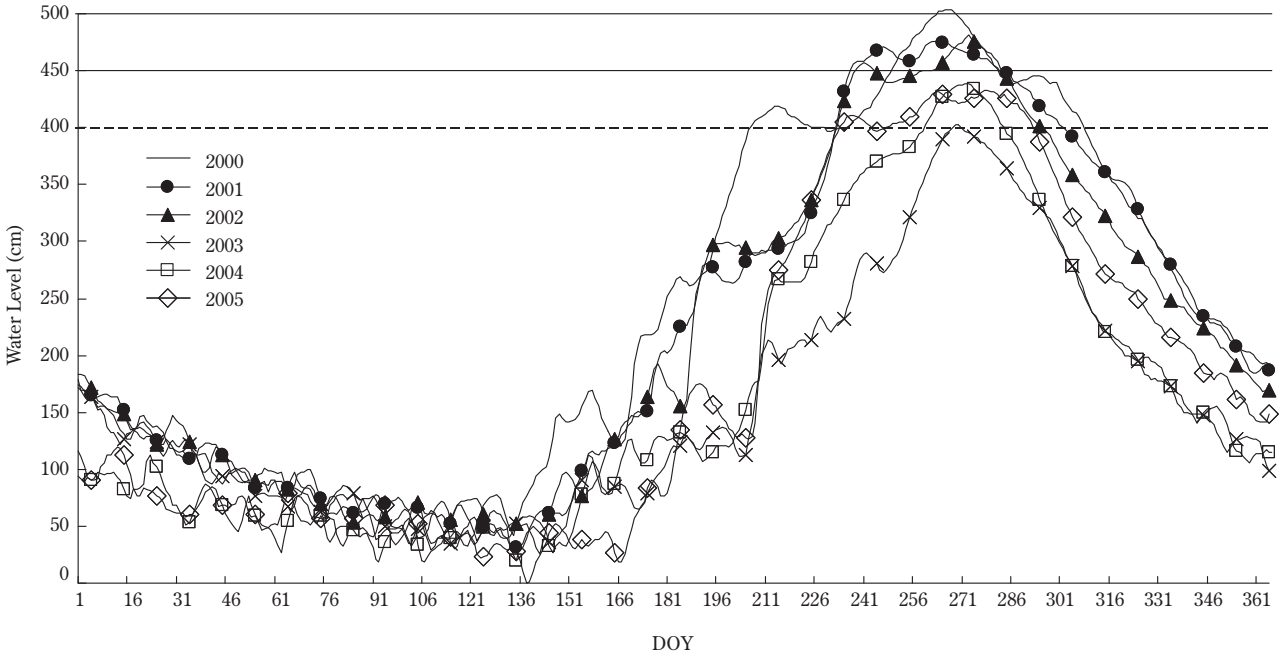

Fig. 51. Daily water-level data recorded at Tan Chau station from 2000 to 2005.

Table 7. Total number of days that the daily water-level in Tan Chau station exceeded the reference level.

	400cm <	450cm <	500cm <
2000	97	33	6
2001	70	46	−
2002	64	25	−
2003	2	−	−
2004	25	−	−
2005	46	−	−

The estimated duration, start and end dates of flood inundation in the target flood-prone area from 2000 to 2005 are shown in Fig. 52. The seasonal flood hydrograph in 2000 began 4-6 weeks earlier than usual (Mekong River Commission, 2005). The WFFI algorithm reveals that the estimated end date of inundation in 2000 was much later than in the other years, and the estimated duration of inundation in 2000 was also much longer. In 2003, characterized by a small flood, the start date was later, the end date earlier, and the duration of flood inundation shorter than in the other years. The estimated duration of inundation thus appears to be useful for detecting differences in the flood scale. The estimated end dates of inundation cycles also appear to be related to the flood scale. It is thus reasonable to assume that the annual change in the estimated end dates reflects the natural discharge periods related to the annual flood intensity (Sakamoto et al., 2007).

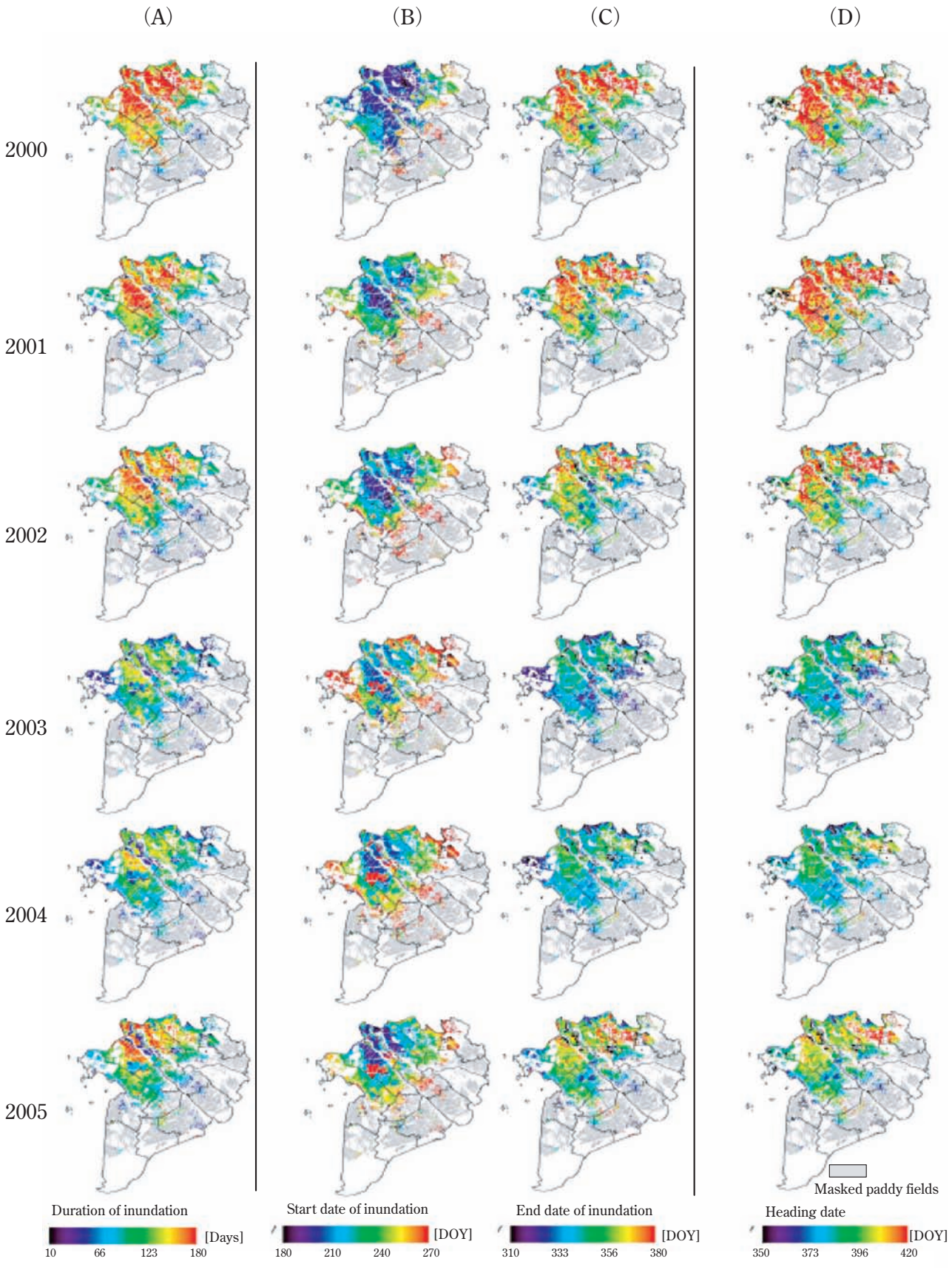

Fig. 52. WFFI estimation of (A) duration, (B) start date, and (C) end date of annual inundation in the flood-prone area from 2000 to 2005. (D) Estimated heading date after the end of the inundation cycle.

5.5.2. Spatial distribution of the estimated heading date of *the winter–spring rice*

The spatial distribution of estimated heading date after the flood season is also shown in Fig. 52. Most of flood–prone area is characterized by heading date of DOY 370–420 from January 1st of the preceding year（with respect to crops planted in the normal year）. This cropping season corresponds to *the winter–spring rice*（*Lua Dong Xuan* in Vietnamese）, the sowing and harvesting seasons for which are Nov/Dec and Feb/Mar in the following year. However, there are some regions with estimated heading dates of earlier than DOY 350 in the An Giang Province after 2003, particularly in the riverside and river island areas between the Mekong and Bassac rivers, where the rice cropping system changed from double cropping to triple cropping（described in detail later）. Because of the triple peaks in the temporal EVI profile, most of the region corresponds to triple cropping area, excepting for the mixed pixel effects due to the cash crop area. However, it is considered that these miss–detected regions including the triple rice–copping area will be negligibly small with respect to the entire target area and can be ignored.

5.5.3. Rice cropping system in target area

The observed EVI data, smoothed EVI time profile, and temporal water condition（*flood/mixture*）are shown in Fig. 50. The EVI derived from MODIS data increases with rice crop growth during the vegetative growth stage, and decreases during the reproductive stage. Thus, the EVI data for point A（Fig. 49）show that the double rice cropping avoiding the flood season was conducted continuously from 2000 to 2006. In point B（Fig. 50）, on the other hands, the triple rice–cropping area, which was changed from double cropping in 2003, was returned to double rice cropping in 2006. This result indicates that one more rice cropping in the early period of the flood season（the third cropping rice）were possible in 2003, attributable to the construction of a dike system enclosing the paddy fields in point B（Sakamoto et al., 2006; 2007）.

5.5.4. Comparison between estimated end date of inundation and heading date of *the winter–spring rice* in flood–prone area

Comparison of the estimated heading date of *the winter–spring rice*（Fig. 52D）with the end date of flood inundation（Fig. 52C）reveals correlated spatial patterns of "early" or "late" in each year. The heading date and the flood–inundation end date were both late in the three provinces of An Giang, Dong Thap, and Long An than the lower provinces of Can Tho, Kien Gian, Ben Tre, and Vinh Long（see Fig. 49）. This may be related to the spatial pattern of flood expansion and drainage under geographical constraints. Floodwater flows into the flood–prone area via rivers and canals, and across the Vietnam–Cambodia border through Dog Thap and Long An（Long, 2003; Sakamoto et al., 2007）.

Temporal profile of average daily EVI data（Fig. 53）represents *the winter–spring rice* growth of the region A（Fig. 49, ca. 450ha）. In this region, double cropping was conducted from 2000 to 2005（see Fig. 50）. According to seasonal change of the areal ratio of the *Flood* or *Mixture* pixels, the "early" or "late" of the flood recession season in each year reflects the yearly change of flood intensity（see Fig. 52）. The average daily EVI data increase rapidly with decreasing areal ratio of *Flood* or *Mixture* pixels. As suggested by the end dates of inundation and heading dates of *the winter–spring rice*, which were latest in 2000 and earliest in 2003, there appears to be close relationship between termination of the flood season and the onset of *winter–spring* cropping. Scatter plots of both dates are shown in Fig. 54. Although the plotted data include error due to mixed pixel effects of neighboring land coverage and poor observation conditions, most plots in each year are distributed around a specific liner relation with slope of 1 and intercept of 40 days（[*Estimated heading date*] = [*Estimated flood–inundation end date*] + 40days）. The aggregate of these plots（Fig. 54）reveals an uneven distribution caused by the difference in annual flood intensity. Nevertheless, it is clear that there is a positive linear relationship between the end date of inundation and the heading date of *the winter–spring rice* in the flood–prone area. The widely cultivated *winter–spring rice* in the upper VMD is a high–yielding, non–photoperiod sensitive variety with a shortened growth period（90–100 days; personal communication）. Given that the *Mixure* pixels derived by the WFFI algorithm indicate mixed pixels of the water, soil and vegetation（Sakamoto et al., 2007）, the last ca. 20–30 days of the estimated

duration of flood inundation may include early-season growth indicative of newly sown rice.

The determination coefficient when comparing these estimations of the noticed pixel with the adjacent 8 pixels in the 6 years from 2000 to 2005 is mapped in Fig. 55. The upper region around the Mekong and Bassac rivers and the flood flow path from the Bassac river to the Gulf of Thailand are characterized by a high determination coefficient. The possible reason for the relative lower coefficient of the other regions is the weaker fluctuation in flood intensity due to the geographic location (see Fig. 50), except for the mixed-pixel effects. The appropriate soil-water conditions for direct seedling are generally when the soil is wet, but not flooded deeply. The soil-water condition can be controlled using a small agricultural pump, allowing sowing date of *the winter-spring rice* to be started earlier by draining the flooded water. However, such a drainage pump is not usually used until the flood level naturally decreases to 40-50cm (personal communication) due to fuel-cost performance. Thus, the sowing season for *the winter-spring rice* in the flood-prone area remains closely dependent on the timing of flood recession, spatially and temporally.

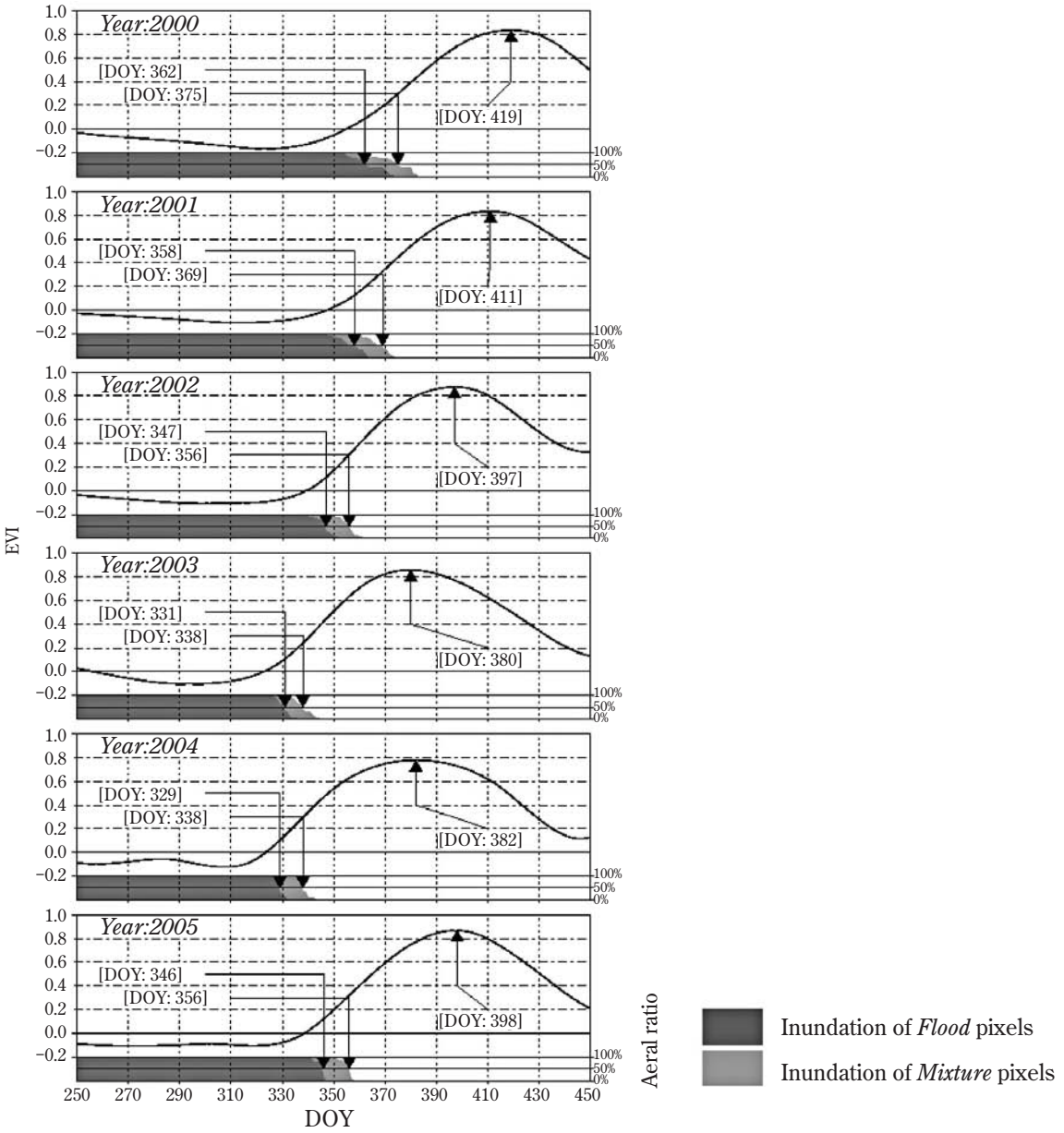

Fig. 53. Temporal profile of average daily EVI and areal ratio of "*Flood*" and "*Mixture*" pixels derived by the WFFI method from the mid-flood season to the end of the subsequent-crop season (DOY : 250-450) over the period from 2000 to 2005. Arrows indicate the dates corresponding to the maximal point in the temporal EVI profile and the half point (50%) in the areal ratio of "*Flood*" and "*Mixture*" pixels.

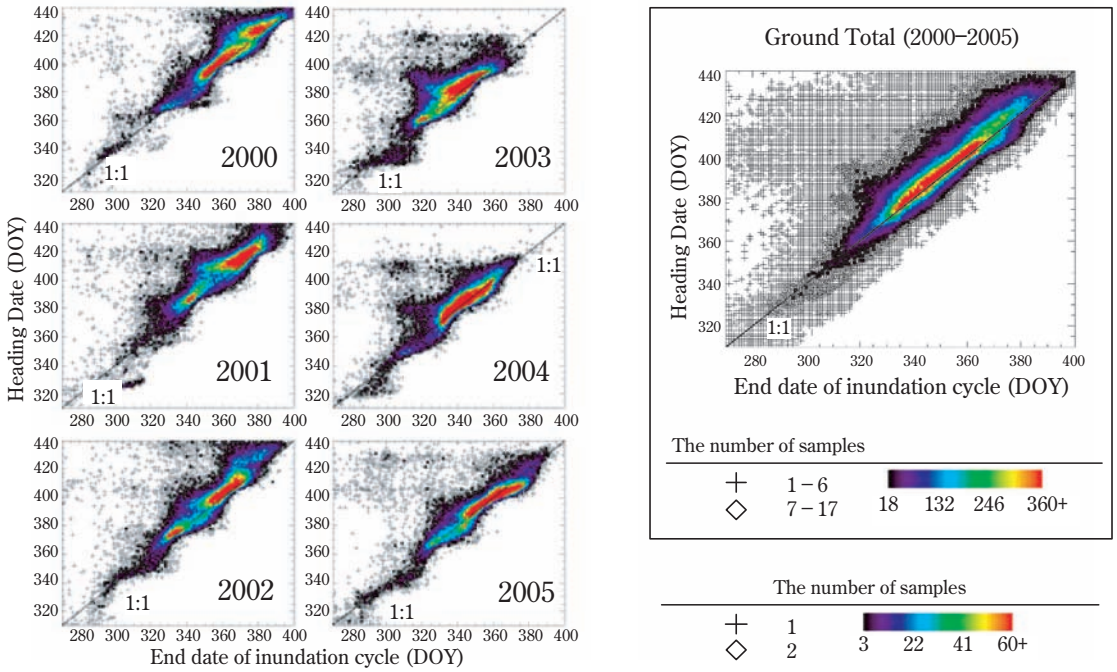

Fig. 54. Comparison between estimated end date of inundation cycles and subsequent heading date in the flood-prone area from 2000 to 2005. The summation of the comparisons in each year is shown on the right.

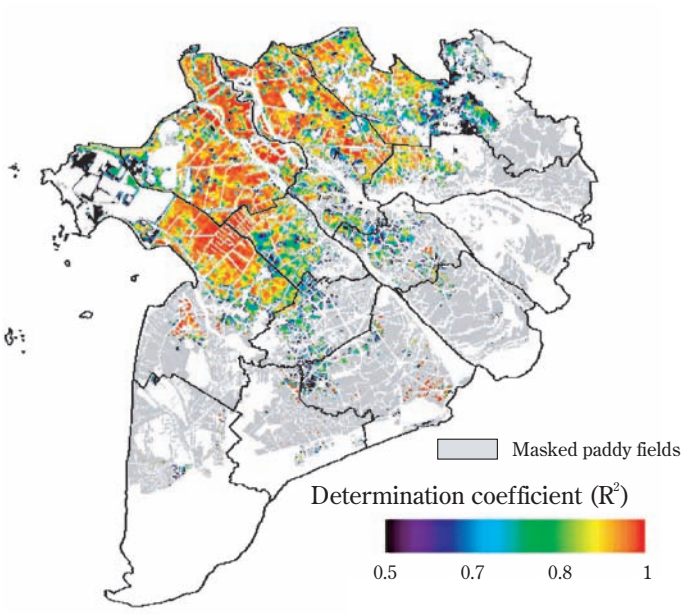

Fig. 55. Map of determination coefficient (R^2) between the end of the inundation cycle and the subsequent heading date in the flood-prone area of the VMD.

5.5.5. Triple cropping area in An Giang province

The spatial distribution of the estimated heading date of *the third cropping rice* in An Giang Province is shown in Fig. 56. The thematic map classifying the annual changes in triple cropped areas is shown in Fig. 57. The region in the foot hills of Tinh Bien and Tri Ton districts is classified as single rainy-season rice in the land use data. As there is a high possibility of error in this determination due to the mixed-pixel effect, these areas are excluded from analysis. The annual change in the areal ratio of triple rice-cropped area to the area of paddy fields in the 9 districts is shown in Fig. 58.

In 2000, triple rice cropping was not the predominant in this region, although the northern part of Cho Moi and eastern

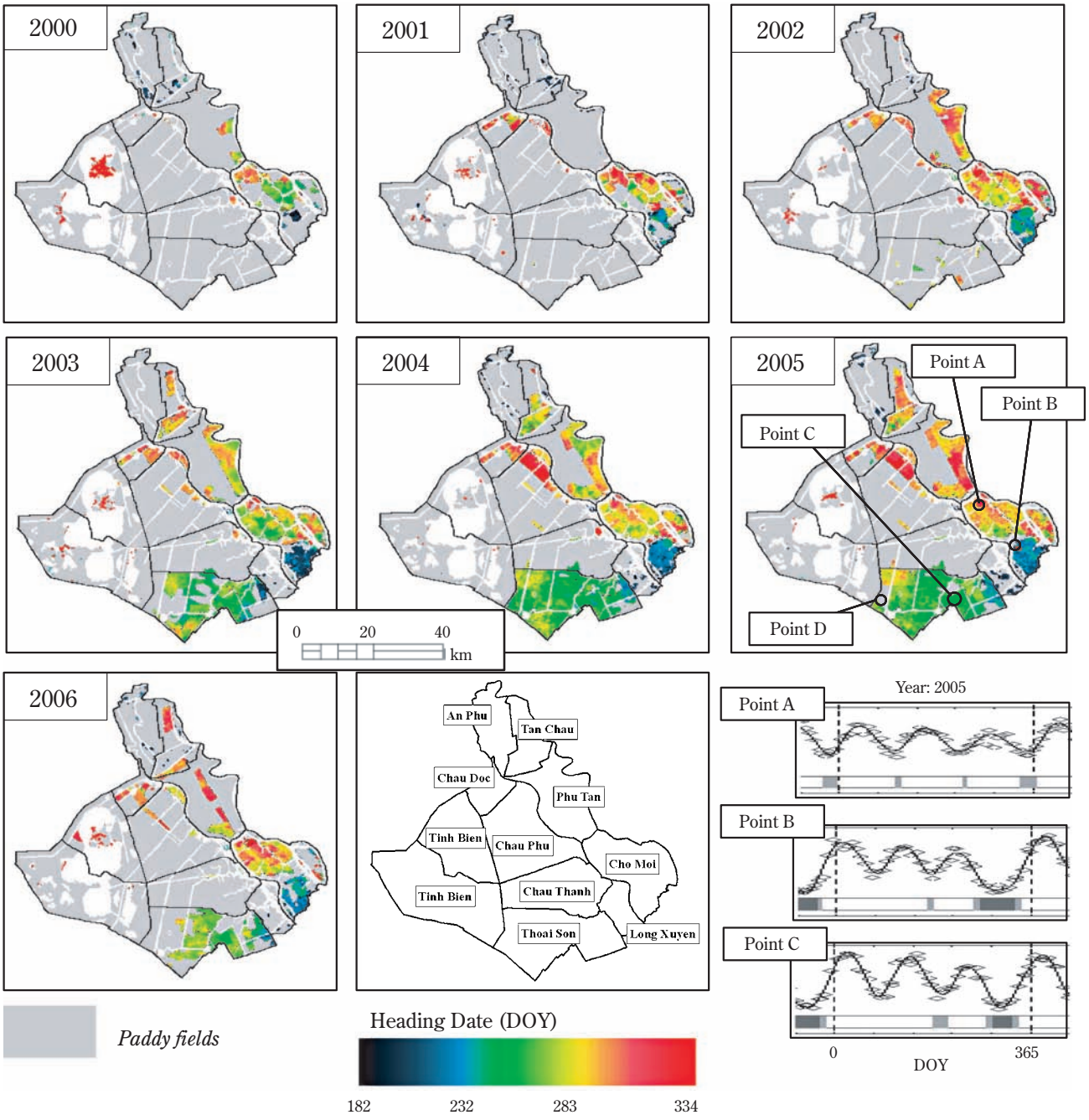

Fig. 56. Spatial distribution of the heading date of the third crop in An Giang province. Temporal EVI profiles with the estimated flood inundation in areas A, B, and C in 2005 are shown on the lower right.

Phu Tan exhibited some triple rice cropping (Fig. 56, 57). The most remarkable land-use change occurred in Thoai Son between 2002 and 2003 (Sakamoto et al., 2007). Due to constructions of water-resource infrastructure including dike system in 2003 to protect *the third cropping rice* against early-flood inundation, it became possible to conduct triple rice cropping in the area. The fractional area of triple rice cropping in the Thoai Son expanded from 5% to 60% in one year from 2002 to 2003, reaching 91% in 2004 (Fig. 57). The average areal ratio of triple rice-cropped area in the 9 districts considered here reached 42.4% in 2004 and 42.5 % in 2005 (Fig. 58). Although the start/end year of triple rice cropping varies between individual fields, the triple rice cropping has been conducted continuously in certain places for successive years (Fig. 57). In 2006, the ratio of triple rice-cropped area decreased drastically in 6 districts, while new triple rice-cropped area was initiated in small places of Chau Doc, Chau Phu, Tan Chau, and Phu Tan (Fig. 57). This implies that the available area for the triple rice cropping expanded potentially and continuously through this period.

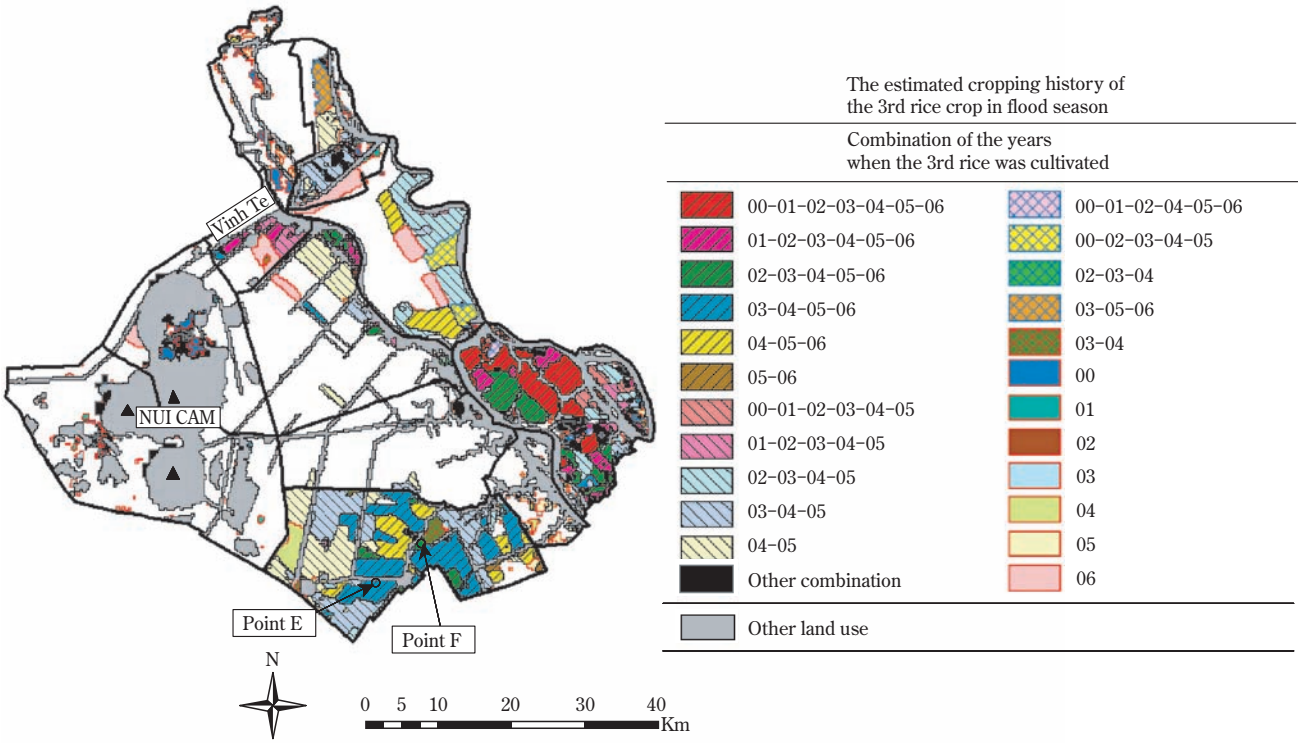

Fig. 57. Estimated cropping history of third crop in the flood season. Legend shows the combination of cropping years detected from temporal EVI data.

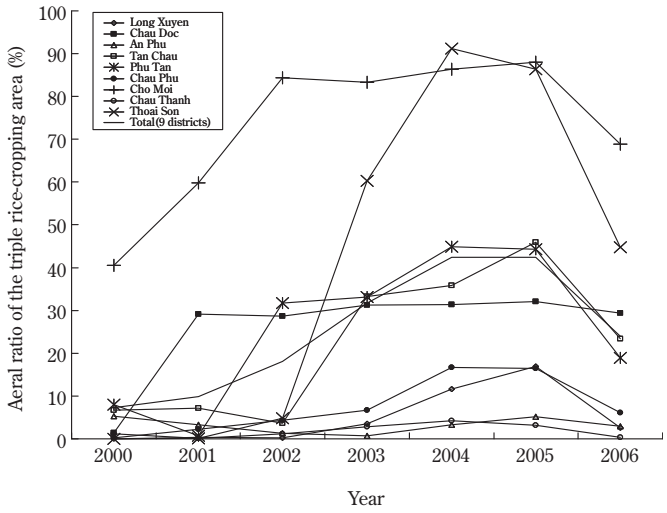

Fig. 58. Yearly change of the areal ratio of triple cropping to the entire paddy fields area in each district.

After the catastrophic flood in 2000, the Vietnamese Government introduced disaster mitigation slogan called as a "*Living with Flood*". This scheme had the effect of shifting the cropping calendar 3 months ahead in order to avoid the flood season. The existing embankments were also reinforced, and a small-scale dike system was constructed to protect the crops (Le et al., 2007; Tinh and Hang, 2003). Triple rice cropping was prompted in Phu Tan and Tan Chau (Fig. 56, 57) by a large-scale development project "*North Vam Nao Water Control Project*" undertaken by An Giang Province and an Australian overseas aid program (Australian Mekong Resource Centre, 2005). This project was implemented between December 2001 and September 2006, involving the construction of a large ring-dike system and water-control infrastructure to the total cost of A$31.4 million (Australian contribution, A$19.5 million). This infrastructure keeps

seasonal floodwater out, allowing rural farmers to increase rice productivity by growing three rice crops per year.

The estimated heading dates in the triple rice-cropped area (Fig. 56) varied regionally. Unlike the case of *the winter-spring rice*, the estimated heading date of *this third cropping rice* did not change substantially on an annual basis. That's why it was assumed that the improved infrastructure appears to control the soil-water conditions well through irrigation and drainage during the early season of flood inundation.

While the characteristic rice-cropping systems for 2005 are shown in Fig. 56 (points A, B and C) as determined from the temporal EVI profile and the water condition (*mixture/flood* pixels), the past experience of the triple rice cropping in these points was also confirmed from farmers interview in a field survey (February, September 2007). Southern Cho Moi (point B) had the earliest heading date for *the third cropping rice* in 2005 (Fig. 56). The inundation period prior to *the third cropping rice* in points B and C was longer than that in point A. The dike system is sometimes opened to allow floodwater into the fields (Sakamoto et al., 2007) to facilitate agricultural production by flushing pollution and pests (e.g., agro-chemicals, insects, and rats) and providing natural fertilizer via sedimentation (Long, 2003). Surplus water is also required for preparation of the land and sowing of following *winter-spring paddy crop*, as this practice reduces the irrigation cost in the dry season. In western Thoai Son (point D), where the triple rice-cropping system was conducted only once in 2004 (Fig. 56), the paddy fields were already enclosed by an embankment. According to an interview with farmer, the reason for not cultivating *a third cropping rice* in recent is that the dike system enclosing his paddy fields is susceptible to collapse in the flood season, probably because of the strength poverty due to design mistake. The large water-resource infrastructure was constructed at initiative of local government, but the small-size dikes should be built or maintained by farmer themselves. According to the interview with the farmer located in point E, he has to pay money for repairing the dikes enclosing his paddy field whether he want or not to conduct *third rice cropping*. Furthermore, the maintenance cost increased more than 1.5 times from the initial year of triple rice cropping. If the local leader supervising his paddy field decided to conduct the *third rice cropping*, he has no choice but to follow the decision for earning the dike-maintenance cost. Incidentally, it was confirmed that he decided not to conduct third rice cropping on the flood season in 2007 because of the local leader's decision of once fallow per 3 years. The new obligation such as economic and labor cost for maintenance of their dike system may be imposed on the local farmers.

According to the head of the agricultural sector in An Giang Province, the dramatic decrease in the area of triple cropping in 2006 is attributed to a large outbreak of Brown Plant Hopper (BPH) and Ragged Stunt Rice disease in *the summer-autumn rice* (as second rice cropping) and the related governmental emergency responses (Sai Gon Giai Phong, 2006). Up to 27,000 ha of paddy fields were plagued by pests in An Giag Province, and government encouraged local farmers to destroy any rice fields in which 30% of the crop area was affected (Viet Nam News, 2006). The local government has since strengthened measures aimed at controlling the cropping schedule for preventing the spread of infectious disease, encouraging farmers to leave fields fallow in the flood season and to flush the paddy field once every 3 year (i.e., 8 crops during 3 years). However the local government in district level has no teeth, just encourages to stop the triple-rice cropping, expect for the emergency situation. Final decision of farming system is made by local authority, farmer groups or farmer themselves. According to the interview with the farmer located in point F of Fig 57, it was considered that his local community does not follow the local government recommendation (once fallow per 3 years). As same as the estimated result from WFCS methodology (Fig. 57), he has continuously conducted the triple rice cropping since 2002. It was also confirmed that the third rice crop has been sown in his field on September 2007.

Although the direct cause for the large outbreak of BPH in 2006 is unclear, the rapid increase in rice-cropping intensity in this region may have affected the arthropod diversity and community structure, which is related to rice phenology (Settle et al., 1996; Wilby et al., 2006), and may take changes to the regional pest biodiversity and ecosystem through the discharged the fertilizer and agrochemicals (Bambaradeniya and Amarasinghe, 2003). Due to the Integrated Pest Management (IPM) training programs and media campaign in 1990's, unnecessary spraying of insecticides, particularly in the first 40 days after sowing, has gradually reduced and incomes have increased as a result of reduced

pesticide costs（Heong et al., 1998; Huan et al., 1999; 2005）. However, the nitrogen–rich crops and high crop intensity may provide potentially the better ecological fitness for the Brown Plant Hopper（Lu et al., 2004）, the spread of triple cropping with the high–yield rice variety in Vietnam and a broad range of cropping schedule may complicate the temporal and spatial dynamics of the pest population. Fortunately, the yield decrease of the whole Mekong delta due to the BPH problem was not serious in 2007, probably because of the countermeasures such as the proper IPM practices and the synchronous planting or sowing of two main crops（Summer–Autumn and Winter–Spring）in large area to avoid（escape）the BPH immigration in according with the forecasting system of light insect traps（Nguyen, 2007）. Additionally, Nguyen（2007）suggested that the synchronous planting against BPH immigration is not easy if the third crop（Autumn–Winter）continues as a linkage between the other two main cropping seasons. Thus it was considered that it is important to detect the spatio–temporal changes in rice phenolgoy, cropping system, and flood dynamics for assessment of not only agricultural productivity and but also the pest control.

5.6. Conclusions

The proprietary methods was applied to the time–series MODIS imagery acquired from 2000 to 2007 for understanding the agro–ecological meaning of the dynamic relationship between annual flood inundation and rice –cropping system in the VMD. The names of these methods are WFCP（Wavelet based Filter for determining Crop Phenology）, WFCS（Wavelet–based filter for evaluating the spatial distribution of Cropping Systems）, and WFFI（Wavelet–based filter for detecting spatio–temporal changes in Flood Inundation）. It was also recognized that there is the two–sided interplay between the regional environment and agricultural activity in the VMD through the analysis using remote sensing techniques in this study. It was revealed that the growing season of *the winter–spring rice*（recession rice）in the flood–prone area is strongly dependent on the annual flood scale, and the regional water–resource environment was gradually transformed by the construction of the water–resource infrastructure including a dike system in order to achieve favorable condition for *a third cropping rice* during the flood season.

It is seemed that the rice–cropping intensity and production in the VMD would be continuously increased by the wisdom of mankind that solves the environmental limiting factor for agricultural activity. At the same time, the increased rice–cropping intensity（triple rice cropping）may complicate the population dynamics of pest and diseases, resulting the heavy use of agrochemicals. After large outbreak of BPH in 2006, the local government pays particularly attention to the rice–cropping schedule, has encouraged farmers to leave fields fallow in the flood season and to flush the paddy field once every 3 year in order to take advantage of the positive effect of flood inundation for pest and disease protection. Towards the sustainable development of agricultural activity in rural area, there is a need for a better understanding of agro–ecological meaning in the interplay between the local environment and the agricultural activity from the macro viewpoint. Though the locally–varied land use and corresponding impact on the agricultural environment could not measured from the statistical data, it is considered that it becomes possible to visualize and understand the spatio–temporal relationship between them because of the advantage of remote sensing technology and our new methodologies. Additionally, understanding the regional macro–interrelation between the natural water cycle and agricultural activity is important in evaluation of the impact of global climate change on regional agricultural productivity and ecosystems.

5.7. Summary

The dynamic relationships among annual flood inundation, rice phenology and land–use change in the Vietnamese Mekong Delta（VMD）were evaluated using time–series MODIS imagery with the wavelet–based filter algorithms. A series of wavelet–based methodology（WFCP, WFCS, WFFI）are applied to MODIS time–series imagery acquired between 2000 and 2007 to detect the regional characteristics of *the winter–spring rice* phonology and its relationship with the annual flood regimes. This chapter focuses on the yearly change of the rice–cropping system in the An Giang province from 2000 to 2006. The finding of this chapter is that the cropping season of *the winter–spring rice* in the

flood-prone area of the upper VMD is spatially and temporally linked to the variable flood-recession season and hence the annual change of flood scale. The use of time-series MODIS imagery reveals that there is the spatio-temporal interrelationship between annual flood inundation and the agricultural activities in the VMD. The cropping season for *the winter-spring rice* in the flood-prone area fluctuates depending on the annual change of flood scale. The triple rice-cropped area in the An Giang province expanded from 2000 to 2005, because the construction of a ring-dike system and water-resource infrastructure have made it possible to sustain a *third rice cropping* during the flood season. However the area of *the third rice cropping* in the An Giang Province decreased drastically in 2006 due to the management of pest outbreaks. The rapid land-use change for the agricultural activity may complicate the spatio-temporal configuration of the agricultural environment in the VMD.

Chapter VI
General Discussion

In this study, proprietary methods of satellite imagery were used to detect the rice phenology, rice cropping pattern and flood inundation. The methodologies used were WFCP（Wavelet based Filter for determining Crop Phenology）, WFCS（Wavelet–based filter for evaluating the spatial distribution of Cropping Systems）, and WFFI（Wavelet–based Filter for detecting spatio–temporal changes in Flood Inundation）. These methods were applied the time–series MODIS imagery from 2000 to 2006 in order to reveal spatio–temporal changes of rice phenology and agricultural land–use patterns, with reference to short–to–medium variations in water resources in the Vietnamese Mekong Delta（VMD）. This chapter discusses current and future situations in the VMD, as revealed in this study（Chapter Ⅲ–Ⅴ）, and the results of the field survey conducted from 2005 to 2007.

One of the characteristics of agricultural land use in the VMD is the yearly change of rice–cropping patterns. These patterns, estimated from 2001 to 2005, are shown in Fig. 59. In An Giang Province, for example, the cropping pattern in some areas has changed from double cropping to triple cropping in the upper regions（Fig. 59 A）. Apart from the brown plant hopper（BPH）outbreak in 2006, which prevented triple cropping, it seems that the effects of flooding is no longer in serious restriction for triple rice cropping because of improved hydraulic structures such as canals, sluice gates and dike systems. In Soc Trang Province, triple rice–cropping areas, where dry–season cropping was introduced from 2002 to 2003（Fig. 59 B）, however, reverted to double rice cropping in 2004. In contrast, the triple rice–cropping areas in Bac Lieu Province successively expanded from 2001–2005, except in 2004（Fig. 59 C）. Field interviews revealed that the return to double rice cropping in Soc Trang Province was related to the failure of the dry–season harvest in 2004 due to water shortage probably caused by earlier salinity intrusion. The widely expanded triple cropping area may also cause the water shortage due to the excessive uptake of irrigation water reserved in canal. Recently, the local government has discouraged the triple rice cropping as part of measures to fight BPH. However in Bac Lieu Province, the regulation on triple cropping was not sufficiently strict to prevent farmers continuing to conduct triple cropping in specific areas where fresh irrigation water was available during the dry season. Field surveys in 2007（25th Feb– 3rd March, 1st – 12th June, Fig. 60）showed that opinions on triple rice cropping vary from farmer to farmer. In the flood–inundated area（An Giang Province）, two farmers（Fig. 60 A, B）who conducted triple rice cropping near the Mekong and Bassac rivers considered it to be feasible in the flood season because of the construction of dyes, and preferred triple rice cropping because of stable income. However, two other farmers（Fig. 60 C, D）who also conducted triple rice cropping in the Thoai Son district had a negative opinion. As discussed in Chapter 5, they considered that triple rice cropping in this area had many disadvantages, such as the large amount of labor and money needed to maintain and repair the small dike system, which are eroded easily by annual flood, enclosing their paddy fields.

At the same time, in the coastal area effected by salinity intrusion, farmers who have successfully practiced triple cropping, or who know of their neighbor's best practice with third rice cropping during the dry season（Fig. 60 E, F, G）, hope to continue with or revert to triple cropping, if fresh irrigation water is available in regular seasons, and triple cropping is also not banned by the local government. However, the other farmers（Fig. 60 H, I, J）in Soc Trang Province have a negative impression about the triple rice cropping because they failed to get enough harvests during the trial dry–season cropping in 2003 or 2004, due to the poor quality of the irrigation water. The results of our remote sensing analysis and field surveys clearly show two points. 1）The feasibility of the triple rice cropping depends on the qualitative and quantitative improvement in seasonal water regimes, in particular the control of salinity intrusion and flood protection. 2）If triple rice cropping is not strictly banned, the farmer decides whether to cultivate a third rice crop based on their own and their neighbor's experience, and on the costs and benefits. Moreover, it seems that the increase in the price of rice since 2001 and the higher yield of dry–season cropping（*Winter–Spring rice*）has encouraged farmers to attempt triple rice cropping in the coastal area（Fig. 61, 62）.

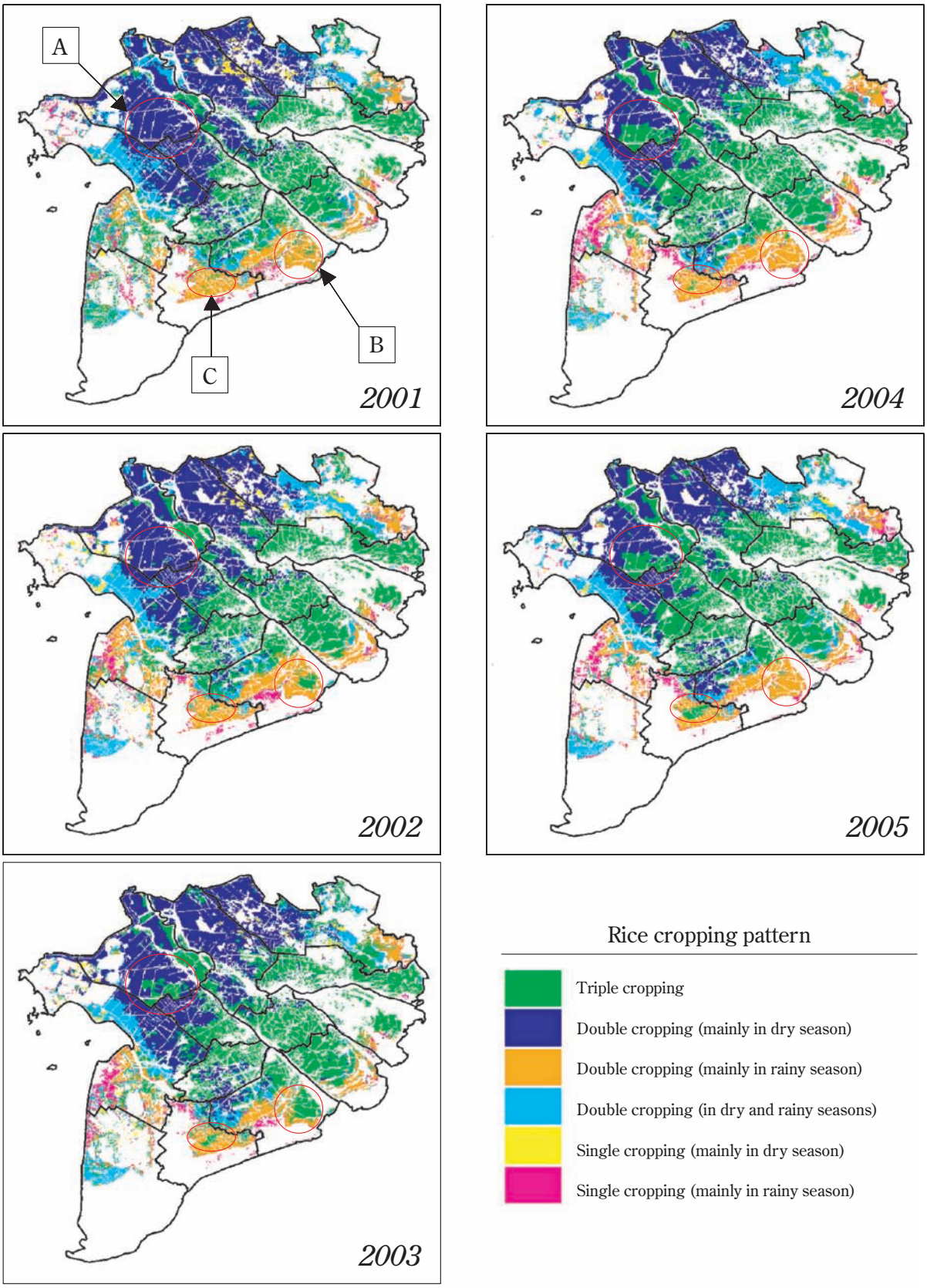

Fig. 59. Rice cropping pattern estimated by WFCS using the time-series MODIS data acquired from 2001 to 2006.

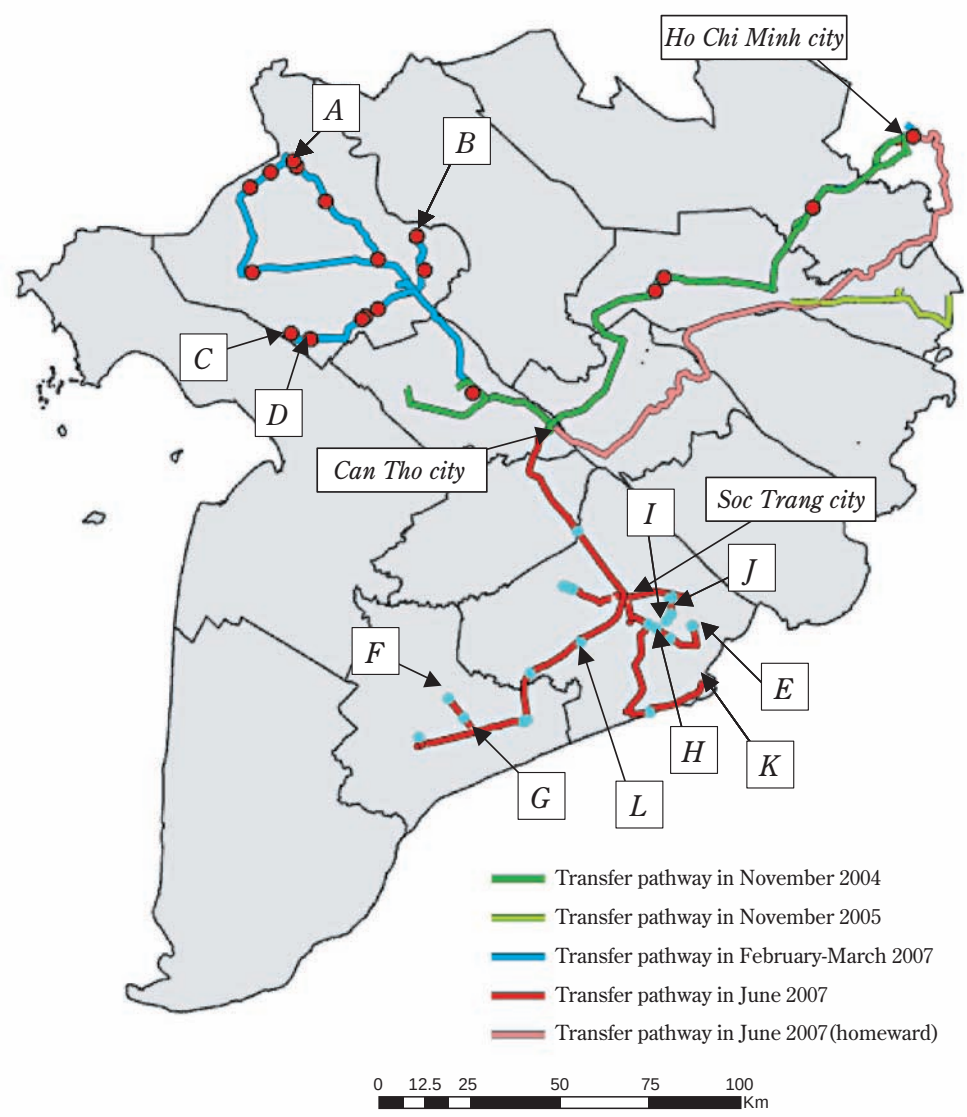

Fig. 60. Transfer pathway in the field surveys conducted since 2004

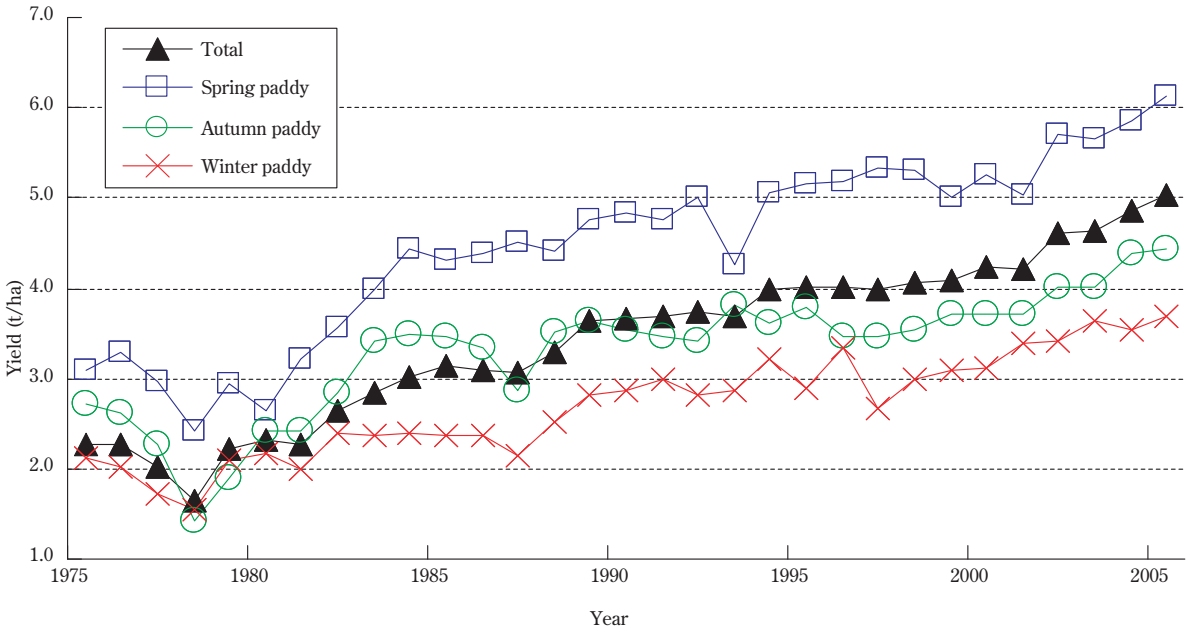

Fig. 61.Annual trend of rice yield in the Vietnamese Mekong Delta

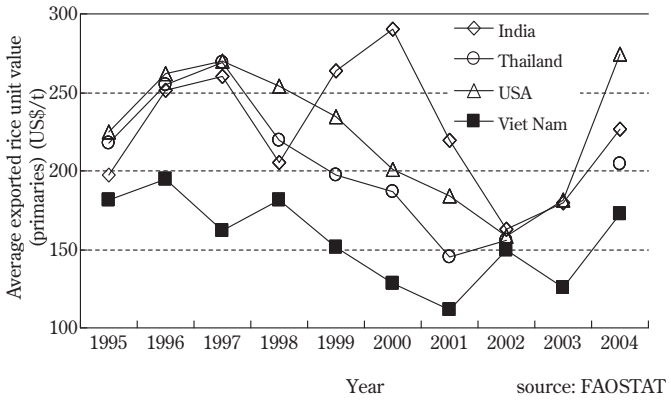

Fig. 62. Trend in price of rice for the major exporters'

The total area planted in rice in the VMD has been stable since 1999 (Fig. 63), while total rice production and the amount of exported successively increased (Fig. 9). The trends in land use and changes in the rice-cropping patterns shown in Chapter 3-5 (Fig. 59) have meant a decrease in the area of paddy fields being converted to shrimp ponds in the coastal area, but an increase in the area under triple rice cropping area as a result of improvements in hydraulic infrastructure. Thus, it could be said that the decrease in the rice planting area in the low rice-yield region has supported the recent increase in rice yield in the VMD, as well as an improvement in rice cultivars. The increase in crop intensity has enhanced Vietnamese rice production, but the diversified rice-cropping season in the VMD may need the more powerful control of the integrated pest management (IPM) for regulating the BPH population. According to the latest presentation about the countermeasure of BPH, the synchronous planting for large areas effectively controlled the BPH damage to avoid the BPH immigration in according with the forecasting system of light traps set up from the regional to local level.

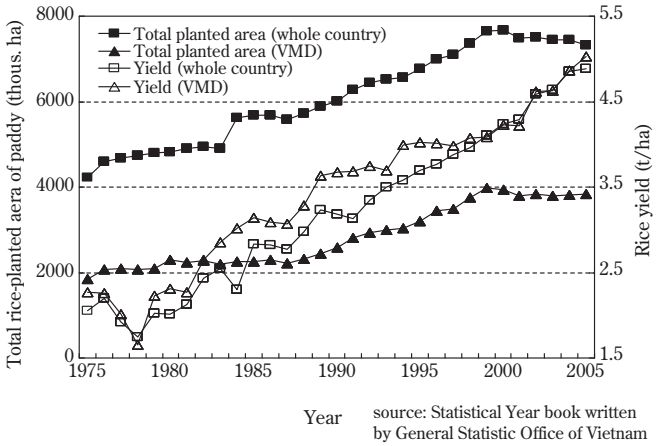

Fig. 63. Annual trend in the total rice-planted area and rice yield in the whole of Vietnam and in the VMD

The other characteristic of the VMD is the rapid change in land use from agricultural area and forestry to shrimp ponds in the coastal area, as explained in Chapter 4. This change was detected by WFFI, as revealed an expansion of the long-term water bodies in the coastal area from 2000 to 2004 (Fig. 42). This phenomenon is confirmed by the statistical data on aquaculture. Throughout the country, most of the area that increased from 2000 to 2005 as inland aquaculture is used for brackish-water shrimp farming (Fig. 64). The increased area of brackish-water shrimp farming in the VMD accounts for 70% of the increased area over the whole country (Fig. 65). Furthermore, 3 provinces in the VMD (Ca Mau,

Bac Lieu and Soc Trang）cultivate about 60% of the country's farmed shrimp（Fig 66）. As discussed in Chapter 5, the main trigger for this rapid expansion in shrimp farming in the VMD was a policy decision of the Vietnamese Government in 2000 to relax regulations on changing land use. The recent growth in the shrimp aquaculture industry may provide greater benefit than the low–yield rice cultivation in the coastal area, but would have a negative impact on the local people and environment. Actually, shrimp farmers interviewed（Fig. 60 K, L）said that their income from shrimp farming was 10 times greater than that from rice farming. However, many shrimp farmers have failed because the shrimp–disease outbreaks, and some farmers have had to sell their lands to pay off debts. In some regions on the boundary of shrimp farming and rice farming areas（Fig. 60 L）, conflict has arisen between farmers over control of irrigation water salinity. Where shrimp farmers increase the salinity of irrigation water, rice production suffers, and rice farmers have no choice but to change to shrimp farming whether they like or not. Some shrimp farmers have been reported destroying sluice gates, built to prevent the intrusion of salt water from the coastal area from which their benefit.

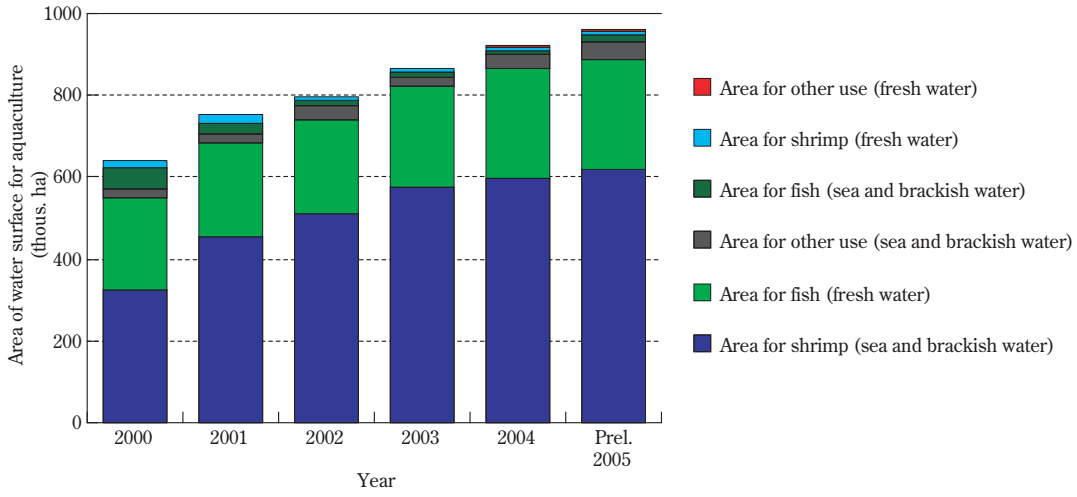

Fig. 64. Different types of inland aquaculture in the whole of Vietnam

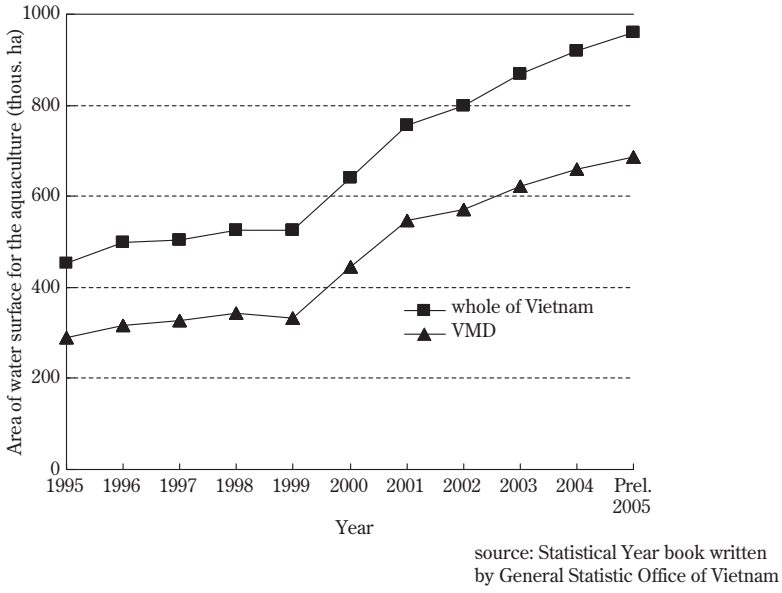

Fig. 65. Annual area of inland aquaculture in whole of Vietnam and in the VMD

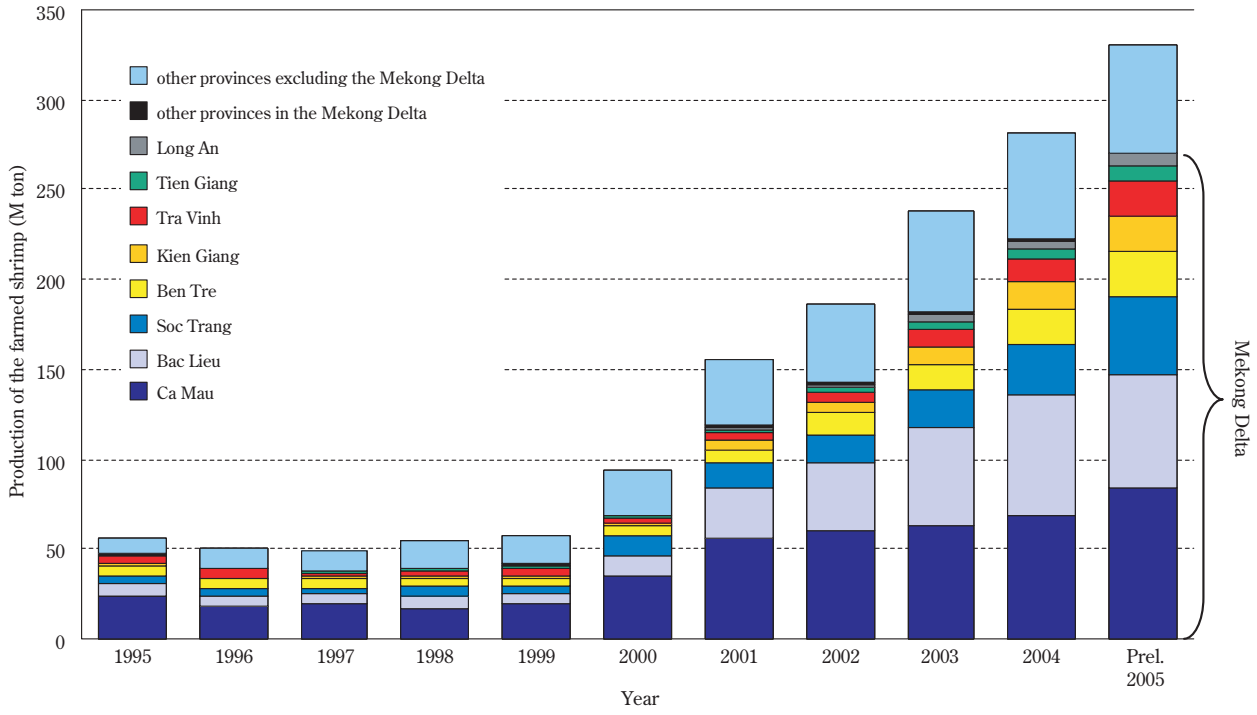

Fig. 66. Trend in the farmed shrimp production of each province of Vietnam

As mentioned above, after the introduction of the market-oriented economic system and the relaxation of regulations on land-use change, farmers now seem to view agriculture as a source of cash income rather than as a bread-and-butter job. The construction of hydraulic infrastructure and policy change on land use can easily transform the rural environment, and bring great benefit to agricultural production in the VMD, especially as a result of a determination to resolve the environmental limitations. However, as agriculture intensifies, heavy use of agrochemicals and water resources will have increasingly negative effects on the region's natural environment and ecosystem, which could never be measured in economic terms or shown by accurate statistical data. The developed countries are partly responsible for the unseen ecological losses that accompany agricultural progress in the developing world because they enjoy the benefits of the increasingly globalized free-market system by importing cheaper agricultural commodities (Japan, the EU and the US, for example, are the biggest importers Vietnamese shrimp).

The intensity of flood inundation during rainy seasons (Chapter Ⅳ) and of salinity intrusion during the dry season fluctuate yearly, due to short- to medium-term fluctuations in the global climate such as El Nino and La Nina. It was clearly shown that the sowing season of *winter-spring rice* in the upper VMD strongly depends on the flood intensity, which fluctuates annually spatially and temporally (Chapter Ⅴ). Changes in the water cycle caused by global warming may seriously affect the intensity and frequency of fluctuations in seasonal water resources. In addition, there is no doubt that the quantity of water-resource use in the upstream countries will increase as a result of the increasing demands for irrigation water in the expanding paddy fields, particularly in Cambodia, which has the second highest (1.73%) population growth after Laos (2.37%) of the six riparian countries (Vietnam:1.00%; China:0.61%; Thailand:0.66%; Myanmar:0.82%). Dam construction in the upper regions (e.g. the Nam Theun 2 Hydroelectric Project in Laos; the Chinese successive dam projects Gongguoqiao, Xiaowan, Manwan, Dachaoshan, Nuozhadu, Jinghong, Ganlanba, and Mengsong) will also affect the variability of seasonal water flow in the VMD. It is not known whether the intensified and more mono-cultural agricultural system, such as that being established in the VMD, will produce high and sustainable economic benefit in the future.

In this study, I have described the rapid changes in agricultural land use and rice cropping patterns, as well as their

macro relationship with seasonal water–environment changes in the VMD visually, using WFCP, WFCS and WFFI. Although there is no doubt that satellite remote sensing is a powerful tool to derive the land–surface information for the purpose of environmental research, it cannot conserve or change the global environment directly, based on an analysis of historical satellite imagery. However, I consider remote sensing technology useful for understanding the impact of human activities on the environment from a global perspective, and for examining the close relationship between human agricultural activity and the fluctuating natural environmental resources. This understanding may become a trigger for raising awareness about the global environment by reminding us of the changes in local cultivated and natural environments. Additionally, the up–to–date information of the agricultural production in foreign countries, which are derived from satellite imagery, would be useful intelligence for assessing the food security issues in Asia, as well as Japan. The significance of a thematic map or an animated movie（e.g., showing spatio–temporal changes in crop phenology and flood inundation）can be easily comprehended, even for people without technical knowledge.

I consider that the following two points realized through the case study in the VMD are important for those in advanced countries, including local policy makers. 1）If the regulation of the land use is relaxed, free–market and free –trade systems would rapidly reform local agricultural land use in developing countries and increase agricultural production efficiency, such as rice and shrimp production for export in the VMD. 2）While agricultural production and cropping systems strongly depend on the spatio–temporal variability of natural resources（water quantity and quality, solar radiation, rainfall, temperature, soil and so on）, there is a possibility that productivity of these intensified and mono –cultural agricultural systems could become less stable because of global climate change, and the possible competition for water–resource use among neighboring farmers or countries who share the same water sources. I hope that new knowledge on the macro relationship between the fluctuating natural environment and agriculture will help achieve environmentally friendly global food–supply system that brings sustainable prosperity for both consumers and producers.

Acknowledgements

I would like to express my profound gratitude to Professor Mikio Umeda for his detailed supervision of the writing of this dissertation. I am also grateful to Professor Shigeto Kawashima and Professor Naoshi Kondo for their valuable advice and careful review of this manuscript. This study, particularly the sections on the Mekong Delta, would not have been possible without the assistance and contribution provided by Drs. Masayuki Yokozawa and, Akihiko Kotera from NIAES, Dr. Nhyan van Nguyen from Sub-NIAPP and Dr. Cao van Phung from CLRI. I would like to special thanks to Drs. Hiroyuki Ohno and Naoki Ishitsuka as colleagues at the former Remote Sensing Unit; Drs. Hitoshi Toritani, Tsuneo Kuwagata, Yasuo Ishigooka, Shinkichi Goto, and Toshihiro Hasegawa of Agro-Meteorology Division in NIAES, Drs. Yoshio Inoue, Katsuo Okamoto, David Sprague, Nobuhiro Minaka, Nobusuke Iwasaki, and Kentaro Ohigashi of Ecosystem Bioinformatics Division for the meaningful discussion in the group seminar; Drs. Toshiaki Imagawa and Ichiro Taniyama of the research coordinator, Dr. Tetsuhisa Miwa of the director of Ecosystem Bioinformatics Division, for the supervision as the research executives before and after 5 pm. I am especially grateful to Drs. Masayuki Yokozawa and Katsuo Okamoto for their guidance and patient support of my first research papers written in Japanese and English, respectively. I would also like to acknowledge Ms. Trinh Thi Long, Dr. Vo Khac Tri, Mr. To Quang Toan and Dr. Nguyen Duy Khang, from the Southern Institute for Water Resources Research, for their valuable and constructive comments on the research manuscript, and conducting the field survey in the Mekong Delta. We would like to thank Dr. Makoto Nakai of NIAES for technical support with GIS data; Dr. Katsuyuki Shimizu of NIRE and Dr. Takeshi Watanabe of JIRCAS for their valuable suggestions of the research. I offer my special thanks to Dr. Takao Masumoto of NIRE for valuable comments and for providing the MRC Inundation maps used in Chapter Ⅳ; and to Director Nguyen Van Phuong of the Department of Agriculture and Rural Development for his valuable comments, and without whose support I could not have conducted the field survey in An Giang Province.

Appendix A
List of Figures

1. Time-series self sufficiency ratio of total food and grains in Japan from 1960 to 2005
2. Time-series food self-sufficiency ratio of the G7 from 1961 to 2003
3. Time-series grain self-sufficiency ratio of the G7 from 1961 to 2003
4. Cereal grains production, consumption, export and end-year stock from 1960 to 2006
5. Time-series data of soybean import from 1964 to 2006
6. Time-series data of soybean export from 1986 to 2006
7. Time-series harvested area of soybean from 1986 to 2006
8. Global market share trend of exported rice from 1960 to 2006
9. Quantity of rice production and exported rice for the whole of Vietnam and the VMD from 1961 to 2004
10. Quantity of frozen shrimp imported to Japan from 1988 to 2006
11. Major five countries' share of Japan's imported frozen shrimp from 1988 to 2006
12. Wavelet function (Coiflet 4) and sine function
13. Locations of the 30 test sites
14. Comparison between statistical data and the dates of phenological stages estimated by methods using Wavelet transform and Fourier transform.
15. One-to-one comparison between statistical data and phenological dates estimated by methods using Wavelet transform and Fourier transform. DOY = day of year
16. One-to-one comparison between statistical data and growing periods estimated by methods using Wavelet transform and Fourier transform.
17. Original EVI data and time profile smoothed by Wavelet transform and Fourier transform for data from Shiga_Kohoku (see Fig. 12).
18. The Mekong Delta showing provinces and river gauge stations.
19. Hydrometeorological data for An Giang Province. (A) Average monthly air temperature and precipitation in 2002. (B) Average monthly water level at the Chau Doc and Tan Chau stations from 1998 to 2002.
20. Land-use map for 2002 (Source: Sub-National Institute for Agricultural Planning and Projection of Vietnam)
21. Estimated number of crops per year in 2002 and 2003
22. Comparison of the number of crops per year between the estimate for 2002 and the reference land-use data
23. Validation of the overestimated number of crops in 2002 for the eastern Soc Trang Province. (A) Comparison of the number of crops per year between the reference land-use data and the number estimated from the smoothed EVI time profile in 2002. (B) Landsat ETM+ image (R: G: B = Band 5: Band 4: Band 3) for 12 January 2002. (C) Landsat ETM+ image for 13 February 2002. Temporal EVI data profiles of pixels α and β are shown in the upper right.
24. Validation of the underestimated number of crops in 2002 in eastern Dong Thap Province. (A) Comparison of the number of crops per year between the reference land-use data and the number estimated from the smoothed EVI time profile in 2002. (B) MODIS false-color image (R:G:B = Band 6: Band 2: Band 1) acquired on DOY 297-304 in 2002. The temporal EVI data for pixels γ and δ are shown on the right.
25. Comparison of the estimated number of crops per year between 2002 and 2003.
26. Average daily EVI data in areas where the number of crops per year decreased from three in 2002 to two in 2003 in the regions ε and ζ shown in Fig. 25.
27. MODIS false-color images of An Giang Province during the same period (DOY 297-304) in 2002 and 2003. R:G:B = Band 6: Band 2: Band 1.
28. Temporal EVI data for areas in which the cropping system changed from double in 2002 to triple in 2003. The data

refer to pixels η and θ in Fig. 27.

29. Comparison of the number of crops per year between 2002 and 2003 in eastern Soc Trang Province (A) and MODIS false-color images for 2002 and 2003 (enlargement of region I in Fig. 5 and region VI in Fig. 8) of the same region. (B) MOIDS 8-day composite image for DOY 65-72 in 2002. (C) MODIS 8-day composite image DOY 65-72 in 2003. R:G: B = Band 6: Band 2: Band 1.
30. Spatial distribution of heading dates in 2002 and 2003. The seasonal results for 2002 are shown on theleft and those for 2003 on the right: (a, e) period 1 (January, February, March); (b, f) period 2 (April, May, June); (c,g) period 3 (July, August, September); and (d, h) period 4 (October, November, December).
31. Time-series rainy-season water-level data at the Chau Doc station in 2001 and 2002.
32. Spatial distribution of cropping patterns in 2002 (A) and 2003 (B). Cropping patterns are described according to the estimated heading seasons (see Fig. 30). For example, the legend "1-2" means that two heading dates were estimated, one in period 1 (January to March) and another in period 2 (April to June).
33. Location map of the study area. The 24 provinces delineated by red boundaries are used as base units for area comparisons between WFFI and MRC products. Seven kinds of Land Use/Land Cover were selected with reference to the land use map of the Vietnamese Mekong Delta in 2002. Blue lines represent major rivers and canals. Regions I and II, as outlined by black rectangles, are further considered in Fig. 43 and 45, respectively.
34. Daily water-level data recorded at Tan Chau Station [Lat. 10.8°N, Long 105.2°E] from 2000 to 2004.
35. Flowchart of the workings of the Wavelet-based Filter for detecting the spatio-temporal changes on Flood Inundation (WFFI).
36. Domain-averaged smoothed Indexes [EVI, LSWI, and DVEL] of seven Land Use/Land Cover types for 2002. The locations of the seven Land Use/Land Cover areas shown in Fig. 33.
37. Temporal changes in the areal ratio of *Flood* and *Mixture* pixels in the three types of paddy fields and shrimp farms. The locations of these areas (Triple-cropped irrigated rice, Double-cropped irrigated rice, Double-cropped rainfed rice, and shrimp farm) are shown in Fig. 33.
38. Spatial comparison of WFFI products, MRC products, and MODIS 8-day composite false-color and daily false-color images for the study area, as shown in Fig. 1. (A1, 2, 3) WFFI products. (B1, 2, 3) MRC products. (C1, 2, 3) MODIS 8 -day composite false-color images. (D1, 2, 3) MODIS daily false-color images. R:G:B = Band 6: Band 2: Band 1.
39. Comparison of inundated areas predicted by WFFI and MRC products at the province level. Target provinces and regions are delineated by red lines in Fig. 33.
40. Distribution of the water-surface area derived from Landsat images. The colors; Blue, Green, and Red indicate the areas of water-surface, not water-surface, and non-analysis respectively. The numbers of the Landsat images are the same as the ID numbers listed in Table 6.
41. Comparison of the inundated area at a 10-km grid level between the Landsat-derived results and the WFFI products.
42. Maximum estimated extent of the floodplain over the period 2000 to 2004.
43. Seasonal changes in the extent of the estimated area of *Flood* pixels within Dong Thap and Long An Provinces.
44. Spatial distribution of inundated areas on the first day of every month from June to January of the following year. Areas of blue indicate the distribution of *Flood* pixels and areas of green indicate *Mixture* pixels.
45. Temporal changes in flood inundation around the Cambodia-Vietnam border during flood seasons over the period: 2000-2004 (enlargement of Region I in Fig. 1). Areas of blue indicate *Flood* pixels, while areas of green indicate *Mixture* pixels.
46. Spatial distribution of the start date, end date, and duration of inundation cycles over the period from 2000 to 2004.
47. Start date, end date, and duration of inundation cycles within An Giang and Can Tho Provinces (enlargement of Region II in Fig. 33.). The colors used for the start date, end date, and duration are the same as those used in Fig. 46.
48. Total area planted in rice, and Area of water surface used for aquaculture and the production of farmed shrimp in Ca

Mau and Bac Lieu Provinces from 2000 to 2004. Sources: Bac Lieu Statistical Office (2005), Ca Mau Statistical Office (2005), and General Statistics Office (2005).

49. Location of study area. The objective flood–prone area is defined by the inundation period (2–6 months) of "*Flood*" pixels in 2000 estimated by the WFFI methodology.
50. Smoothed EVI time profile with observed EVI data from 2000 (DOY 57) to 2007 (DOY 56) in (A) an area in which the cropping system did change in the observation period (area A in Fig. 49), and (B) an area in which the cropping system changed from double cropping to triple cropping (area B in Fig. 49).
51. Daily water–level data recorded at Tan Chau station from 2000 to 2005.
52. WFFI estimation of (A) duration, (B) start date, and (C) end date of annual inundation in the flood–prone area from 2000 to 2005. (D) Estimated heading date after the end of the inundation cycle.
53. Temporal profile of average daily EVI and areal ratio of "*Flood*" and "*Mixture*" pixels derived by the WFFI method from the mid–flood season to the end of the subsequent–crop season (DOY: 250–450) over the period from 2000 to 2005. Arrows indicate the dates corresponding to the maximal point in the temporal EVI profile and the half point (50%) in the areal ratio of "*Flood*" and "*Mixture*" pixels.
54. Comparison between estimated end date of inundation cycles and subsequent heading date in the flood–prone area from 2000 to 2005. The summation of the comparisons in each year is shown on the right.
55. Map of determination coefficient (R^2) between the end of the inundation cycle and the subsequent heading date in the flood–prone area of the VMD.
56. Spatial distribution of the heading date of the third crop in An Giang province. Temporal EVI profiles with the estimated flood inundation in areas A, B, and C in 2005 are shown on the lower right.
57. Estimated cropping history of third crop in the flood season. Legend shows the combination of cropping years detected from temporal EVI data.
58. Yearly change of the areal ratio of triple cropping to the entire paddy fields area in each district.
59. Rice cropping pattern estimated by WFCS using the time–series MODIS data acquired from 2001 to 2006.
60. Transfer pathway in the field surveys conducted since 2004
61. Annual trend of rice yield in the Vietnamese Mekong Delta
62. Trend in price of rice for the major exporters'
63. Annual trend in the total rice–planted area and rice yield in the whole of Vietnam and in the VMD
64. Different types of inland aquaculture in the whole of Vietnam
65. Annual area of inland aquaculture in whole of Vietnam and in the VMD
66. Trend in the farmed shrimp production of each province of Vietnam

Appendix B
List of Tables

1. Comparison of root mean square error (RMSE) of the estimated phenological date and growing period against the statistical data.
2. Number of cases that the estimated dates are within the period from beginning to end of each phonological seasons in statistical data.
3. Confusion matrix of the number of crops per year between the amount estimated in 2002 and the land–use data.
4. Confusion matrix of the number of crops per year between the amount estimated in 2002 and 2003.
5. Sown paddy area and area dedicated to aquaculture from 2001 to 2003 (thousands Ha).
6. Estimated accuracy of WFFI products relative to the inundation area derived from Landsat images.
7. Total number of days that the daily water–level in Tan Chau station exceeded the reference level.

References

1) Akiyama, T., K. Kawamura, A. Fukuo and Z.Z. Chen (2002) : Sustainable grassland management using GIS, GPS and remote sensing data in Inner Mongolia. *Application on remote sensing technology for the management of agricultural resources, China Agricultural Scientech Press*, Beijing, 13–19
2) Alcaraz, D., J. Paruelo and J. Cabello (2006) : Identification of current ecosystem functional types in the Iberian Peninsula. *Global Ecology and Biogeography*, **15**, 200–212
3) An Giang Statistical Office (2003) : Statical yearbook An Giang Province 2002 : An Giang., p. 276 An Giang Statical Office., An Giang
4) Anderson, E., G.R. Brakenridge and S. Caquard (2005) : Dartmouth Atlas of Global Food Hazard: E100N20. Dartmouth Flood Observatory, Hanover, USA, Available at. http: //www.dartmouth.edu/~floods/hydrography/E100N120.html
5) Australian Mekong Resource Centre, U.o.S. (2005) : Dealing with Confilict and Risk. Water Governance in Context, *Project final report Working paper #5* Available at http: //www.mekong.es.usyd.edu.au/projects/water_governance.htm, 1–11
6) Azzali, S. (2000) : Mapping vegetation–soil–climate complexes in southern Africa using temporal Fourier analysis of NOAA–AVHRR NDVI data. *International Journal of Remote Sensing*, **21**, 973–996
7) Bac Lieu Statistical Office (2003) : Statical yearbook Bac Lieu Province 2002: Bac Lieu., p. 198 Bac Lieu Statical Office, Bac Lieu
8) Bac Lieu Statistical Office (2005) : Statical yearbook Bac Lieu Province 2004: Bac Lieu., p. 199 Bac Lieu Statical Office, Bac Lieu
9) Bambaradeniya, C.N.B. and F.P. Amarasinghe (2003) : Biodiversity associated with the Rice Field Agroecosystem in Asian Countries, IWMI Working Paper 63, p. 29 International Water Management Institute, Colombo, Sri Lanka
10) Binh, T., N. Vromant, N. Hung, L. Hens and E. Boon (2005) : Land Cover Changes Between 1968 and 2003 In Cai Nuoc, Ca Mau Peninsula, Vietnam. *Environment, Development and Sustainability*, **7**, 519–536
11) Bormanb Am, K.M.J. and T.P. Tuong (2001) : ORYZA2000: modeling lowland rice., p.235 International Rice Research Institute. Manila, Philippines
12) Brandt, J.S. and P.A. Townsend (2006) : Land use – land cover conversion, regeneration and degradation in the high elevation Bolivian Andes. *Landscape Ecology,* 21, 607–623
13) Brivio, P.A., R. Colombo, M. Maggi and R. Tomasoni (2002) : Integration of remote sensing data and GIS for accurate mapping of flooded areas. *International Journal of Remote Sensing*, **23**, 429–441
14) Bryant, R.G. and M.P. Rainey (2002) : Investigation of flood inundation on playas within the Zone of Chotts, using a time–series of AVHRR. *Remote Sensing of Environment*, **82**, 360–375
15) Cabinet Office , G.o.J. (2006) : Abailable at: http: //www8.cao.go.jp/survey/
16) Central Intelligence Agency (2007) : The World Factbook, Available at: https: //www.cia.gov/library/publications/the–world–factbook/index.html
17) Cho, K. (2005) : Vietnamese agriculture and farming village under Market–Oriented Economy (in Japanese). p. 326 Tsukuba–shobo, Tokyo, Japan
18) Dartmouth Flood Observatory (2006) : Dartmouth Flood Observatory, Dartmouth atlas of global flood hazard, Available at http: //www.dartmouth.edu/~floods/index.html
19) Daubechies, I. (1988) : Orthonormal bases of compactly supported wavelets. Comm. Pure *Appl. Math*, **41**, 909–996
20) Dijk, V.A.N. (1987) : Smoothing vegetation index profiles–An alternative method for reducing radiometric disturbance in NOAA/AVHRR data. *Photogrammetric Engineering and Remote Sensing*, **53**, 1059–1067
21) Dingkuhn, M. and P.Y. Le Gal (1996) : Effect of drainage date on yield and dry matter partitioning in irrigated rice.

Field Crops Research, **46**, 117–126

22) Disaster Management Unit (2004) : Disaster Management Unit, Total annual damage caused by flood and storm in Vietnam, Available at http: //www.undp.org.vn/dmu/index.html

23) Echeverria, C., A.C. Newton, A. Lara, J.M.R. Benayas and D.A. Coomes (2007) : Impacts of forest fragmentation on species composition and forest structure in the temperate landscape of southern Chile. *Global Ecology and Biogeography*, **16**, 426–439

24) EOS (2007) : NASA earth observing system data gateway. Available at. http: //edcimswww.cr.usgs.gov/pub/imswelcome/

25) Estellès, P., H. Jensen and L. Sanchez (2002) : Sustainable development in the Mekong Delta., p. 108 Afdeling for Miljostudier/Center for Environmental Studies, Aarhus

26) Fang, H.T. and D.S. Huang (2004) : Noise reduction in Lidar signal based on discrete wavelet transform. *Opt. Commun*, **233**, 67–76

27) FAO (1999) : Global climate maps, Available at http: //www.fao.org/sd/EIdirect/climate/EIsp0002.htm

28) FAOSTAT (2007) : FAO statistical databases. Available at http: //faostat.fao.org/

29) Frolking, S., J.B. Yeluripati and E. Douglas (2006) : New district-level maps of rice cropping in India: A foundation for scientific input into policy assessment. *Field Crops Research*, **98**, 164–177

30) Fujii, H. (2004) : Hydrological survey and water balance of the Cambodian floodplain in the Mekong River (in Japanese and English Abstract). *Technical Report of the National Institute For Rural Engineering*, **202**, 127–140

31) Fujii, H., H. Garsdal, P. Ward, M. Ishii, K. Morishita and T. Boivin (2003) : Hydrological roles of the Cambodian floodplain of the Mekong River. *International Journal of River Basin Management*, **1**, 1–14

32) Gao, B. (1996) : NDWI--A normalized difference water index for remote sensing of vegetation liquid water from space. *Remote Sensing of Environment*, **58**, 257–266

33) General Statistics Office (2000) : Statistical data of vietnam, agriculture, forestry and fishery 1975–2000., p.586 Statistical Publishinng House, Hanoi

34) General Statistics Office (2004) : Statistical yearbook 2003. p. 778 Statistical Publishinng House., Hanoi, Vietnam

35) General Statistics Office (2006) : Statistical yearbook of Vietnam 2005. p. 738 Statistical Publishinng House., Hanoi, Vietnam

36) Gilbert, M., X.M. Xiao, P. Chaitaweesub, W. Kalpravidh, S. Premashthira, S. Boles and J. Slingenbergh (2007) : Avian influenza, domestic ducks and rice agriculture in Thailand. *Agriculture,Ecosystems & Environment*, **119**, 409–415

37) Giri, C., T.A. Moe, S. Shrestha and J. Aschbacher (2000) : Multi-temporal analysis of the VEGETATION data for land cover assessment monitoring in Indochina. Vegetation-2000. Lake Maggiore, Italy, April 3–6

38) GLCF (2006) : Global land cover facility, Available at http: //www.landcover.org

39) GSO (2007) : General Statistics Office of Vietnam. Abailable at: http: //www.gso.gov.vn/

40) Gupta, A.D., M.S. Babel and P. Ngoc (2004) : Flood assessment in the Mekong Delta, Vietnam. Proceedings of the Asia Pacific Association of Hydrology and Water Resources (APHW), 2nd Conference held at the Suntec International Convention and Exhibition Center, Available at: http: //www.wrrc.dpri.kyoto-u.ac.jp/~aphw/APHW2004/APHW2004.html

41) Hara, M., S. Okada, H. Yagi, T. Moriyama, K. Shigehara and Y. Sugimori (2003) : Developing and evaluation of the noise reduction filter for the time-series satellite image (in Japanese, with English abstract). *Journal of the Japan Society of Photogrammetry and Remote Sensing*, **5**, 48–59

42) Harris, A.R. and I.M. Mason (1989) : Lake Area Measurement Using Avhrr – a Case-Study. *International Journal of Remote Sensing*, **10**, 885–895

43) Haruyama, S. and K. Shida (2006) : Flood risk evaluation of the Mekong River Delta utilizing JERS-1 SAR images (in Japanese with English abstract). *Journal of Geography*, **115**, 72–86

44) Heinl, M., A. Neuenschwander, J. Sliva and C. Vanderpost (2006) : Interactions between fire and flooding in a southern African floodplain system (Okavango Delta, Botswana). *Landscape Ecology*, **21**, 699–709

45) Henry, J.B., P. Chastanet, K. Fellah and Y.L. Desons (2003) : ENVISAT multi-polarised ASAR data for flood mapping. *Proceedings of IGRASS'03*, Toulouse, France

46) Heong, K.L., M.M. Escalada, N.H. Huan and V. Mai (1998) : Use of communication media in changing rice farmers' pest management in the Mekong Delta, Vietnam. *Crop Protection*, **17**, 413–425

47) Heremans, R., A. Willekens, D. Borghys, B. Verbeeck, J. Valckenborgh and M.e.a. Acheroy (2005) : Automatic detection of flooded areas on ENVISAT/ASAR images using an objected-oriented classification technique and active contour algorithm. Proceedings of the 31st International Symposium on Remote Sensing of the Environment. June 20 –24, 2005 St. Petersburg, Russia

48) Higgins, P.A.T. (2007) : Biodiversity loss under existing land use and climate change: an illustration using northern South America. *Global Ecology and Biogeography*, **16**, 197–204

49) Hirose, K., Y. Maruyama, D.V. Quy, M. Tsukada and Y. Shiokawa (2001) : Visualization of flood monitoring in the lower reaches of the Mekong River. *Proceedings of 2nd Asian Conference on Remote Sensing*. 314–319 November 5–9 2001, Singapore,

50) Hoanh, C.T., H. Guttman, P.Droogers and J. Aerts (2003) : Water, climate, food, and environment in the Mekong Basin in Southeast Asia. Contribution to project ADAPT, adaptation strategies to changing environments. Final report, p. 58 Available at http: //sheba.geo.vu.nl/~ivmadapt/downloads/Mekong_FinalReport.pdf

51) Hori, H. (1996) : The Mekong: Development and its environmental effects (in Japanese)., p. 476 Kokon-Shoin Publishing., Tokyo

52) Huan, N.H., V. Mai, M.M. Escalada and K.L. Heong (1999) : Changes in rice farmers' pest management in the Mekong Delta, Vietnam. *Crop Protection*, **18**, 557–563

53) Huan, N.H., L.V. Thiet, H.V. Chien and K.L. Heong (2005) : Farmers' participatory evaluation of reducing pesticides, fertilizers and seed rates in rice farming in the Mekong Delta, Vietnam. *Crop Protection*, **24**, 457–464

54) Huete, A., K. Didan, T. iura, E.P. Rodriguez, X. Gao and L.G. Ferreira (2002) : Overview of the radiometric and biophysical performance of the MODIS vegetation indices. *Remote Sensing of Environment*, **83**, 195–213

55) Humphreys, E., L.G Lewin, S. Khan, H.G. Beecher, J.M. Lacy, J.A. Thompson, G.D. Batten, A. Brown, C.A. Russell, E.W. Christen and B.W. Dunn (2006) : Integration of approaches to increasing water use efficiency in rice-based systems in southeast Australia. *Field Crops Research*, **97**, 19–33

56) Huu-Thoi, N. and A. Gupta (2000) : Assessment of Water resources and salinity intrusion in the Mekong Delta. *Water international*, **26**, 86–95

57) IPCC Working Group I (2001) : Climate Change 2001: The Scientific Basis., p. 881 Cambridge University Press, Cambridge

58) Ishitsuka, N., G. Saito, T. Murakami, S. Ogawa and K. Okamoto (2003) : Methodology development for area determination of rice planted paddy using RADARSAT data. (in Japanese with English abstract). *Journal of the Remote Sensing Society of Japan*, **23**, 458–472

59) ITT Visual Information Solutions, http: //www.ittvis.com/index.asp

60) Jackson, T.J., D. Chen, M. Cosh, F. Li, M. Anderson, C. Walthall, P. Doriaswamy and E.R. Hunt (2004) : Vegetation water content mapping using Landsat data derived normalized difference water index for corn and soybeans. *Remote Sensing of Environment*, **92**, 475–482

61) Jakubauskas, M.E., D.R. Legates and J.H. Kastens (2002) : Crop identification using harmonic analysis of time-series AVHRR NDVI data. *Computers and Electronics in Agriculture*, **37**, 127–139

62) Ji, R., B.Y. Xie, D.M. Li, Z. Li and X. Zhang (2004) : Use of MODIS data to monitor the oriental migratory locust plague. *Agriculture Ecosystems & Environment*, **104**, 615–620

63) Jin, Y.Q.（1999）：A flooding index and its regional threshold value for monitoring floods in China from SSM/I data. *International Journal of Remote Sensing*, **20**, 1025–1030

64) Kang, S., S.W. Running, J.H. Lim, M. Zhao, C.R. Park and R. Loehman（2003）：A regional phenology model for detecting onset of greenness in temperate mixed forests, Korea: an application of MODIS leaf area index. *Remote Sensing of Environment*, **86**, 232–242

65) Karlsen, S.R., A. Elvebakk, K.A. Hogda and B. Johansen（2006）：Satellite-based mapping of the growing season and bioclimatic zones in Fennoscandia. *Global Ecology and Biogeography*, **15**, 416–430

66) Kazama, S.（2001）：Report on flood and inundation in the Mekong River Basin in 2000（in Japanese with English abstract）. *Japan Society for Natural Disaster Science*, **19**, 493–500

67) Kazama, S.O., Y. Muto, K. Nakatsuji and K. Inoue（2002）：STUDY ON THE 2000 FLOOD IN THE LOWER MEKONG BY FIELD SURVEY AND NUMERICAL SIMULATION. Proc. 13th congress the APD/IAHR, **1**, 534–539

68) Kerr, J.T. and J. Cihlar（2003）：Land use and cover with intensity of agriculture for Canada from satellite and census data. *Global Ecology and Biogeography*, **12**, 161–172

69) Khan, V.M., R.M. Vilfand and P.O. Zavialov（2004）：Long-term variability of air temperature in the Aral sea region. *Journal of Marine Systems*, **47**, 25–33

70) Kimball, J.S., K.C. McDonald, S.W. Running and S.E. Frolking（2004）：Satellite radar remote sensing of seasonal growing seasons for boreal and subalpine evergreen forests. *Remote Sensing of Environment*, **90**, 243–258

71) Koger, C.H., L.M. Bruce, D.R. Shaw and K.N. Reddy（2003）：Wavelet analysis of hyperspectral reflectance data for detecting pitted morningglory（Ipomoea lacunosa）in soybean（Glycine max）. *Remote Sensing of Environment*, **86**, 108–119

72) Koizumi, T.（2006）：U.S. Ethanol Policy; Impacts on Corn Market in Jpanese with English Abstract. *Journal of Agricultural Policy Research*, **11**, 53–72

73) Kono, Y.（2001）：Canal Development and Intensification of Rice Cultivation in the Mekong Delta: A Case Study in Cantho Procince, Vietnam. *Southeaset Asian Studies*, **39**, 70–85

74) Kurosu, T., M. Fujita and K. Chiba（1995）：Monitoring of rice crop growth from space using the ERS-1 C-bandSAR. *Geoscience and Remote Sensing, IEEE Transactions on*, **33**, 1092–1096

75) Kuusemets, V. and U. Mander（2001）：Nutrient flows and management of a small watershed. *Landscape Ecology*, **17**, 59–68

76) Laugier, O., K. Fellah, N. Tholey, C. Meyer and P. De Fraipont（1997）：High temporal detection and monitoring of flood zone dynamic using ERS data around catastrophic natural events: The 1993 and 1994 Camargue Flood events. *Proceedings of the third ERS Symposium, ESA SP-414*, 559–564

77) Le, T.V.H., H.N. Nguyen, W. Eric, T.C. Tran and H. Shigeko（2007）: The combined impact on the flooding in Vietnam's Mekong River delta of local man-made structures, sea level rise, and dams upstream in the river catchment. *Estuarine Coastal and Shelf Science*, **71**, 110–116

78) Li, Z. and M. Kafatos（2000）：Interannual Variability of Vegetation in the United States and Its Relation to El Nino/ Southern Oscillation. *Remote Sensing of Environment*, **71**, 239–247

79) Liew, S.C., S.P.Kam, T.P. Tuong, P. Chen, V.Q.Minh and H. Lim（1998）：Application of multitemporal ERS-2 synthetic aperture radar indelineating rice cropping systems in the Mekong River Delta, Vietnam. *Geoscience and Remote Sensing, IEEE Transactions on*, **36**, 1412–1420

80) Liu, Z., F. Huang, L. Li and E. Wan（2002）：Dynamic monitoring and damage evaluation of flood in north-west Jilin with remote sensing. *International Journal of Remote Sensing*, **23**, 3669–3679

81) Long, T.T.（2003）：Impacts of flow regimes on environmental conditions in the Mekong Delta of Vietnam. *Integrating Environmental Impacts into Water Allocation Models of the Mekong River Basin*, Workshop in Ho Chi Min City, Vietnam

82) Lu, Z.X., K.L. Heong, X.P. Yu and C. Hu (2004) : Effects of plant nitrogen on ecological fitness of the brown planthopper, Nilaparvata lugens Stal in rice. *Journal of Asia-Pacific Entomology*, **7**, 97-104

83) Ludwig, J.A., G.N. Bastin, J.F. Wallace and T.R. McVicar (2007) : Assessing landscape health by scaling with remote sensing: when is it not enough? *Landscape Ecology*, **22**, 163-169

84) Mahmood, R. (1997) : Impacts of air temperature variations on the boro rice phenology in Bangladesh: implications for irrigation requirements. *Agricultural and Forest Meteorology*, **84**, 233-247

85) McFeeters, S.K. (1996) : Use of the normalized difference water index (NDWI) in the delineation of open water features. *International Journal of Remote Sensing*, **17**, 1425-1432

86) McKenney, B. and P. Tola (2002) : Natural resources and rural livelihoods in Cambodia: A baseline assessment, Working paper 23, p. 116 Cambodia Development Resource Institute, Phnom Penh, Cambodia

87) Mekong River Commission (2005) : Overview of the hydrology of the Mekong Basin. p. 73, Mekong River Commission, Vientiane, LaoPDR

88) Minh, H.N.T. and T. Kawaguchi (2002) : Overview of Rice Production System in the Mekong Delta?Vietnam. *J. Faculty Agric. Kyushu Univ*, **47**, 221-231

89) Ministry of Agriculture, F.a.F.o.J. (2003) : Statistical year book for crops. P. 239 Tokyo: Nourin Tokei Kyokai, Tokyo

90) MLIT (1997) : Ministry of Land, Infrastructure and Transport Government of Japan, Download site for distributing digital national information Available at: http: //nlftp.mlit.go.jp/ksj/

91) Neefjes, K. (2002) : Lessons from the floods Voice of the people, local authorities, and disaster management agencies from the Mekong Delta in Vietnam, p. 6 Available at http: //www.undp.org.vn

92) Nguyen, N.V., H.M. Do, A.N. Nguyen and K.V. Le (2004a) : Rice production in the Mekong Delta (Vietnam) : Trends of development and diversification. *Mekong Rice Conference 2004: Rice the Environment, and Livelihoods for the Poor* 15-17. Ho Chi Minh City, Vientam

93) Nguyen, V.H. (2007) : Considering BPH as a factor to adjust the cropping patterns of rice production in the Mekong Delta. *CLRRI-IRRI international conference "Better Rice, Better Environment and Better Life"*., 83-86 Cuu Long Delta Rice Research Institute, Cantho, Vietnam

94) Nguyen, V.L. (2000) : Crop diversification in Vietnam. In K.P.M.a.J.D. Frank (Ed.), Crop diversification in the Asia-Pacific Region p. 189. FAO Regional Office for Asia and the Pacific, Bangkok

95) Nguyen, V.N., M.H. Do, N.A. Nguyen and V.K. Le (2004b) : Rice production in the Mekong delta (Vietnam) : Trends of development and diversification. *Mekong Rice Conference 2004: Rice the Environment, and Livelihoods for the Poor* 8-18 in Ho Chi Minh City, Vietnam 15-17 October

96) Park, J., R. Tateishi and M. Matsuoka (1999) : A proposal of the Temporal Window Operation (TWO) method to remove high-frequency noises in AVHRR NDVI time series data (in Japanese, with English abstract). *Journal of the Japan Society of Photogrammetry and Remote Sensing*, **38**, 36-47

97) Pham, V.C., Q.C. Tran, X.T. Le, V.P. Nguyen, T.V. Tran and T.H. Le (2003) : Rice mapping by SAR in the service of land resources exploitation in the Mekong Delta. *Proceedings of the Regional Conference on Digital GMS*, 55-60, in Bangkok, 26-28 February 2003

98) Reed, B.C., B. White and J.F. Brown (2003) : Phenology: An integrative environmental science. P. 592 Kluwer Academic Publishers, Dordrecht

99) Ribbes, F. (1999) : Rice field mapping and monitoring with RADARSAT data. *International Journal of Remote Sensing*, **20**, 745-765

100) Roerink, G.J. (2000) : Reconstructing cloudfree NDVI composites using Fourier analysis of time series. *International Journal of Remote Sensing*, **21**, 1911-1917

101) Rogers, A.S. and M.S. Kearney (2004) : Reducing signature variability in unmixing coastal marsh Thematic Mapper scenes using spectral indices. *International Journal of Remote Sensing*, **25**, 2317-2335

102) Sai Gon Giai Phong (2006) : Plant hopper epidemic threatens national granary. In: Available at http: //www.saigon-gpdaily.com.vn/index.html

103) Saito, G., N. Mino, Y.Q. Li and Y. Yasuda (2002) : Seasonal changes of vegetation index obtained from NOAA/AVHRR data in China and Japan. *Application on remote sensing technology for the management of agricultural resources*, China Agricultural Scientech Press, Beijing, 13–19

104) Sakamoto, T., N.V. Nguyen, A. Kotera, H. Ohno, N. Ishitsuka and M. Yokozawa (2007) : Detecting temporal changes in the extent of annual flooding within the Cambodia and the Vietnamese Mekong Delta from MODIS time-series imagery. *Remote Sensing of Environment*, **109**, 295–313

105) Sakamoto, T., N.V. Nguyen, H. Ohno, N. Ishitsuka and M. Yokozawa (2006) : Spatio-temporal distribution of rice phenology and cropping systems in the Mekong Delta with special reference to the seasonal water flow of the Mekong and Bassac rivers. *Remote Sensing of Environment*, **100**, 1–16

106) Sakamoto, T., M. Yokozawa, H. Toritani, M. Shibayama, N. Ishitsuka and H. Ohno (2005) : A crop phenology detection method using time-series MODIS data. *Remote Sensing of Environment*, **96**, 366–374

107) Sawada, Y., N. Mitsuzuka and H. Sawada (1999) : Classification of vegetation types by time series data analysis of vegetation index (in Japanese, with English abstract). *Proceedings of the 27th Conference of the Remote Sensing Society of Japan* in November 1999, 73–74

108) Sawada, Y., H. Sawada and H. Saito (2000) : Monitoring seasonal variations of vegetation by high-temporal-resolution spaceborne sensor (in Japanese). *Proceedings of the Academic Conference of the Japan Society of Photogrammetry and Remote Sensing*, Tottori in 16–17 November 2000, 209–212

109) Settle, W.H., H. Ariawan, E.T. Astuti, W. Cahyana, A.L. Hakim, D. Hindayana and A.S. Lestari, (1996) : Managing tropical rice pests through conservation of generalist natural enemies and alternative prey. *Ecology*, **77**, 1975–1988

110) Sheng, Y. and P. Gong (2001) : Quantitative dynamic flood monitoring with NOAA AVHRR. *International Journal of Remote Sensing*, **22**, 1709–1724

111) Shibayama, M. and T. Akiyama (1989) : Seasonal visible, near-infrared and mid-infrared spectra of rice canopies in relation to LAI and above-ground dry phytomass. *Remote Sensing of Environment*, **27**, 119–127

112) Sipaseuth, Inthapanya, P., P. Siyavong, V. Sihathep, M. Chanphengsay, J.M. Schiller, B. Linquist and S. Fukai (2001) : Agronomic practices for improving yields of rainfed lowland rice in Laos. *Increased Lowland Rice Production in the Mekong Region*, 31–40 Vientiane, Laos 30 October – 2 November 2000

113) Sivanpillai, R., A.V. Latchininsk, K.L. Driese and V.E. Kambulin (2006) : Mapping locust habitats in River Ili Delta, Kazakhstan, using Landsat imagery. *Agriculture Ecosystems & Environment*, **117**, 128–134

114) Soc Trang Statistical Office (2003) : Statical yearbook Soc Trang Province 2002. Soc Trang: Soc Trang Statical Office, Soc Trang

115) Soc Trang Statistical Office (2005) : Statical yearbook Soc Trang Province 2004. Soc Trang: Soc Trang Statical Office

116) Tanaka, M., T. Sugimura and S. Tanaka (2000) : Cover. Monitoring water surface ratio in the Chinese floods of summer 1998 by DMSP-SSM/I. *International Journal of Remote Sensing*, **21**, 1561–1569

117) Tanaka, M., T. Sugimura, S. Tanaka and N. Tamai (2003) : Flood-drought cycle of Tonle Sap and Mekong Delta area observed by DMSP-SSM/I. *International Journal of Remote Sensing*, **24**, 1487–1504

118) Tanaka, S., T. Sugimura and M. Tanaka (1991) : Observation of flooded area in Bangladesh by MOS/MSR on an all-weather condition (in Japanese with English Abstract). *Remote Sensing Society of Japan*, **11**, 77–85

119) Thenkabail, P.S., M. Schull and H. Turral (2005) : Ganges and Indus river basin land use/land cover (LULC) and irrigated area mapping using continuous streams of MODIS data. *Remote Sensing of Environment*, **95**, 317–341

120) Tinh, D.Q. (2003) : Flood kindergarten: Community need to community solution. Living with risk turning the tide on disasters towards sustainable development, United Nations Inter-Agency Secretariat of the International Strategy for Disaster Reduction, Switzerland, Available at: http: //www.unisdr.org/eng/public_aware/world_camp/2003/pa-

camp2003-kit-eng.htm

121) Tinh, D.Q. and P.T. Hang (2003) : Living with floods in the Mekong river delta of vietnam. *The 3rd World Water Forum*. Kyoto, Shiga and Osaka, Japan

122) Tong, P.H.S., Y. Auda, J. Populus, M. Aizpuru, A. Al Habshi and F. Blasco (2004) : Assessment from space of mangroves evolution in the Mekong Delta, in relation to extensive shrimp farming. *International Journal of Remote Sensing*, **25**, 4795-4812

123) Trang, T.Q. (2005) : Water resources management in Viet Nam. *Workshop on the Water in Mainland Southeast Asia,Siem Reap, Cambodia, Nov.30-Dec.2, 2005*., Center for Khmer Studies, Siem Reap, Cambodia, November 30-December 2, 2005, Available at http: //www.khmerstudies.org/events/Water/water.htm

124) Tuong, T.P., S.P. Kam, C.T. Hoanh, L.C. Dung, N.T. Khiem, J. Barr and D.C. Ben (2003) : Impact of seawater intrusion control on the environment, land use and household incomes in a coastal area. *Paddy and Water Environment*, **1**, 65-73

125) UN/ISDR (2004) : Risk management of water-related hazards. *WMO Bulletin*, **53**, 23-28

126) USDA (2007) : United States Department of Agriculture. Abailable at: http: //www.usda.gov/wps/portal/usdahome

127) Ut, T.T. and K. Kajisa (2006) : The impact of Green Revolution on rice production in Vietnam. *Developing Economies*, **44**, 167-189

128) Vermote, E.F. and A. Vermeulen (1999) : MODIS algorithm technical background document, atmospheric correction algorithm: spectral reflectances (MOD09). Nasa contract NAS5-96062

129) Viet Nam News (2006) : Pests, diesease suck life out of Mekong Delta rice fields. Available at http: //vietnamnews.vnagency.com.vn

130) Viovy, N., O. Arino and A.S. Belward (1992) : Best index slope extraction(BISE). A method for reducing noise in NDVI time-series. *International Journal of Remote Sensing*, **13**, 1585-1590

131) Wang, Y. (2002) : Mapping Extent of Floods: What We Have Learned and How We Can Do Better. *Natural Hazards Review*, **3**, 68-73

132) Wang, Y. (2004) : Seasonal change in the extent of inundation on floodplains detected by JERS-1 Synthetic Aperture Radar data. *International Journal of Remote Sensing*, **25**, 2497-2508

133) Wang, Y., J.D. Colby and K.A. Mulcahy (2002) : An efficient method for mapping flood extent in a coastal floodplain using Landsat TM and DEM data. *International Journal of Remote Sensing*, **23**, 3681-3696

134) Wardlow, B.D., J.H. Kastens and S.L. Egbert (2006) : Using USDA crop progress data for the evaluation of greenup onset date calculated from MODIS 250-meter data. *Photogrammetric Engineering and Remote Sensing*, **72**, 1225-1234

135) Wassmann, R., N.X. Hien, C.T. Hoanh and T.P. Tuong (2004) : Sea Level Rise Affecting the Vietnamese Mekong Delta: Water Elevation in the Flood Season and Implications for Rice Production. *Climatic Change*, **66**, 89-107

136) WFP (2007) : World Food Programme. Abailable at: http: //www.wfp.org/english/

137) Wilby, A., L.P. Lan, K.L. Heong, N.P.D. Huyen, N.H. Quang, N.V. Minh and M.B. Thomas (2006) : Arthropod diversity and community structure in relation to land use in the mekong delta, vietnam. *Ecosystems*, **9**, 538-549

138) Wilson, D.R., R.C. Muchow and C.J. Murgatroyd (1995) : Model analysis of temperature and solar radiation limitations to maize potential productivity in a cool climate. *Field Crops Research*, **43**, 1-18

139) Xiao, X., S. Boles, S. Frolking, C. Li, J.Y. Babu, W. Salas and B. Moore Iii (2006) : Mapping paddy rice agriculture in South and Southeast Asia using multi-temporal MODIS images. *Remote Sensing of Environment*, **100**, 95-113

140) Xiao, X., S. Boles, S. Frolking, W. Salas, B. Moore Iii, C. Li, L. He and R. Zhao (2002a) : Landscape-scale characterization of cropland in China using Vegetation and Landsat TM images. *International Journal of Remote Sensing*, **23**, 3579-3594

141) Xiao, X., S. Boles, S. Frolking, W. Salas, B. Moore Iii, C. Li, L. He and R. Zhao (2002b) : Observation of flooding and

rice transplanting of paddy rice fields at the site to landscape scales in China using VEGETATION sensor data. *International Journal of Remote Sensing*, **23**, 3009–3022

142) Xiao, X., S. Boles, J.Y. Liu, D.F. Zhuang, S. Frolking, C.S. Li, W. Salas and B. Moore (2005)：Mapping paddy rice agriculture in southern China using multi-temporal MODIS images. *Remote Sensing of Environment*, **95**, 480–492

143) Zalinge, N.V., P. Degen, C. Pongsri, S. Nuov, J.G. Jensen and V.H. Nguyen (2003)：The Mekong River system. *Proceedings of the Second International Symposium on the Management of Large Rivers for Fisheries.* , 335–357, Phnom Penh Cambodia in February 11–14 2003.

144) Zhan, X., R.A. Sohlberg, J.R.G. Townshend, C. DiMiceli, M.L. Carroll, J.C. Eastman, M.C. Hansen and R.S. DeFries (2002)：Detection of land cover changes using MODIS 250 m data. *Remote Sensing of Environment*, **83**, 336–350

145) Zhang, X., M.A. Friedl, C.B. Schaaf, A.H. Strahler, J.C.F. Hodges, F. Gao, B.C. Reed and A. Huete (2003)：Monitoring vegetation phenology using MODIS. *Remote Sensing of Environment*, **84**, 471–475

MODIS画像を用いたベトナムメコンデルタ農業の時空間解析

坂本利弘

摘　要

日本の食料自給率（2005年時の供給熱量ベース）は、40% と先進７カ国の中で最も低い。日本は、その食料海外依存度の高さから、世界的な食料価格の変動の影響を最も受け易い国と言える。近年の経済発展に伴う中国の大豆輸入量の増加や世界的なエネルギー政策の転換（バイオエタノール政策）は、世界の穀物需給バランスを不安定にさせつつあり、世界的な問題となっている。さらに、地球温暖化による農業生産影響、増加し続ける世界人口、鈍化する穀物生産性を考えれば、世界の食料需給バランスが将来にわたって安定し続けると言うことはできないだろう。他方、食料増産・生産性向上を目的とした集約的農業の展開は、発展途上国の農業環境にさらなる負荷を与えるかもしれない。世界の食料生産と密接な関係にある日本は、自国の食料安全保障を議論する前提として、急速に変わり行く世界の農業生産現場やそれを取り巻く農業環境を客観的に理解し、世界の農業環境情報を独自の手法によって収集・整理する必要がある。そこで、筆者は、衛星リモートセンシング技術を活用することによって、地球規模の視点で、時間的・空間的な広がりを持って変わり行く農業生産活動とそれを取り巻く農業環境情報を把握・理解するための時系列衛星データ解析手法の確立を目指すこととした。本研究では、インドシナ半島南端に位置するベトナム・メコンデルタを調査対象領域とした。ベトナムは、タイに次ぐ世界第２位のコメ輸出国であり、その輸出米の９割近くが、ベトナム・メコンデルタで生産されたものである。筆者は、ベトナム・メコンデルタを世界の食料安全保障を考える上で重要な食料生産地帯の一つであると考え、本地域における農業環境及び土地利用パターンの時空間変化を明らかにするための MODIS データを用いた新たな時系列解析手法の開発を行った。

本研究において提案する時系列解析手法は、次の三つである。1. Wavelet-based Filter for Crop Phenology（WFCP), 2. Wavelet-based Filter for evaluating the spatial distribution of Cropping System（WFCS), 3. Wavelet-based Filter for detecting spatio-temporal changes in Flood Inundation（WFFI). WFCP は、時系列植生指数（EVI）を平滑化するためにウェーブレット変換手法を利用しており、日本の農業統計データを用いた検証結果から、水稲生育ステージ（田植日、出穂日、収獲日）を約９－12日（RMSE）の精度で推定可能であることが示された。WFCP を基に改良された WFCS は、水稲作付パターンの年次把握を可能にし、ベトナムメコンデルタにおける水稲作付時期の空間分布が、上流部において毎年雨期に発生する洪水と沿岸部において乾季に発生する塩水遡上によって特徴づけられていることを明らかにした。WFFI は、時系列水指数（LSWI）と植生指数（EVI）から、湛水期間、湛水開始日・湛水終息日を広域把握し、メコン川洪水強度の年次変化を地域スケールで評価することを可能にする。そして、ウェーブレット変換を利用した一連の手法を、2000～2006年までの MODIS 時系列画像に適用することによって、メコンデルタ上流部の洪水常襲地帯において、冬春米の作付時期が、年次変化する洪水規模に依存していることを明らかにした。また、An Giang 省において、堤防建設（輪中）や水利施設の建設によって、洪水期における水稲三期作が可能になった地域が、2000～2005年にかけて拡大していることを明らかにした。本研究で提案した MODIS 時系列画像を利用した時系列解析手法（WFCP、WFCS、WFFI）によって、ベトナムメコンデルタにおける水稲生産が水資源の量的（洪水）・質的（塩水遡上）変動影響を受ける一方、洪水対策の実施によって、栽培体系を二期作から三期作に変更している地域があることを明らかにした。